Universität Kassel
Fachbereich Ökologische Agrarwissenschaften
Fachgebiet Agrartechnik
Prof. Dr. sc. agr. Oliver Hensel

Design and development of a diagonal-airflow batch dryer for spatial drying homogeneity

Dissertation zur Erlangung des akademischen Grades Doktor der Agrarwissenschaften (Dr. agr.)

von
M.Sc. Ing. Waseem Amjad
aus Pakistan

2016

Die vorliegende Arbeit wurde vom Fachbereich Ökologische Agrarwissenschaften der Universität Kassel als Dissertation zur Erlangung des akademischen Grades “Doktor der Agrarwissenschaften” angenommen.

Tag der mündlichen Prüfung: 12.07.2016

Erster Gutachter : Prof. Dr. Oliver Hensel
Zweiter Gutachter : Assoc. Prof. Dr. Anjum Munir

Mündlicher Prüfer: Prof. Dr. Dr. Peter von Fragstein
Prof. Dr. Eva Schlecht

Im Selbstverlag: Waseem Amjad

Bezugsquelle: Universität Kassel, FB Ökologische Agrarwissenschaften
Fachgebiet Agrartechnik
Nordbahnhofstr. 1a
37213 Witzenhausen

Acknowledgements

This dissertation is submitted to the Faculty of Organic Agricultural Sciences, University of Kassel. The research described herein was conducted under the dynamic supervision of Prof. Dr. Oliver Hensel in the Department of Agricultural and Biosystems Engineering, University of Kassel.

I am extremely grateful to my supervisor Prof. Dr. Oliver Hensel for his endless support and the way he encouraged the research work, in short he has been a tremendous mentor for me. I would like to thank my second supervisor Dr. Anjum Munir for his all-time invaluable scientific guidance. His advices on both research as well as on my career have been invaluable. I am indeed thankful to German Academic Exchange Services (DAAD) to provide financial support for my study. I am also indebted to Dr. Albert Esper, CEO Innotech drying technology GmbH for co-funding this project and providing technical support as well. I am also thankful to my committee members, Prof. Dr. Dr. Peter von Fragstein and Prof. Dr. Eva Schlecht for serving as my committee members and for providing brilliant comments and suggestions.

I found myself lucky to have nice, cooperative and friendly department fellows. I owe appreciation to all of my colleagues especially Christian Schellert, Heiko Tostmann for their logistic support and Dr. Uwe Richter, Dr. Barbara Sturm, Dr. Stuart and Dr. Franz for their timely technical and scientific support. For the non-scientific side of my thesis, I particularly want to thank my friend Dr. Shafique Maqsood for his all time help, guidance and support in any sort of problem during my stay in Witzenhausen.

Special thanks and love to my mother and father for their prayers and encouragement; also to my elder brother. Undoubtedly, my wife (Syeeda Iram Touqeer) deserves a special word of appreciation for her moral support and patience during the course study.

Table of contents

Table of Figures

List of Tables

Nomenclature

Symbol/Abbreviation	Unit	Remarks
T	k	Temperature
m	kg/s	Mass flow rate
h	kJ/kg	Enthalpy
cp	kJ/kg k	Specific heat
v	m/s	Air velocity
W	kJ/s	Energy utilization
Q	kJ/s	Heat energy
M	kg	Mass
SEE	....	Standard error of estimate (chapter 4)
SEE	MJ/kg	Specific evaporation energy (chapter 5)
SPE	MJ/kg	Specific product energy
P	kJ/s or kW	Work rate/power
Ex	kJ/kg	Specific exergy
Exr	kJ/s	Exergetic rate
U	-	Total uncertainty in measurement
F	%	Exergetic factor
IP	kJ/s	Improvement potential rate
V	m^3	Volume
hc	$kW/m^2.k$	Convective heat transfer coefficient
L	kJ/kg	Latent heat of vaporization
X	kg water/kg dry mass	Moisture content of the product
$\bar{X}$	kg water/kg dry mass	Average moisture content of the product in time interval Δt
$\bar{T}$	K	Average temperature of time interval Δt
Y	kg water/kg dry air	Moisture added to air, humidity in air
$\bar{Y}$	kg water/kg dry air	Average air humidity in time interval Δt
t	s	Time
A	m^2	Thermal communication area
DR	$kg/m^2.s$	Rate of moisture removal per unit surface area
Q	m^3/s	Volumetric flow rate
Sv	m^3/kg	Specific volume

Subscripts

i	-	inlet and initial
o	-	outlet
a	-	ambient and air
iw	-	water/moisture in inlet air
ew	-	evaporated water/moisture
ow	-	water/moisture in outflow air
hi, ho	-	heater inlet and outlet
fo	-	fan outlet

dci	-	drying chamber inlet
bi,bo	-	bucket inlet and outlet sides
p	-	Product
t	-	total (for chapter 4) beginning time of a difference interval (for chapter 6)
t+1		end time of a difference interval
r	-	Rate
k	-	k^{th} component
v		Vapour
w		Water

Greek symbols

ω	g of water / kg of dry air	Specific humidity
η	%	Efficiency
ϕ	%	Relative humidity
ρ	kg/m^3	Density

List of publications:

The following research articles have been published out of this work.

- **Amjad, W**., Munir, A., Esper, A., Hensel, O. (2015). Spatial homogeneity of drying in a batch type food dryer with diagonal air flow design. Journal of Food Engineering, 144 (1): 148–155. doi.org/10.1016/j.jfoodeng.2014.08.003

- **Amjad, W.,** Hensel, O., Munir, A. Esper, A. (2015). Batch drying of potato slices: Kinetic changes of color & shrinkage in response of uniformly distributed drying temperature. Agricultural Engineering International: CIGR Journal, 17(3): 296-308.

- **Amjad, W**., Hensel, O. Munir, A., Esper, A., Sturm, B. (2016). Thermodynamic analysis of drying process in a diagonal-batch dryer developed for batch uniformity using potato slices. Journal of Food Engineering, 169: 238-249. doi.org/10.1016/j.jfoodeng.2015.09.004

1 General introduction

The present work was carried out at Department of Agricultural and Biosystems Engineering, University of Kassel with the collaboration of Innotech Drying Technology *(Innotech Ingenieursgellschaft GmbH)* to develop a batch type food dryer for spatial drying homogeneity in order to reduce energy consumption and to get product of uniform final quality.

Drying is a widely used method for preservation of fruits and vegetables but an energy intensive unit operation due to high latent heat of water evaporation. Different drying methods are used for the drying of fruits and vegetables like steam drying, microwave drying, vacuum drying but more than 85% of industrial dryers are of the convective type with hot air or direct combustion gases as the drying medium, and over 99% of the applications involve removal of water (Mujumdar 2007). The total energy demand of the dryer is significantly higher with the actual amount depending on the thermal efficiency of the drying systems. Therefore, drying time and product quality are main considerations for any industrial drying process (Chua et al., 2001). In convective drying process, the reduction in drying time and maximum retention of product quality is directly linked with drying temperature which determines the rate of energy utilization (Araya-Farias and Ratti, 2008). In convective dryer (especially large in volume), uniform distribution of drying heat is much important both from drying rate and energy consumption points of view and it depends upon airflow. Therefore uniform air distribution over the food products is required for successful drying operation.

Batch type food dryers are the most extensively applied dryers for the drying process of agricultural products due to simple design, low cost and easy maintenance. But the main problem of the dryer is the lack of drying homogeneity. Factors of high energy requirement and low efficiency (25% to 50%) continue to force researchers for its improvement (Mujumdar, 2006a). The achievement of drying uniformity is always a challenging task and it becomes more difficult for large batch drying systems. Keeping in view the energy consumption, dryer's manufacturers modify the designs to improve the overall energy utilization because dryer's design (type, configuration, mode of heating, heat recovery) effects energy consumption (Kudra, 2004). It could be obtained through a proper distribution and guidance of the drying air inside the drying space (Ghiaus, Margaris, & Papanikas, 1998). For all the food products in the drying chamber, it is difficult to get uniform exposure to the drying air in the batch dryers. Normally, in convective dryers, the air moves from one side/bottom (inlet) of the drying chamber to the other side/top (outlet) of the drying chamber

causing over and under drying of material lying at front/bottom and tail/top of the drying chamber respectively. Several researchers reported different ways to overcome this problem. The majority of designs employ air recirculation systems and incorporating of air guiders in the drying chamber. Such designs and methods implemented to improve convective tray dryer performance have been reviewed by Misha et al. (2013). It reports that drying homogeneity is key factor in the reduction of drying time and production of uniform quality dried product. The use of air deflectors/guiders in batch drying systems is a common practice to overcome the problem of drying heterogeneity. Their use make the dryer's geometry complicate (Margaris 2006) which not only increase the dryer construction cost but also result in velocity pressure drop. So more energy is consumed in the drying process.

Uniform exposure of entire food product to air especially without the addition of baffle plates is still need to be investigated. Presently, an energy efficient dryer that is able to produce uniform quality product is still not widely available on the market (Müller and Mühlbauer 2011). In industrial air dryers, the effect of flow heterogeneity is particularly difficult to resolve. Optimization of the air distribution inside the drying chamber of a batch dryer remains a very important point, due to its strong effect on drying efficiency (Tzempelikos et al., 2012). The achievement of drying uniformity is always a challenging task for large batch drying systems. Therefore, in the present research a new batch type dryer with diagonal airflow design has been developed for spatial drying homogeneity. The main idea behind the design was to make a possibility for all the food buckets to be exposed to air uniformly. The study presents the development, computational based simulation, numerical and experimental evaluation, thermal analysis and mathematical modelling of the system.

Objectives of the studies

The overall objective of this study was to investigate a batch type food dryer for spatial drying homogeneity without the use of any baffle plate in the drying chamber and assessment of the design both with numerical (CFD) and experimental approaches. The ultimate objective of uniform air distribution is to get dried product of uniform quality throughout the drying chamber due to dependence of quality change on drying temperature. More the uniform drying air distribution, more would be the uniformity in the final quality of dried product. In order to meet the overall objective, following specific objectives were defined for research activities.

1. To design and investigate a batch type food dryer with the help of computational techniques, capable to dry the perishable food products (fruits and vegetables) uniformly. Assessment of design both numerically and experimentally.
2. Design of an imaging system to evaluate the performance of the dryer for spatial uniform quality assessment. The change in product color was taken as quality parameter to be investigated on-line along with the entire length of the drying chamber.
3. To perform the thermodynamic analysis of the dryer. In context of reducing energy consumption, optimized air distribution is important for the energy consumption, therefore thermal analysis was also aimed to conduct. This objective also helped to sort out the dryer component to be improved.
4. To develop mathematical model for the drying kinetics of food product and the dynamics of the dryer. It would help to analyze the influence of various drying conditions on the drying time and to overcome the practical difficulties in getting optimum dryer design and drying conditions.

The following chapters give the detail discussions for the aforementioned objectives. The work is presented in the form of state of the art, design and development of dryer, assessment of airflow distribution through simulation and experimental measurements, energy and exergy analyses of the drying process and mathematical modelling. In order to resize the dryer for the required capacity, simulation based design assessment method is also presented as an example.

2 State of the art

This chapter presents the review of literature related to the importance of batch food dryers and associated problems, efforts made to overcome these problems, applications of computational approach in food drying, and the details of the need of thermal analysis.

2.1 Batch type food dryers

Various types of dryers have been used in the domestic and industrial sectors like batch dryers, drum dryers, tunnel dryers, fluidized bed dryers, spray dryers, flash dryers, rotary dryers, vacuum dryers and freeze dryers. Among these, batch type food dryers are widely spread equipment used for food dehydration. For fruits and vegetables, the commonly used batch dryers are named as tray dryers. The food with an acceptable thickness is used to put on the trays. Uniform airflow distribution over the trays is the key to the success of drying operation. One major drawback of this dryer is the spatial heterogeneity of air distribution in the drying chamber. The amount of heat at all sections of the dryer and relative humidity are the main variables effecting the rate of food drying. Parameters commonly used to evaluate the dryers include thermal performance, quality of dried product, and cost of dryer and payback period. The trays inside the dryer can be stationary or moveable. Batch dryer with stationary trays are common due to simple design but variations of final moisture contents of the product at various places are invited due to poor airflow distribution. On the other hand movement of the trays increase the drying rate but this type is seldom used due to complex design and more energy requirement.

2.2 Problem of drying homogeneity

Batch type food dryers are widely used due to their simple design requirement. But problem of uneven air distribution encounter in most batch type drying systems. This leads to problems of low drying efficiency and lack of homogeneity of the products being dried (Mirade, 2003; Misha et al., 2013). Most of the research in batch drying processes has targeted the effect of drying temperature and air velocity as primary influencing parameters on the quality of dried products while the lack of uniformity in air flow is a crucial factor.

Non-uniform air distribution effect the pattern of air velocity and the drying temperature which translates into drying heterogeneity in the drying chamber (Mujumdar, 2006).

Air distribution has been considered as primary design parameter by many researchers (Adams and Thompson, 1985; Ayensu and Asiedu 1986; Mathioulakis et al., 1998; Kiranoudis 1999; Shawik 2001; Mirade 2003; Babalis et al., 2005; Margaris et al., 2006; Gül ah and Cengiz, 2009; Amanlou and Zomorodian, 2010; Jacek et al., 2010; Tzempelikos D.A 2012, Darabi et al., 2013). The majority of designs employ recirculation of air. It is quite easy to handle the issue of drying heterogeneity in small size dryers i.e. mostly solar cabinet dryers but challenges come while dealing dryers of large capacity. Therefore, the use of baffle plates/air straighteners is a common practice to overcome this problem in large drying chamber (Janjai et al., 2006; Roman et al., 2012). Apart of the benefits to use air guiders, it causes not only increase in dryer construction cost but also results in velocity pressure drop. So, more energy is consumed in the drying process. Many researchers reported various airflow designs in convective batch drying systems to increase energy efficiency and product uniformity.

Gülah et al., (2009) designed a swirling flow new drying system. They installed air directing elements inside the drying chamber and a rotating element at the entrance to get shorter drying time. Jacek et al., (2010) improved temperature uniformity by changing the position of heater and the baffle directing the air flow. Tzempelikos et al., (2012) designed a batch-type tray air (BTA) dryer with guide vanes and a flow straightener section to get flow uniformity in the drying section. Nagle et al, (2010) modified an industrial longan dryer by introducing air deflector in the plenum and insulation. An increase in thermal efficiency of 1.51–4.27% was reported by introducing inverted mesh and insulation respectively. Tippayawong et al., (2009) developed a new recirculating air dryer to enhance energy utilization in traditional longan fruit dryer. In order to get uniform airflow across the full cross section of the dryer, they attached smoothly curved air plenums at both ends of heating and drying chambers. It yielded an average thermal efficiency of 29%, compared to 19% for the existing design. Ehiem (2009) developed an industrial batch dryer. The dryer was joined together with a frustum shape diffuser to spread hot air to the drying products (on six trays) at the same time. It resulted a mean thermal efficiency of 82%. But such diffusers are not appropriate in large drying units without perforated screens and air guiders to distribute air over the high column of trays. Precoppe et al., (2014) improved the batch uniformity and the energy efficiency of a dryer by designing chamber's air inlet to a single slit from double-slit.

The difference in the moisture content of litchis on the top tray and bottom tray was reduced from 24% to 4%. It increased dryer energy efficiency from 33 to 42 %.

2.3 Significance of drying temperature for food quality

The process of drying accelerate depending on the specified drying temperature and rate of airflow. Temperature difference between drying air and product determines the drying rate. Reduction of dry matter and increase of energy cost are the consequences of over drying, while under drying facilitate the spoilage process of product. In food drying process, the effect of drying temperature on the quality parameters has been reported by numerous researchers. Krokida et al. (2003) studied the effect of air drying conditions on drying kinetics of vegetables such as potato, carrot, pepper, garlic etc. They found out that drying temperature is the most important factor affecting the drying rate. Babalis et al. (2004) showed that drying air temperature significantly affects the drying kinetics during thin layer drying of figs. Ramalloa and Mascheronib (2012) evaluated the effect of drying time and air temperature on the pineapple quality (color and texture) under constant air velocity of 1.5m/s, and drying temperature of 45^{o}C was stated as best condition for pineapple preservation. Shahabi et al. (2013) investigated the effect of drying air temperature and air velocity for hot air drying of green tea using computer vision system. Fractional conversion model was found acceptable to describe the color parameters accurately that drying temperature showed significant effect on color values. Marcel et al. (2014) studied the color loss of pineapple slices during hot air drying process (40-60^{o}C) in parallel airflow and transverse airflow conditions. Significant effect of drying temperature on color change was reported. Parallel airflow was found good to obtain high color quality at 60^{o}C. Therefore, it can be deduced that drying temperature is the main influencing factor to determine the quality of the final product (Farias and Ratti 2008; Elamin and Akoy, 2014).

Therefore, uniform distribution of drying temperature in the drying chamber is vigorously needed to vaporize water equally from the product lying throughout the drying chamber. A product which dries faster will exhibit different quality parameters than which dries slower. The achievement of drying uniformity is always a challenging task and it becomes more difficult for large batch drying systems. In a convective air dryer (especially large in volume), uniform distribution of drying temperature is vital both from quality retention and energy consumption points of view. Major quality attributes such as nutritional, physical, and chemical mainly depend on the drying temperature and rate of heat flow.

Therefore, it is important to distribute this heat uniformly to get uniform quality for the final dried product. It could be obtained through proper air distribution inside the drying chamber to get uniform heat distribution. It is very important to control the rate of moisture removal for better quality of the dried materials. Whatever the temperature is specified for a certain product, uniformity in final quality can only be achieved if all the product have uniform exposure to that temperature.

2.4 Computer applications in food drying

Computers are increasingly being used for design development, simulation and control of food processes. Application of simulation software is very important to predict the performance of different kinds of drying systems. Chauhan et al., (2015) comprehensively reviewed the application of different software being used in the drying systems.

The use of computational fluid dynamics (CFD) simulation software is increasing as a viable technique for effective and efficient design solutions (Norton and Sun, 2006), prediction of air velocity and temperature profiles in the drying units (Darabi et al., 2013). Progresses in computing efficiency and affordable cost have made its use vigorously for the analysis and investigation of airflow and temperature distribution in the drying systems. The problem stated by user is expressed in scientific form by CFD. The final calculation done by computer, enable the user to inspect and interpret the results of simulation. The entire simulation process can be divided into three steps, pre-processing (generating geometry in "2D or 3D form, developing problem domain i.e. meshing), processing (applying boundary conditions to the geometry, solver which is a process of equation discretization), and post processing (evaluation of the data both numerically and graphically). High costs and time requirement for experiments have enhanced the adoption rate of CFD. During last decade, many researchers reported the use of CFD for the design of various types of drying systems (Shawik, 2001; Mirade, 2003; Bartzanas et al., 2004; Margaris and Ghiaus, 2006; Ghiaus and Gavriliuc, 2007; Chen et al. 2008; Jacek, et al., 2010; Amanlou and Zomorodian, 2010; Krawczyk et al., 2011; Darabi et al., 2013). Numerical results obtained from flow simulation software are needed to be validated by experimental results due to the use of approximate models in CFD (Xia and Sun, 2002).

Recently CFD has been integrated into ANSYS Workbench as ANSYS Fluent, providing a powerful and comprehensive procedure for product design and optimization due to its bidirectional parametric CAD connectivity, powerful automated meshing, pervasive

parameter management and integrated optimization tools. Therefore, use of ANSYS-Fluent CFD based simulation is increasing for food drying processes. CFD was applied for the assessment of design functionality.

2.5 Importance of thermal analysis and modelling

In context of reducing energy consumption, drying temperature and its uniform distribution is important for the reduction of drying time and maximum retention of product quality in a convective drying process (Krokida et al., 2003; Babalis et al., 2004; Araya-Farias and Ratti, 2008). Batch type food dryers are the most extensively applied dryers. The distribution of drying temperature is linked with air flow, therefore uniform air distribution over the food trays is required for successful operation both from drying rate and energy consumption points of view. Recently, several studies have been undertaken to overcome the problems of energy consumption and product quality deterioration through the drying uniformity in hot air dryers (Tippayawong et al., 2009; Ehiem 2009; Amanlou and Zomorodian, 2010; Darabi et al., 2013; Roman et al., 2012; Precoppe et al, 2014).

Keeping in view the value of energy consumption, several researchers have reported the thermodynamic analysis for thermal systems but there is a lack of work on the energy and exergy analyses of the food drying processes in the literature (Akpinar et al., 2005). Some studies were reported conducting energy and exergy analyses to evaluate the tray or batch dryer's performance. Erbay and Icier (2011) reported the use of energy and exergy analyses to evaluate the performance of a tray dryer using olive leaves as drying material. They found drying temperature as more influencing parameter than air velocity. Midilli and Kucuk (2003) conducted the energy and exergy analyses of the shelled and unshelled pistachio drying in a solar cabinet dryer. They suggested considering the order, structure and water contents of the products for reducing the energy utilization and exergy losses during the drying process. Akpinar et al. (2006) conducted the thermodynamic analysis of single layer drying of pumpkin slices in a cyclone type dryer. On the basis of the energetic and exergetic results, they concluded that exergy losses are directly proportional to the energy utilization in the drying chamber. Icier et al. (2010) investigated the effects of drying air temperature on the exergy loss, exergy efficiency and exergetic improvement potential for the drying of broccoli florets using three different drying systems. A direct relation was found between exergy loss and drying temperature both in the tray and heat pump dryer. Maximum exergy efficiency and improvement potential were reported for fluidized bed dryer and heat pump

dryer respectively. Colak and Hepbasli (2007) used exergy analysis method for the performance evaluation of a tray dryer using green olive as test material. The drying temperature of 70^{o}C and air mass flow rate of 0.015 kg/s were found optimum for maximum exergy efficiency. Hancioglu et al. (2010) performed energy and exergy analyses methods to investigate the performance of a tray dryer using parsley. The use of higher temperature and lower air velocity were reported for higher energy and exergy efficiencies.

These thermal analyses, especially exergy analysis provides useful information in the design of the drying system. The outcomes of these analyses mainly vary depending upon the dryer configuration and the product being used. Therefore, dryers with different designs can give different values of energy and exergy analyses for the same product. Thus, the ultimate objective of a modified or new design is to improve the results in the form of less energy consumption and better product quality. Energy and exergy analyses are rarely made for food processes. Detailed literature review has shown that little work has been done on the energetic and exergetic analyses for the hot-air batch drying of fruits and vegetables. In case of potatoes, only Akpinar et al. (2005) worked on the single layer drying process of potatoes via a convective hot-air cyclone type dryer reported by Aghbashlo et al. (2008). So to present more work on the energy and exergy analyses for this product using different drying unit would provide another way to overcome the problems related to energy and exergy throughout the drying process of potato. Therefore, potatoes were used for all the drying experiments to meet different objectives. Thermodynamic analysis of the newly developed dryer was performed which helped to sort out the system components requiring improvement.

3 Development of diagonal-batch dryer for spatial homogeneity of drying

A new batch type dryer with diagonal airflow design (along with the length of drying chamber) has been developed. ANSYS-Fluent has been used to predict the profile of air distribution in the drying chamber by applying the appropriate boundary conditions. A spatial homogeneity of air distribution was found in the drying compartment. In order to assess the working of the dryer, a series of drying experiments were conducted using potatoes (slices, 4mm thickness) as drying material. The results, expressed as drying curves for all the food buckets, showed high values of coefficient of determinants (R^2). The simulated results of airflow distribution along the length of the dryer were compared with experimental measured data. This comparison revealed a good correlation coefficient of 87.09%.

3.1 Introduction

The process of drying, the drying medium and the geometry of the drying chamber determine the uniformity of drying and thus the quality of the finished products (Tzempelikos et al., 2012). It means that after selecting a drying process and drying medium, configuration of the drying chamber is the critical design parameter. It decides the uniform air flow over the entire product in the drying chamber. Therefore, the design of airflow is one of the most important factors in the designing of batch type food dryers. The present study was conducted to design a new batch type food dryer named as diagonal-batch dryer due to its diagonal airflow design. In order to get spatial uniform drying without air guiders in the drying chamber, the food buckets were arranged diagonally along with the length of dryer. The main objectives of this part of the study were to design an air flow pattern in such a way that the entire product should be exposed to warm air uniformly, conducting airflow simulation by using ANSYS Fluent to find air flow distribution, drying experiments to evaluate the design using sample food product (potatoes) and comparing the experimental data for air flow distribution with that of simulated.

3.2 Materials and methods

3.2.1 Description of the dryer

Figure 3.1 illustrates the designed batch dryer (11 m×1.20 m×1.25 m). It consisted of three major parts namely: connector, lower half, which is the heating chamber, and upper half, the drying chamber. The heating chamber was positioned at the bottom of the drying chamber to reduce space requirement. The heating chamber was made up from a constant speed axial tube fan (Dia. 0.7 m, 453 m^3/h, 2.2 kW) and an electric water–air heat exchanger. A water pump was used for the water circulation in the system along with a pressure gauge and thermal expansion valve (to absorb excess water pressure). A connector was used to connect the lower half to the upper half of the dryer. In the drying chamber, twenty-five food buckets (each was of dimension 0.6m×0.4m×0.29m) were arranged diagonally on a guiding track (for easy loading and unloading of food buckets). Each bucket covered a distance of 0.4m in the drying chamber.

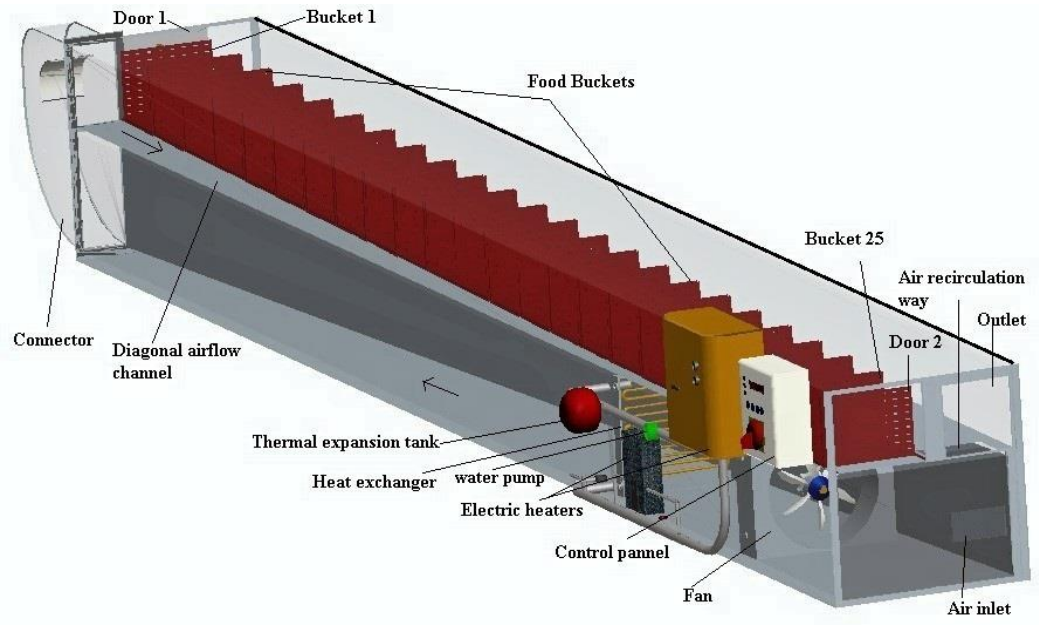

Figure 3.1: Diagonal-airflow batch food dryer for spatial homogeneity of drying

These diagonally arranged buckets gave a shape of diagonal airflow channel at an angle of 1.42^o with the wall of the drying chamber in longitudinal direction. It is the distinct designing feature of the dryer to make possibility for the drying air to pass equally through all the buckets. The walls of dryer were made of polyurethane foam sandwiched into galvanized iron sheets for easy machining and excellent insulation. Two opening doors (0.65 m×0.36 m) were installed for the loading and unloading of buckets (both sides of the drying chamber). A

rectangular passage (0.30 m×0.15 m) was made just before the outlet door (0.30 m×0.15 m) for air recirculation. This passage was opened and closed with the flap of outlet door. The operation of the outlet door (opening/closing time of flap) was controlled based on set temperature. A control panel was used to set temperature and time (three different temperatures can be set for three different intervals of drying time for a drying process). More technical details of the dryer can be found in appendix 1.

Velocity pressure increase and decrease as the air proceeds through the channel, depending on the cross-sectional area of the flow. The aspect ratio of an airflow channel is significant to control the pressure drop. The higher the aspect ratio, the higher-pressure loss in the rectangular airflow system (Hassan and Yue, 2002). Therefore, the aspect ratio of the diagonal channel was gradually decreased along with the length of drying chamber to maintain uniform velocity pressure inside the channel, forcing the air to pass equally across all the food buckets (Figure 3.2).

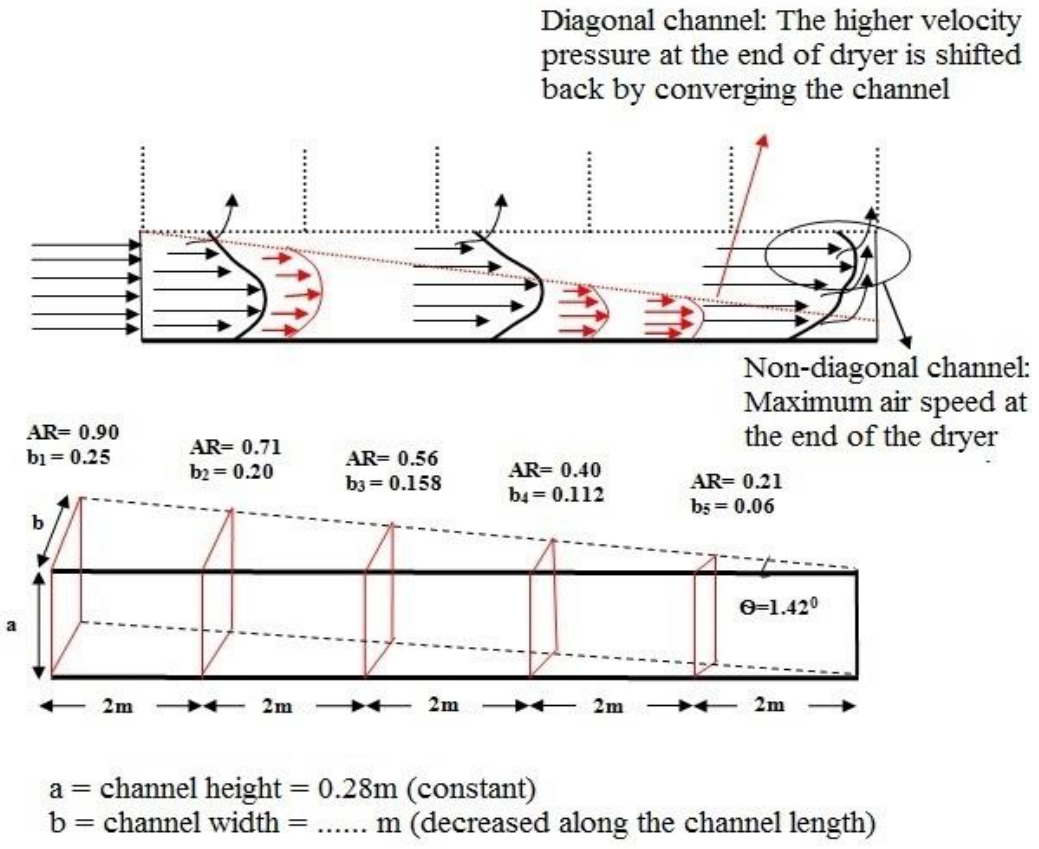

Figure 3.2: Diagonal airflow channel in the drying chamber

The diagonal form of the channel shifted back the higher velocity pressure developed at the end of the dryer (in case of straight airflow) to provide possibility for the drying air to pass across all the buckets equally.

3.2.2 Design considerations

The empirical knowledge serve as basis for the design of a batch tray dryer while modelling and simulation help to improve the design and product quality. Drying process is a complex phenomenon and various factors are involved which need to take into consideration. Mainly these factors are the quantity of product, loading and unloading of product, mass of the moisture to be removed from the product, quantity of air required, selection of type and size of fan, amount of energy required, rates of heat and mass transfer and energy efficiency (Ahmed and Rahman 2012). Some basic equations used for design computation are given below.

After selecting a perishable product which needs to be dried, the amount of moisture to be removed to get the desired final product moisture can be calculated as (Ichsani and Dyah, 2002).

$$M_w = M_{pi}\left(\frac{X_i - X_f}{100 - X_f}\right) \qquad 1$$

Where M_w and M_{pi} are the mass of moisture to be removed and initial mass of product respectively in kg; X_i and X_f are the initial and final moisture contents of products respectively in % (wet basis).

The mass of drying air which is required to dry the specified amount of product can be calculated using basic energy balance equation (Ichsani and Dyah, 2002).

$$M_a C_{pa} \Delta t = M_w L \qquad 2$$

Where M_a, C_{pa}, Δt and L are the mass of drying air (kg), specific heat capacity of air (kJ/kg. k), difference in the initial and final temperature of drying air and latent heat of evaporation of free water (kJ/kg).

After calculating the quantity of air, the size of the fan can be determined by calculating the volumetric flow rate of air given by Axtell (2002).

$$q = m_a \times sv_a \quad (3)$$

Where q is the volumetric air flow rate (m^3/s), m_a is the mass air flow rate (kg/s) and sv is the specific volume of the drying air in (m^3/kg).

The quantity of heat required can be calculated as (Axtell 2002).

$$Q = m_a(\Delta h) \quad (4)$$

Where Q is amount of heat energy (kJ/s), m_a is the mass air flow rate (kg/s) and Δh is the difference in specific enthalpy of air at drying temperature and at inlet (kJ/kg).

Uniform distribution of that calculated amount of air in the drying chamber is very important to save energy consumption as well as to get the drying homogeneity. Therefore, the arrangement of food trays/shelves/buckets is important to overcome this problem, to avoid the back pressure caused by these loaded trays and to get an appropriate airflow through the trays. Following steps can be considered for it.

a	**Batch size:** It is the amount of the food materials to be dried in one batch	In diagonal dryer = 150kg
b	**Drying area:** The drying area needed per kg of food material depends upon batch size and loading density	Loading density: $5kg/m^2$ ($1kg/0.2m^2$) This means that for 150kg batch, $30m^2$ drying area is required.
c	**Tray area:** The number of trays and tray area are calculated based on available area and tray load.	Total trays area should be $30m^2$. Now, for the size of a tray, length to breadth ratio has to be optimized based on good airflow. Circulation of air at velocities of 1 – 10 m/s is desirable to improve the surface heat transfer coefficient and to eliminate stagnant air pockets.
d	**Air distribution:** Placement of trays mainly depends upon uniform air velocity over all the material being dried. This defines the shape (dimensions) of drying chamber.	Distance between two trays is based on tray load. There should be a clearance of not less than 4cm between the material in one tray and the bottom of the 2nd tray immediately above. In the current study, it is 4.5 cm

3.3 Simulation of the design

3.3.1 Simulation details

ANSYS-Fluent was used for the air flow simulation into the ANSYS Workbench platform. It provides a comprehensive suite of computational fluid dynamics (CFD) software for modeling fluid flow and other related physical phenomena (Fluent user's guide 2005). The geometry of the dryer was modeled and analyzed for two configurations of air flow channels named as straight air flow channel and diagonal air flow channel (θ=1.42^o). The simulation with straight flow channel was done to assess the suitability of diagonal air flow design and to show a comparative change in the air flow regime in the drying chamber.

The main purpose of the simulation was to predict the profile of air distribution; therefore only the concerning parts of the dryer (connector and the drying chamber) were designed and simulated in 3D model. The geometry was developed in ANSYS Design-Modeler. The use of 3D model enabled to assess the flow variation along with the depth of the drying chamber which was not assessable in 2D model. Keeping in view the importance of air flow pattern, the case was simulated as steady state condition (just to show the distribution of air). For boundary conditions, lower part of the connector was taken as air inlet, receiving heated drying air from the heat exchanger. A value of 5 m/s normal to air inlet was assigned as inlet velocity. The standard k-ε turbulence model was used for air flow turbulence. The characteristics and settings of simulations are tabulated in Table 3.1.

Table 3.1: 3D Model properties and settings of the simulations

Number of elements	9613901 (straight airflow) 9542733(diagonal airflow)
Volume main body	4.36667 m^3
Grid type	3D, tetrahedral, unstructured
Turbulence model	k-ε standard
Discretization	Second-order upwind
Wall friction model	no slip
Inlet air velocity (normal to air inlet)	5.0 m/s
Mass flow inlet	1.31688 kg/s
Outlet pressure	0 Pa

The resistance to air flow due to food product was assumed negligible due to single layer and small thickness (4mm thick slices). So food was not modeled as solid objects nor as a porous media. Practically, a single layer of food samples was loaded on each tray of bucket

(4-5 trays in a bucket), so application of porous media was not applicable as food product. The main concern was that if the region of food buckets gets uniform air distribution, it would facilitate the uniform drying.

3.3.2 Simulated results

Figure 3.3 shows comparative path lines of air velocity for straight air flow (a) and diagonal air flow (b) channels. In straight airflow channel, air entered in the upper half of the dryer (drying chamber) and moved directly to the end of the drying chamber as was expected. It caused higher air velocity at the end of the drying chamber especially through the last bucket (avg.7m/s) comparative to other parts of the drying chamber where zones of higher and lower

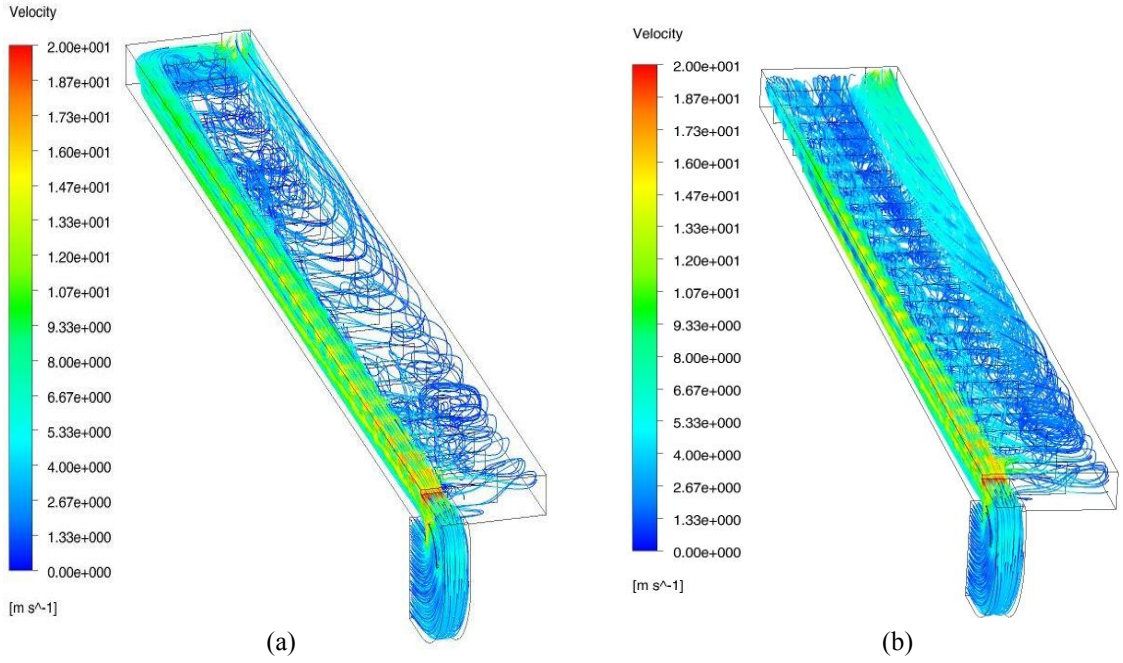

Figure 3.3: Path lines of air velocity for straight (a) and diagonal (b) airflow cases

airflow were observed. On the other hand, the design with diagonal airflow channel showed a good air distribution through the buckets (Figure 3.3b). In this arrangement, the air converged as it moved towards the end of the drying chamber due to its diagonal flow. It resulted almost same velocity pressure at the inlet side of the buckets (inlet flow channel) causing uniform air flow through all the food buckets. At the outlet side of the buckets (outflow channel), velocity path lines showed the occurrence of almost an equal outflow from each bucket. It strengthens the diagonal air flow design for uniform air distribution along with the length of the drying chamber. In order to visualize the air distribution along with the depth of the

drying chamber (along the height of the buckets), planes were drawn at three positions (bottom, middle and top) of the drying chamber in ANYSY Fluent solution (Figure 3.4).

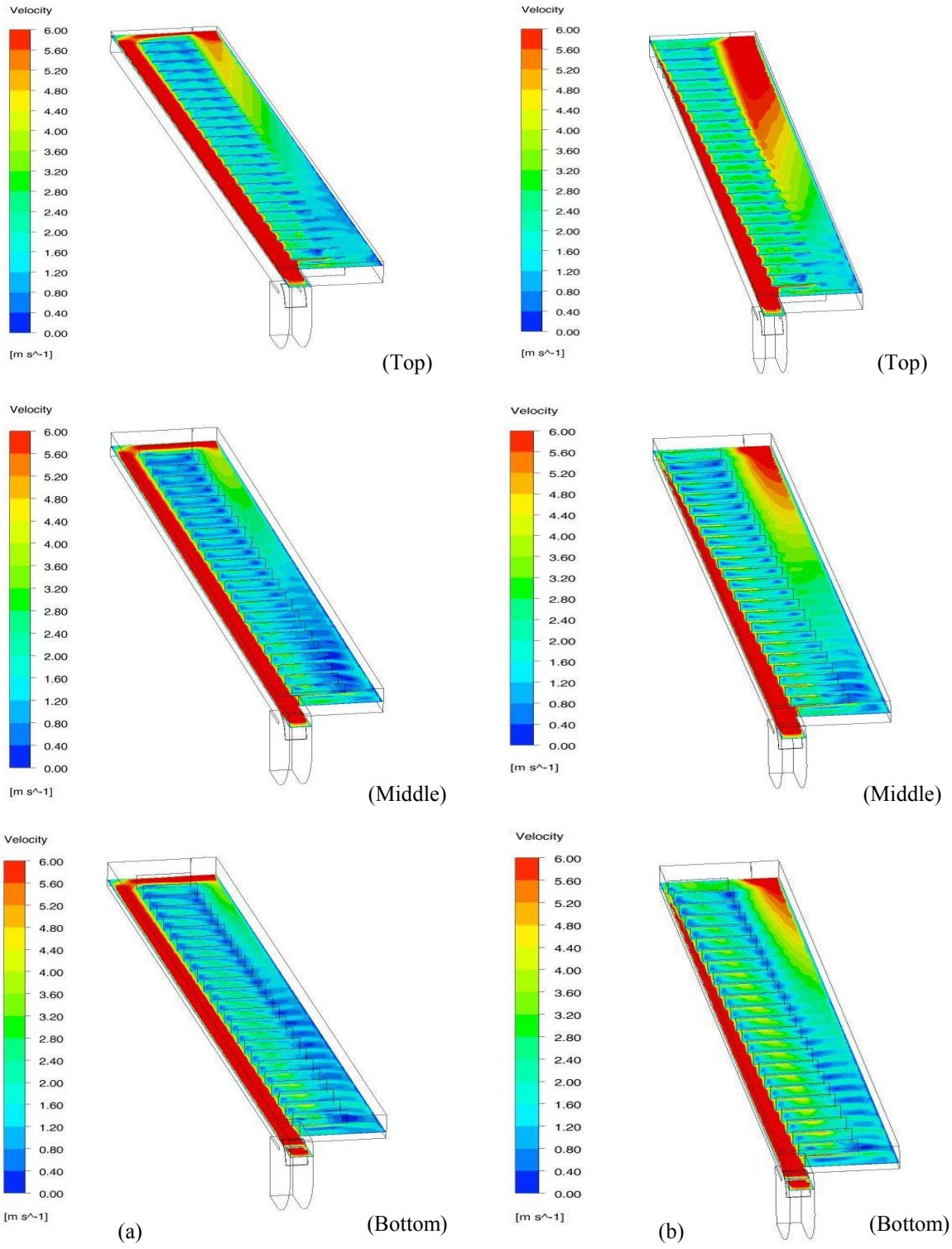

Figure 3.4: Contours of air velocity at top, middle and bottom positions of the drying chamber for the straight (a) and diagonal (b) airflow cases

Figure 3.4 shows velocity contours at three different positions of the drying chamber for both straight (Figure 3.4a) and diagonal (Figure 3.4b) air flow designs. It is a more effective way to get through the analysis of air distribution in a system. The air velocity decreased as air entered into the buckets, so the velocity scale was reduced to 6 m/s to assess the air flow variations through the buckets clearly. In straight airflow design, velocity contours at all three positions of the drying chamber showed a higher flow at the end of the dryer, same as it was observed with velocity path lines (Figure 3.3a). The velocity contours for diagonal airflow design at three positions showed a uniform air distribution, same as it was observed with actual velocity scale (Figure 3.3b). It can be observed from the velocity contours of the planes drawn at three positions, showed uniformity of air flow not only along with the length of dryer but also along the heights of buckets as well (Figure 3.4b). So the simulated analysis for diagonal airflow pattern gave good uniformity of air distribution through the concerned region (food buckets).

3.4. Drying experiments

3.4.1 Procedure

The dryer was instrumented to measure different values needed to assess its working. Air velocity was measured with TA5 hotwire anemometer with a resolution of 0.01 m/s at two positions of lower half of the dryer (after the heat exchanger & at the start of the connector) and at four positions of the drying chamber (at the start point, middle and at the end of diagonal air flow channel and at the outlet). Air temperatures at every one meter distance of the drying chamber were measured by inserting thermocouples (K-type ±1.5 k) at the top of the drying chamber, connected with data logger (Agilent 34970A) to assess temperature distribution throughout the drying chamber. Mini data logger (MSR-145 ±2%, Swiss) was used both at inlet and outlet positions of the drying chamber to measure the relative humidity. Electric weight balance (BIZERBA-Sartorius, ±0.1g) was used for weighting of fresh and dry material for drying rate calculations at different intervals of an experiment.

The experiments were carried out using locally available potatoes. Preliminary trials were conducted with one and two trays of potatoes (single layer) in each food bucket to assess the drying trend along with the length of the drying chamber. After that number of trays was increased to four in each bucket to assess the drying uniformity not only along the length of the dryer but also along the height of each bucket (among four trays). The

perforated trays (69.45% perforation) were inserted in each bucket (0.6m×0.4m×0.29m) at successive intervals (0.058m). These trays in a bucket were loaded with four kilogram of potatoes slices (4mm); each of them was carrying one kilogram of drying material in single layer. These potatoes were sliced with an adjustable cutting thickness cuter (Bosch MAS62). The operating drying temperature (48ºC) was set with a controller installed on the dryer. Potatoes were dried up to twelve percent final moisture contents. During the experiment, periodic weighing method was used for each bucket to calculate its drying rate.

In case of four trays of the drying material, the dryer was not fully loaded due to the difficulty of material handling during the experiments and to avoid the material cost for repetitive trials. So, the drying experiments were divided into five sets of experiments each comprised of five buckets. Each set (five buckets) covered a distance of 2m in the drying chamber, so five sets of experiments covered the entire length of the drying chamber. It was tried to make sure the same drying conditions for all the experiments at their start. Therefore, the drying material was not loaded just after the start of the dryer until the required air conditions were obtained within the drying chamber.

3.4.2 Drying results and discussion

Figure 3.5 shows the experimental results in the form of drying curves plotted for each set of experiments separately to show spatial uniformity in the drying. Although, these drying curves were found quite smooth at various places in the drying chamber but during the constant rate of drying, there were slight variations in moisture contents among the food buckets. It can be observed in first (Figure 3.5a), fourth (Figure 3.5d) and fifth (Figure 3.5e) sets of experiments comparative to the second (Figure 3.5b) and third (Figure 3.5c) sets. As air entered into the drying chamber, it moved towards the end of the dryer and built a velocity pressure within the diagonal airflow channel due to its convergence.

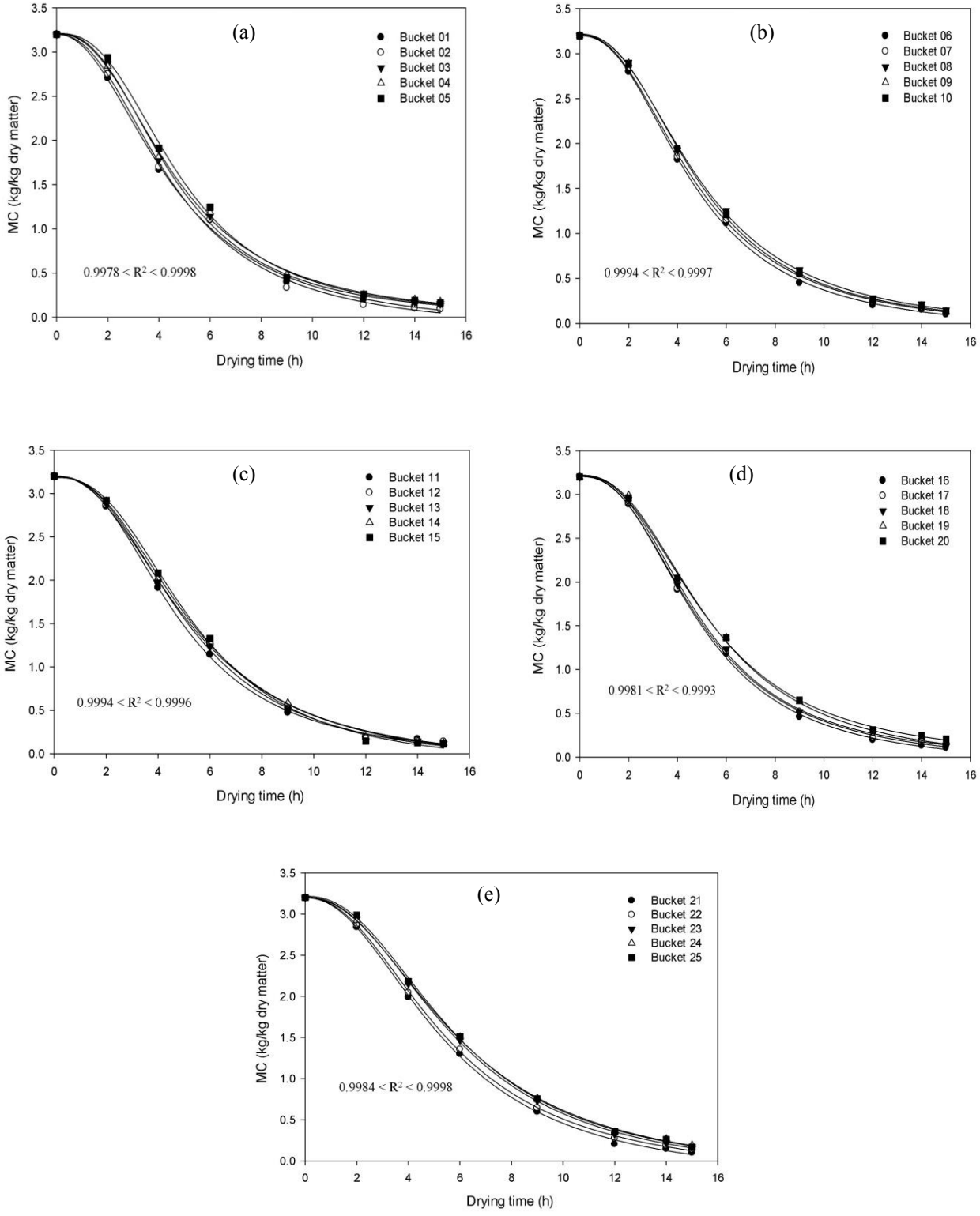

Figure 3.5: Drying curves for five sets of experiments at different places in the drying chamber (a) 1-5 buckets at 2m distance (b) 6-10 buckets at 4m distance (c) 11-15 buckets at 6m distance (d) 16 20 buckets at 8m distance (e) 21-25 buckets at 10m distance.

It was observed from the results for airflow simulation that air flow was not so smooth just at the entrance of airflow channel due to some pushing effect exerted by the incoming air. So, the velocity pressure settled smoother at the middle of airflow channel. That is why there were found slight span of moisture contents in first set of experiment (Figure 3.5a) after second and fourth hours of its drying time comparative to other. Similarly, at the end of airflow channel, due to comparative low air velocity, small variation in moisture contents were found among the food buckets during the constant rate of drying (Figure 3.5d and Figure 3.5e). The observed variations during constant rate of drying occurred because of surface moisture which is loosely bounded and its evaporation rate significantly varies with the slight variation in the air flow. But all the drying material in each set of experiments gave an almost equal final moisture contents during the phase of second falling rate. This was the main objective of the study that whole the product, lying throughout the length of the drying chamber, should come at same drying level with minimum variation. The drying material in all the food buckets was being exposed to incoming warm air uniformly which facilitated the uniform drying.

For each set of the experimental drying data, sigmoid logistic model was found best for curve fitting with high R^2 value using sigmaplot-12 as shown in Figure 3.5. It showed that a smooth drying trend had been shown by all the food buckets under same drying conditions. Drying uniformity is achieved with uniform heat distribution as zones with different airflow cause drying heterogeneity which ultimately reduces dryer efficiency by increasing the energy consumption and the drying time (Kiranoudis et al., 1999; Roman et al., 2012). Because convective heat transfer (h_c) of a product varies with its position in the drying chamber and drying time, so variation in the drying rates effect the quality parameters of drying materials. No doubt drying temperature is important to maintain the quality of dried product as some products are heat sensitive. But the main task is to distribute that temperature uniformly, so the product at all the places of the drying chamber would experience of similar changes in their quality parameters. In diagonal airflow design, the product was dried with uniform drying rate, so it would also result uniform quality drying for other concerning quality parameters because uniform quality drying is dependent on uniform air distribution. This design of airflow provided quite encouraging results by eliminating the factor of zones of over and under drying.

Figure 3.6 shows the comparative drying trend of all the food buckets at different intervals of the drying time. Overall it shows the drying behavior of food material along the entire length of the drying chamber. The variation of moisture contents among the food buckets at various intervals of drying was observed quite low especially as drying proceeded towards its falling rate.

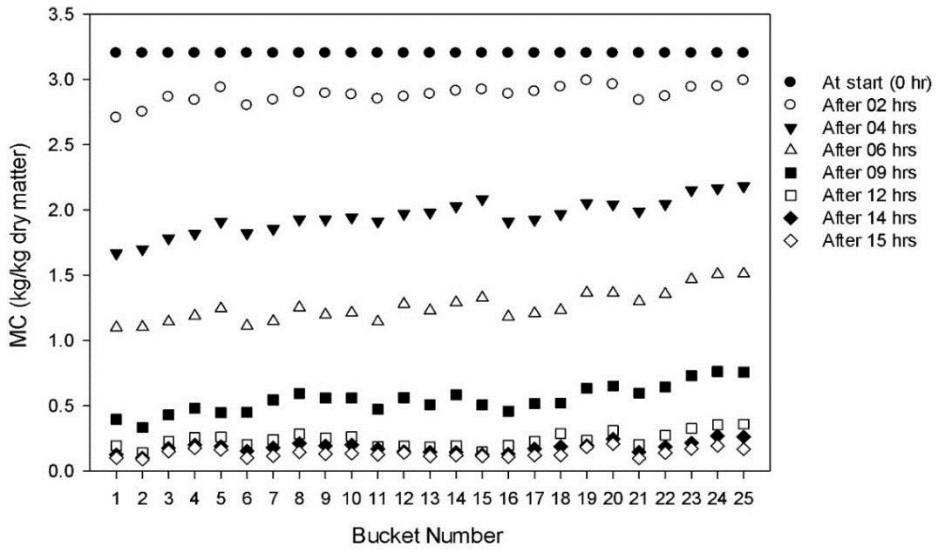

Figure 3.6: Comparative product drying trend among the food buckets at different time intervals of the drying process

Experimental measurements showed that the diagonal airflow design resulted a homogenous air distribution. The measured span of moisture content among the food buckets at a given drying time is tabulated in Table 3.2 in the form of standard deviation. The highest standard deviation was observed during constant rate of drying i.e. after four and sixth hours of drying time.

Table 3.2: Standard deviation among the food buckets at different time intervals

Drying time (hr)	MC (kg/kg dry matter)			
	Median	Minimum	Maximum	Standard Deviation
2	2.89	2.71	2.99	0.07
4	1.94	1.67	2.18	0.13
6	1.23	1.10	1.51	0.12
9	0.55	0.33	0.76	0.11
12	0.24	0.14	0.36	0.06
14	0.18	0.10	0.27	0.04
15	0.13	0.09	0.21	0.03

It was observed that at early stages of the drying process, first one or two buckets in each set showed a less value of moisture content comparative to the rest of the food buckets of that set. This trend can be observed at the drying times of four, six and nine hours especially in the last two sets of the buckets. It could be because of not fully loading the dryer. As mentioned earlier that the dryer was not operated at its full load capacity but with a set of five buckets at every two meter distance of the drying chamber in an experiment. The side walls of the buckets were also perforated, so some percentage of the air coming through the neighbor empty bucket passed over to the adjacent first bucket of the experimental set. It facilitated the evaporation of surface moisture of food lying in the first bucket of the set more than the following buckets of that set. Because surface moisture is loosely bounded so easy to evaporate. But even though the maximum variation (higher standard deviation) was low (Table 3.2). Material started to dry with same moisture contents and ended up at almost same level of moisture. Thus, the diagonal airflow design provided a way to lower down the problem of drying heterogeneity in the batch dryers.

3.5 Comparison between the experimental and the simulated data

Experimental air flow through each bucket was measured by inserting TA5 hotwire anemometer at three points for each bucket (Figure 3.7).

Figure 3.7: Experimental measurement of air velocity at the region comprised with food buckets in the drying chamber

These points were made by drilling three holes in the roof at the place of each bucket to insert the probe of anemometer as shown in Figure 3.7. For a single bucket, six velocity readings were measured for each of its three points at various depths (top, middle, and bottom) and then an average velocity was calculated for that bucket.

In case of airflow simulation, velocity distribution showed turbulence when air entered in each bucket. So the measurements of the velocity distribution inside a bucket at its different positions were necessary to take an average velocity of airflow. For this, in CFD solution, lines were drawn passing through each bucket in longitudinal direction at three points (front, middle and back) with three positions (top, middle, bottom) for each point. Then the values of air velocity were extracted for these lines.

These results of average velocity were compared corresponding with the results extracted from the simulation. The result of statistical analysis showed good correlation (correlation coefficient of 87.09 %) for airflow distribution between the average predicted and the average experimental measured velocity as illustrated in Figure 3.8.

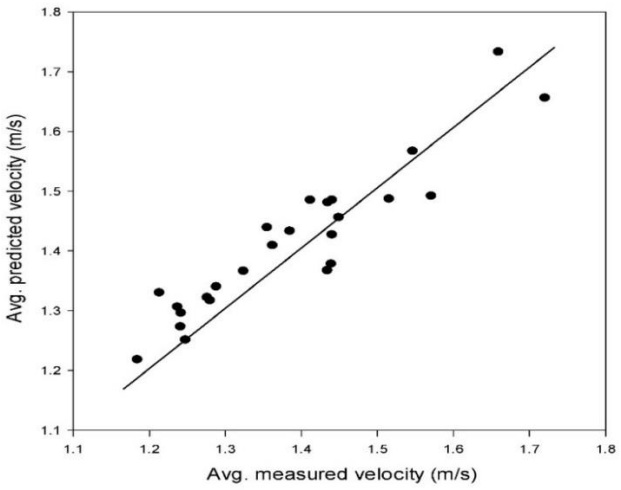

Figure 3.8: Comparison of experimental and predicted average air velocity through buckets

The numerically and experimental air distribution with diagonal airflow design strengthen the design for uniform drying. This comparison of air distribution not only supports the uniformity of drying along the length of drying chamber (in each bucket) but also along its height (all the trays in a single bucket). Practically it was checked by measuring rate of moisture contents reduction for each tray of a bucket and it was found almost uniform. So, uniformity occurred not only along the length of dryer within the food buckets but also found good along the height of each bucket. Therefore, chance of significant variation of drying in direction of depth of drying chamber has been reduced.

Figure 3.9 shows the simulated results for the pressure drop along with the length of the dryer. In CFD analysis two rakes each of with twenty points were drawn, one passing through bucket's place (a) and second passing through the middle of diagonal airflow channel (b). The pressure of inlet air dropped towards the end of the drying chamber as was expected.

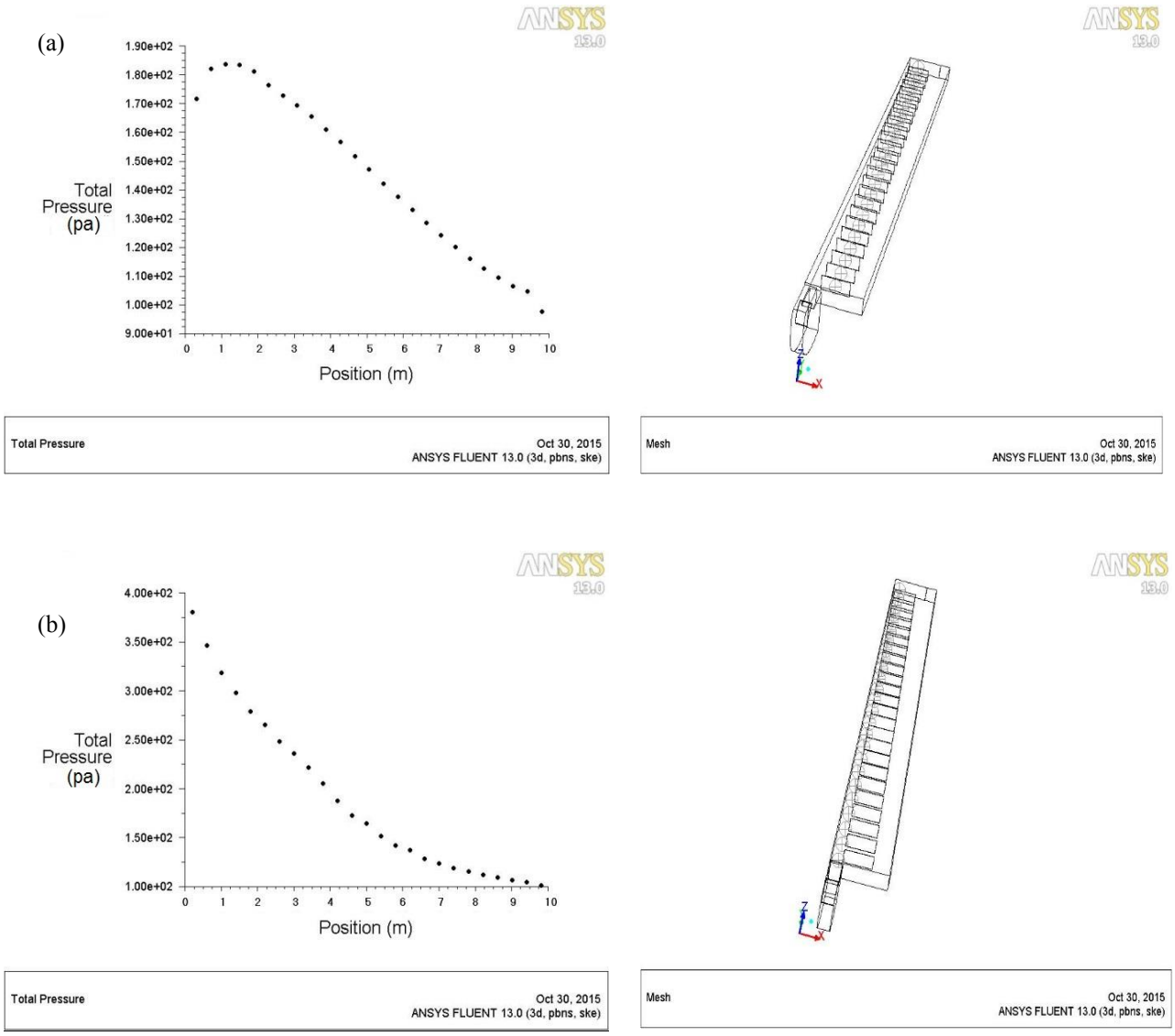

Figure 3.9: Pressure drop along with the drying chamber at the place of food buckets (a) and in the diagonal airflow channel (b)

In place of food buckets, the pressure drop was about only 90pa along with the dryer and 270pa in case of diagonal channel. As the diagonal channel was not a closed conduit, therefore pressure could not be same in the channel from inlet point to the end of dryer. But

this decline did not cause much decrease in pressure at the buckets region, causing almost uniform airflow distribution through food buckets (Figure 3.8).

Experimentally airflow pressure in the diagonal channel was measured at four points along its length. These points were drilled through the wall of the channel. At each point, four measurements were recorded and took average (close to the channel wall, midpoint between channel wall and center of the channel, center of channel and near bucket's inlet). To compare these values with those of simulated, in CFD analysis lines were drawn at the same positions and direction. Average value was calculated from the extracted values for each line. Figure 3.10 shows comparison of experimental and predicted average pressure drop in the diagonal channel. For experimental measurement, a pitot tube connected to pressure gauge was inserted into the airstream. It measured total pressure at single point i.e. only a point velocity reading. This could be the reason for the apparent difference between the experimental and simulated values. Secondly it is important that the pitot tube should be aligned parallel to the airflow and its tip pointing directly into the flow.

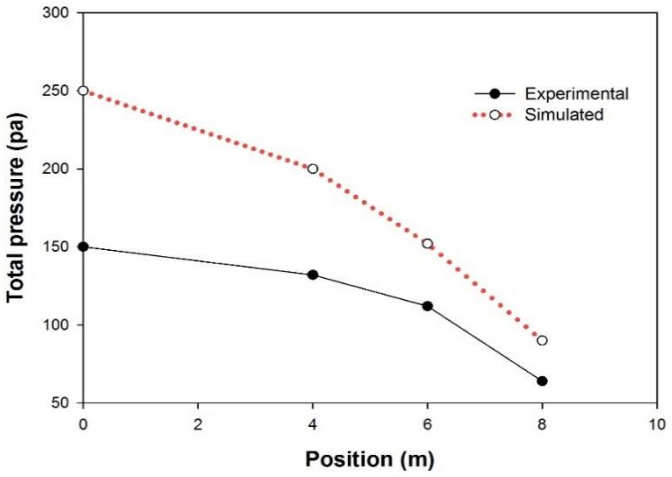

Figure 3.10: Comparison of experimental and predicted average Pressure drop in the diagonal channel

3.6 Conclusion

A new batch type food dryer was developed with distinct feature of diagonal air flow design for uniform air distribution in the drying chamber. The design was modeled and analyzed using ANSYS-Fluent. Numerically and experimentally, a good air distribution was found in the drying chamber which gave assertiveness to the design. It was found that whole the drying material (potatoes slices 4 mm thick, at 48^{o}C) lying in diagonally arranged buckets, dried with almost uniform drying rate. As all the food was being exposed to air at same time

so the remarkable usual fact of under and over drying has been reduced. It shows that this design would ultimately lead to the quality drying because air distribution has significant influence on product quality. Comparison between experimental and predicted average values of air flow through buckets revealed good correlation coefficients of 87.09%. It showed that newly designed dryer is able to distribute air satisfactorily uniform. The pressure dropped along the channel as was expected but this drop did not make significant difference in rate of airflow through buckets.

4 Real-Time measurements of color and moisture content changes in potato slices for the assessment of drying process in diagonal-airflow batch dryer

Uniform quality drying throughout the drying chamber of a dryer is important for a quality oriented drying process. The final quality of the dried products significantly depends upon the drying temperature. A batch type food dryer was developed for spatial drying uniformity (chapter 3). The effect of uniform air distribution on quality changes (color) of dried product was on-line investigated along with the entire length of the drying chamber. The required parameters were measured for 5mm thick potato slices at 60°C using an imaging box and a load cell. The correlations of image attribute (color) with physical parameter of drying (product moisture) were developed for all sections of the drying chamber. The rate of color change was found uniform at all sections with high value of R^2 (0.98). The kinetics of color change showed that changes in values of L^* and b^* fitted well to the first-order kinetic model while values of a^* and ΔE followed zero order kinetic model for all sections of the drying chamber. These results show that spatial uniform drying temperature is important to get uniform change in quality of dried product at all the zones of the drying chamber.

4.1 Introduction

Many factors are involved in maintaining the quality of dried product like medium of drying, food tray material, pre-treatment processes etc. but the drying temperature is the most critical. It is very important to control the rate of moisture removal for better quality of the dried materials. For this, uniformity in heat distribution, associated to air distribution, is important. For the assessment of dried product quality, color and shrinkage are extensively used aspects in the acceptance of the dried product. Consumers tend to associate color and other visual properties with flavor, safety, storage time, nutrition and level of satisfaction (Pedresche et al., 2006). The dehydration level in food quality is usually evaluated by trained visual inspectors (Abdullah et al., 2004). The other way is sampling and instrumentation after specific intervals during the drying process that is comparative precise but an invasive and tedious procedure leading to the loss of quality (Jayas et al., 2000). Preliminary, experiments were also conducted using this approach using a Chroma meter (Konica Minolta CR-410) for color measurement (Amjad et al., 2015a). A new and alternative non-invasive approach is the application of computer vision systems (CVSs) which proved to be convenient and accurate method for real-time measurement of quality parameters, such as for color measurement

(Yam and Papadakis, 2004; Pedreschi et al., 2006) and shrinkage measurement (Fernandez et al., 2005; Martynenko, 2006). The quality changes must be precisely monitored not only for the control of product quality but also for the assessment of drying process for optimization. The successful application of this technique for color measurement for the varieties of foods has been reported in the last decade (Rafiq et al., 2013).

In this study product color change was selected to assess the spatial uniform quality drying in the developed dryer. Spatial drying homogeneity has been shown for the developed diagonal-airflow batch dryer (Amjad et al., 2015b). The objective of this part of the study was to assess the drying process non-invasively for quality homogeneity in response of uniform air distribution throughout the drying chamber. A spatial variation of color parameter was selected as criteria to assess the uniform quality drying.

4.2 Materials and methods

4.2.1 Diagonal- dryer

Same dryer as discussed in previous chapter was used to perform the experiments for the assessment of spatial quality homogeneity in response of uniform air distribution. The detailed functional description of the dryer can be found in chapter 3.

4.2.2 Data acquisition

For real-time image acquisition system, a wooden box named as imaging-box was made of cross sectional area equal to a food bucket's area (0.6m×0.4m), holding a USB CMOS Color Autofocus Camera (DFK 72AUC02-F) which was connected to the computer (Lenovo T500, 2.40 GHz, 3 GB RAM, 148 GB hard disk).

For lightening, eight florescent led bulbs were used for uniform lighting conditions to get sharp contrast at the border of the image by avoiding glitter. The angle between the camera lens axis and the light source axis was 45^{o} for capturing the diffuse reflection responsible for the color (Fernandez et al., 2005). The height of the box was fixed according to the required distance (42cm) between the camera lens and the food sample for quality image with high contrast and pixel resolution. In order to avoid the light and reflection from the room, the inner walls of the imaging box were painted black. The roof/top of the drying chamber was cut at the position of first bucket and the imaging-box was placed over it. An

acrylic sheet was put at the bottom of box to prevent the air to flow into the box as shown in the Figure 4.1. This was repeated throughout the dryer length for all twenty five buckets to acquire data at all places of the drying chamber. As the imaging-box moved to the next place (2nd bucket), the place of the previous bucket (cut part of dryer roof) was covered with a piece of glass sheet with side insulation with king-span air cell tape.

For on-line weight loss measurement, a load cell (KD60±50N of accuracy 0.1%) was sandwiched in two trays such a way that it was mounted on the lower tray and was mechanically connected to the upper moveable tray (holding food samples). Four thermocouples (K-type ± 1.5k) with long probes (10mm diameter) were inserted through the box up to the food tray. Thermocouples and load cell were connected to a data logger (Agilent 34970A) as can be seen in Figure 4.1.

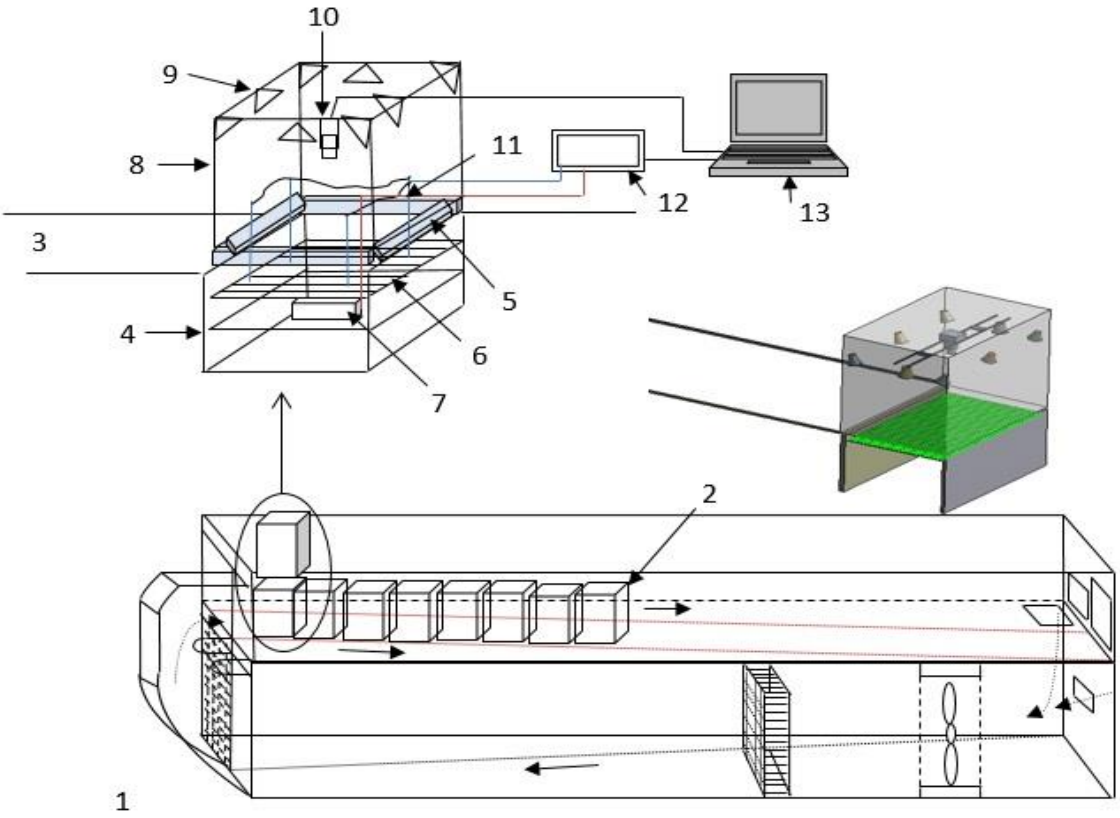

Figure 4.1: Online data monitoring set up. (1)Diagonal-batch dryer (2) diagonally arranged buckets (3) Dryer's roof (4) Food bucket (5) Acrylic sheet (6) Food tray (7) Load cell (8) Imaging box (9) LED lights (10) CMOS camera (11) Thermocouples (12) Data logger (13) Computer

4.2.3 Raw material and drying experiments

Potatoes (variety: Anuschka) were acquired from the university agricultural farm. Potatoes were washed, peeled and sliced of thickness 5mm with an electric slicing machine (Bosch MAS62 slicer, 110 watt, 120 rpm). After that slices were blanched in boiled water for three minutes to inhibit enzymatic reactions. The free water on the surface of blanched potatoes was dried up with clean cloth before loading into the food bucket tray (69.44% perforation). The tray (mechanically connected to the load cell) was loaded with a single layer of half kilogram potato slices. Experiments were conducted at 60^{o}C and potato slices were dried up to 12% of final moisture contents. Images of the potato slices were captured continuously by imaging-box system at an interval of five minutes at their maximum resolution (2048×1536 pixels) as shown in figure 4.2. The digital data was acquired using IC Capture 2.4 software and directly transferred to the connected PC in TIFF format via USB interface. The weight change of the samples was measured continuously after every five minutes.

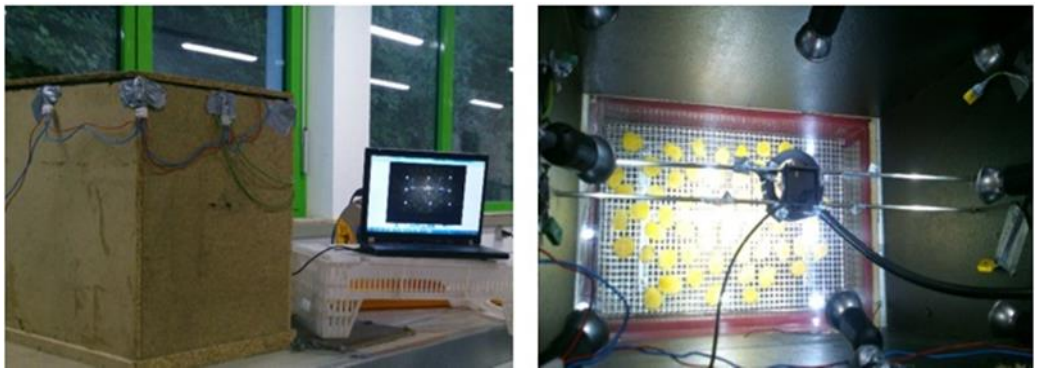

Figure 4.2: Imaging-box made for data acquisition

4.2.4 Image analysis and color feature extraction

The sensitivity of camera sensors and lightning, effect the RGB color measurement (Leon et al, 2006). The effectiveness of image processing mainly depends on computer technology and mathematical algorithms to extract the data from the images and several steps are involved in it such as (a) pre-processing the acquired images (2) segmentation of the images to separate objects from the background (3) conversion of RGB images of the separated objects into L^*, a^*, and b^* color space. In order to accomplish these steps for easier and fast color determination, a computer program was developed in Matlab code. The followed steps for this process are described below.

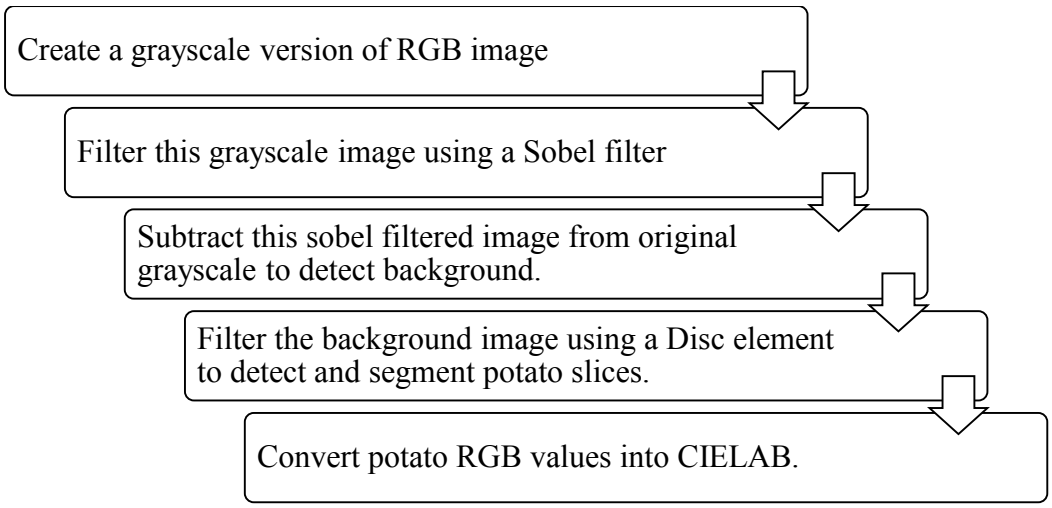

1.Starting image

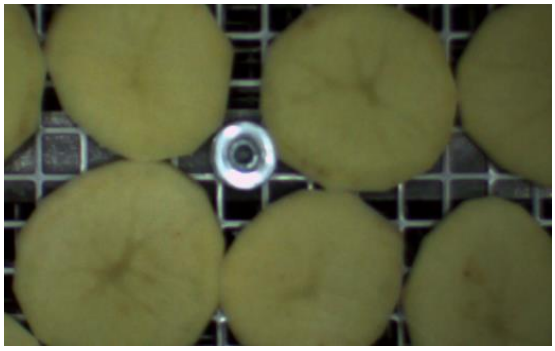

2. Grayscale image

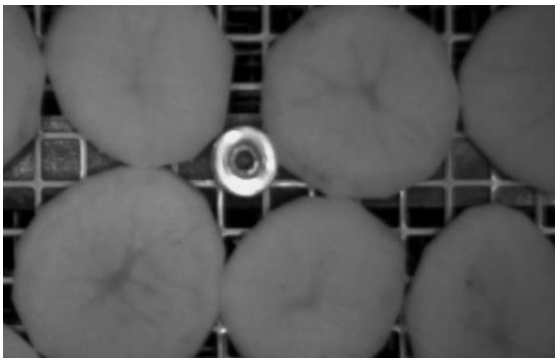

3. Sobel filtered image

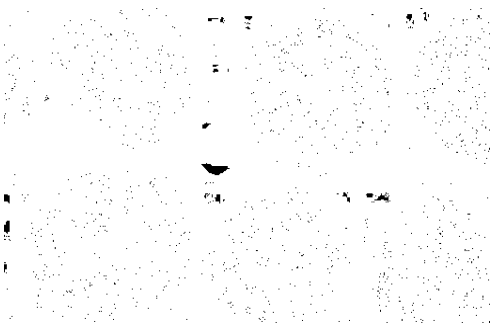

4. Result of subtracting Sobel filtered image from Grayscale image to allow detecting of potatoes

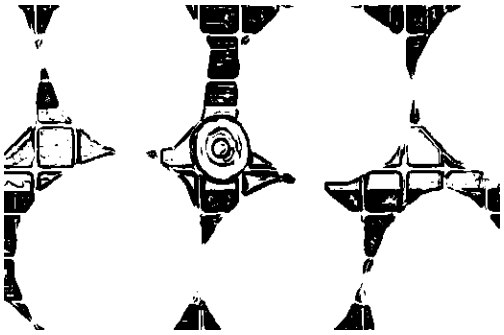

5. Result of disc shaped structuring element filter to detect potatoes

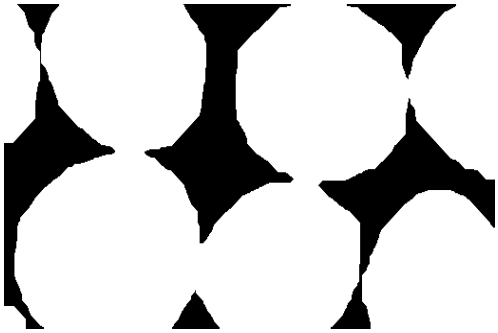

CIE L^*, a^*, b^* color space is used in food research studies as it provides consistent colour (Yam & Papadakis, 2004). The mean values of the extracted colors were expressed in *CIELAB* colors space system as L^* (lightness/darkness), a^* (redness/greenness) and b^* (yellowness/blueness). The ratios of L^*, a^*, and b^* to the corresponding initial values were calculated to normalize these color parameters for reducing the heterogeneity between different raw samples (Niamnuy et al., 2008). These color retention ratios were considered as color feathers and measured for each position (each bucket) of the drying chamber. Sahin and Sumnu (2006) reported the increased use of the total color difference (ΔE) for the determination of color changes in the food products. It was calculated using equation 1 for the determination of food quality changes (Sturm et al., 2014).

$$\Delta E = [(L_0^* - L^*)^2 + (a_0^* - a^*)^2 + (b_0^* - b^*)^2]^{0.5} \quad 1$$

4.2.5 Kinetic modelling

Kinetic modelling is necessary to derive basic kinetic information of a particular food during its processing. For the kinetics of color changes of food materials, the use of zero-order or

first-order kinetics models has been reported by many researchers (Mujumdar, 2000; Sturm et al., 2014). So, the following equations were used for the mathematical modelling for the color changes of potato slices during the convective drying process.

$$C = C_o \pm k_o t \qquad 2$$

$$C = C_o exp(\pm k_1 t) \qquad 3$$

where C is the measured value of color variables (L^*,a^*,b^*) at time t during drying, C_o is the initial value of color variables at the start of drying process, t is the drying time, k_o is the zero-order kinetic constant and k_1 is the first-order kinetic constant. The positive and negative signs indicate formation and degradation of quality parameter respectively.

4.3 Results and discussion

Figure 4.3 shows the drying trend throughout the drying chamber. The span of moisture

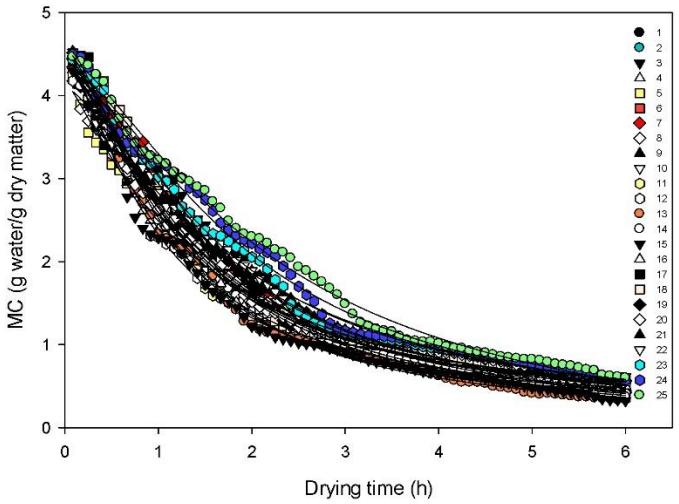

Figure 4.3: Drying curves for all food buckets showing drying uniformity in the drying chamber.

contents among the food buckets at various places of the drying chamber in different intervals of drying time was observed low especially as drying proceeded towards its falling rate. It was also shown in chapter 3 but with destructive approach. Non-destructively measured rate of drying also showed drying uniformity among the food buckets.

4.3.1 Color kinetics

The kinetics of color changes during convective air drying of potato slices have been presented in the form of respective color retention ratios.

4.3.1.1 Lightness retention ratio (L^*/L_0^*)

The L^* represents the light reflecting capacity of the food samples. Figure 4.4 shows the changes in luminosity (L^*) with the change in product moisture contents during the drying process.

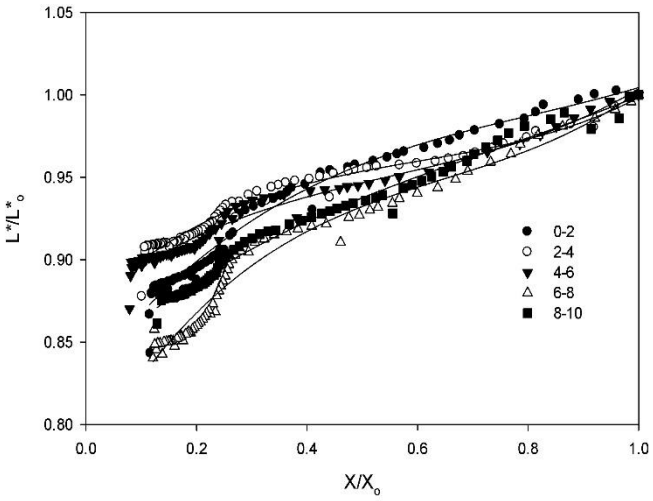

Figure 4.4: Lightness retention ratios vs dimensionless moisture content at five sections of the drying chamber. Each section covered two meter distance of the drying chamber.

It can be clearly observed that the lightness retention ratio (L^*/L_0^*) decreased with the decreasing of moisture content for all the sections of the drying chamber. This change in the brightness of dried potato slices can be taken as a measurement of browning (Lozano and Ibarz, 1997; Lee and Coates, 1999; Avila et al., 1999), which reduced at an average value of lightness ratio from 1-0.84, 1-0.88, 0.99-0.87, 1-0.84 and 1-0.86 for sections 1-5 respectively along with the entire length of the drying chamber. It means that potato slices tended to get little darker as drying proceed and resulted to increase color difference (ΔE). The rate of decrease in lightness retention ratio was observed smooth until X/X_0 = 0.4 and after that product trend to be darker became fast. The blanching treatment during sample preparation inactivated the most of enzymes, so decreasing of L^* could be attributed to the non-enzymatic browning and brown pigment formation (Krokida et al., 1998). It might also be related to an

increase in samples opacity resulting from structural shrinkage due to the moisture evaporation (Contreras et al., 2008). Pedreschi et al. (2007) reported that the luminosity of potato slices decreases more with increase in product temperature. The declining trends in lightness of potato slices at all sections of the drying chamber were found similar which ascertain the fact of uniform temperature availability throughout the drying chamber. It could be related to uniform air distribution within the drying chamber as temperature distribution is associated with airflow in the drying chamber.

4.3.1.2 Redness retention ratio (a^*/a_0^*)

Figure 4.5 shows the relationship between redness retention ratio (a^*/a_0^*) and dimensionless moisture content of the potato slices during drying. The chromatic parameter (a^*) of potato slices increased during the drying process due to non-enzymatic browning reactions.

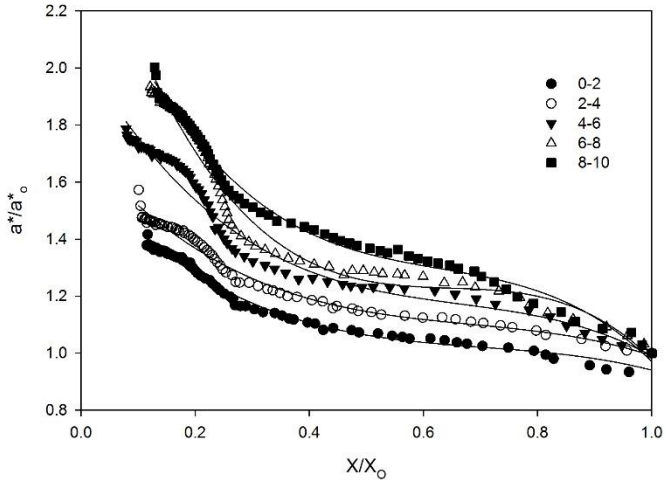

Figure 4.5: Redness retention ratios vs dimensionless moisture content at five sections of the drying chamber.

It is noteworthy that variety of potato used for drying will have a strong effect on color change. There was continues increase in a^*/a_0^* with the reducing moisture content for all sections of the drying chamber. As drying proceeded, the higher product temperature increased the Millard browning reactions (Chua et al., 2002) which resulted in the increment of dried product redness. The results are coincident with those reported by other researchers for potato slices of other varieties like Panda, Saturna and Bintje (Pedreschi et al., 2006; Segnini et al., 1999). The average low initial value of chromatic parameter (a^*) for samples indicated greenness, and increased at the end of the drying process lead to redness. This trend

was observed for all sections of the drying chamber. As a consequence of uniformity in the drying rate due to uniform temperature availability, food products at different positions of the drying chamber showed almost similar changes with maximum difference of 0.3 among values of a^*/a_0^* for all sections.

4.3.1.3 Yellowness retention ratio (b^*/b_0^*)

Figure 4.6 manifests the rate of change in color parameter (b^*/b_0^*) with the dimensionless moisture ratio (X/X0) for different sections of the drying chamber. During the decline of moisture ratio from 1 to 0.3, the yellowness colour retention ratio (b^*/b_0^*) decreased from 1 to an average value of 0.97 for all sections of the drying chamber. This change rate increased at X/X0 <0.3. It could be due the Millard reactions and browning formations led towards the decline of yellowish regions in samples. Therefore, the yellowness of potato slices slightly decreased during the drying process.

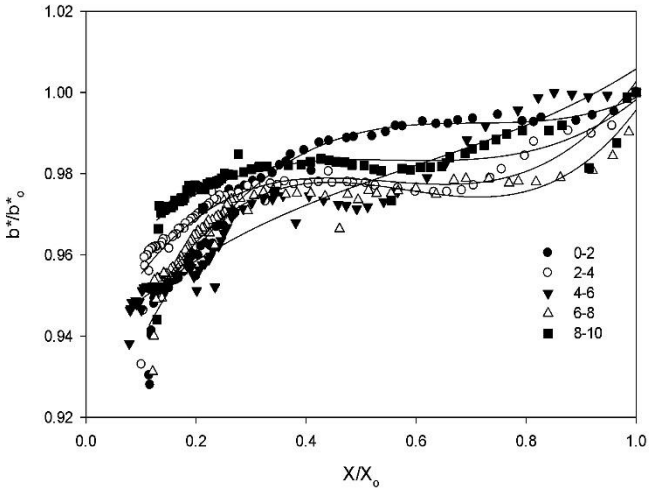

Figure 4.6: Yellowness retention ratios vs dimensionless moisture content at five sections of the drying chamber.

4.3.1.4 Total color difference (ΔE)

The overall color changes in the potato slices were followed by total color difference (ΔE), because this color parameter showed notorious changes during the drying process. Figure 4.7 illustrates the overall color variation for each section of the dryer against the drying time (4.7a) and dimensionless moisture ratio (4.7b). It is obvious from the figures that the ΔE increased with the drying time (decreasing of moisture content) as a result of surface non-

enzymatic browning reactions. It could be observed that the rate of change for all the color parameters (L^*,a^*,b^*) was almost uniform up to moisture ratio of value 0.3 and it became high as drying process forwarded to the end. It showed that potato slices tended to get darker with drying time as indicating by the progressive increase of total color difference. Specifically, this trend can be noticed similar for all sections of the drying chamber, giving the assertiveness to the hypothesis of uniform air distribution in the dryer.

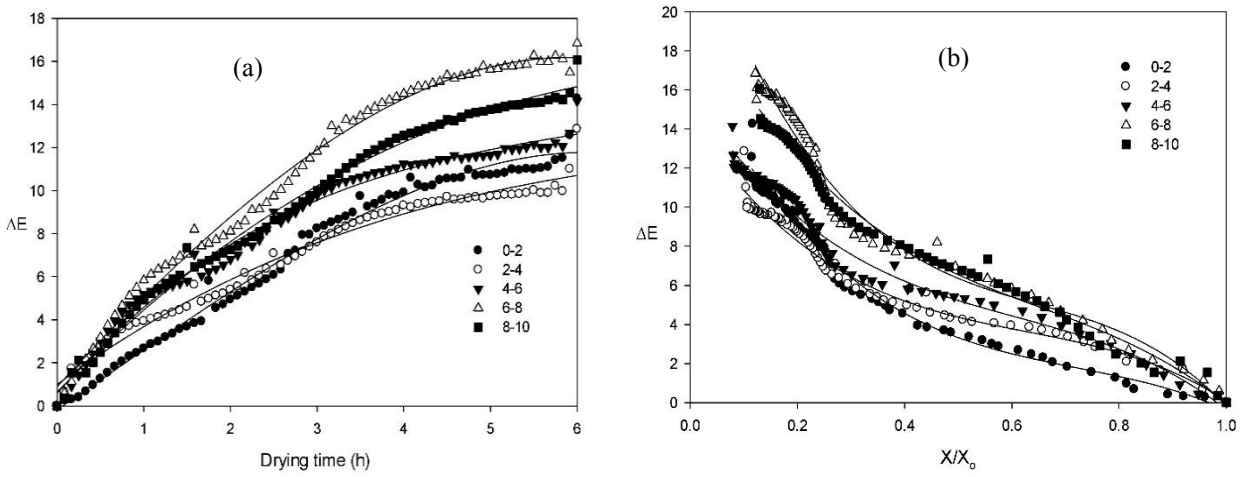

Figure 4.7: Total color difference vs drying time (a) and dimensionless moisture content (b) at five sections of the drying chamber.

At the end of drying process, ΔE varied in the range of 13-17 among the five sections of the dryer. The color calibration performed for a single bucket was taken as reference value for all other buckets to extract the data from the acquired images. Slight disturbance in light distribution was also expected as the imaging box was shifted to the next position after each experiment. So such slight variation in the results could be due to the actual variations in the lightness of respective positions when imaging box was shifted. Although white plate images were taken before the start of each experiment (i.e. for each bucket) and no significant difference was found for the distribution of light. Second reason could be the data representation using single tray of each bucket rather from four trays for true average. The average data for color change from all the trays would reduce the difference.

Non-linear regression analysis was performed and polynomial cubic model was found best fitted to all parameters with high values of coefficient of determinant (R^2) and lower values of standard error of estimate (SEE) using Sigma-plot 12.3 as shown in Table 4.1. These parameter values of curve fitting for each section is actually representing the values for

five buckets. It is clear from the values of standard error of estimate for all the measured (L^*, a^* and b^*) and calculated (ΔE) color parameters for all sections that these observations are very close to the model fitted line of correspondent color parameter. So, the model with the smallest standard error of estimate was the best fit for the sample.

Table 4.1: Results for the fitting of all parameters investigated

Parameter	Section	yo	a	b	c	R^2	SEE
L^*/L_0^*	0-2	0.7775	0.5831	-0.736	0.3776	0.9761	0.0071
	2-4	0.8365	0.2963	-0.2439	0.1104	0.9852	0.0047
	4-6	0.8725	0.2676	-0.3403	0.2039	0.9719	0.0049
	6-8	0.8287	0.4303	-0.4323	0.1778	0.9766	0.0063
	8-10	0.8708	0.3271	-0.4458	0.2463	0.9708	0.0045
a^*/a_0^*	0-2	1.9171	-3.8966	6.0701	-3.1638	0.9827	0.0235
	2-4	2.6368	-6.4056	9.81	-5.061	0.9746	0.0462
	4-6	2.055	-3.4527	4.7983	-2.4098	0.9717	0.0405
	6-8	1.7225	-2.3416	3.1441	-1.5335	0.9837	0.0199
	8-10	1.4973	-2.6409	4.3632	-2.2397	0.969	0.0163
b^*/b_0^*	0-2	0.9082	0.3554	-0.5011	0.2363	0.9695	0.0033
	2-4	0.9332	0.2691	-0.5132	0.3136	0.8835	0.0036
	4-6	0.9369	0.1345	-0.1485	0.0829	0.9503	0.0036
	6-8	0.9142	0.361	-0.658	0.3785	0.8982	0.0038
	8-10	0.9505	0.1786	-0.3205	0.1895	0.7167	0.0041
ΔE vs X/X_o	0-2	17.2694	-53.3176	66.0344	-30.3662	0.9842	0.4871
	2-4	14.4269	-40.9804	56.8272	-30.2032	0.9783	0.4331
	4-6	15.8243	-41.4389	55.6911	-30.4416	0.9778	0.5304
	6-8	25.2353	-78.2122	109.0213	-56.2342	0.9769	0.7626
	8-10	20.8228	-53.0769	65.8531	-33.6718	0.9886	0.4608
ΔE vs Drying time	0-2	-0.169	2.7292	0.0633	-0.0311	0.9838	0.4926
	2-4	0.9947	2.9689	-0.2907	0.0109	0.9778	0.4377
	4-6	0.5715	4.6179	-0.6467	0.0353	0.9856	0.4281
	6-8	0.8976	4.3459	-0.1533	-0.0244	0.9915	0.4497
	8-10	0.6459	4.1372	-0.3356	0.0067	0.9925	0.3745

4.3.2 Color modelling

It was observed that L^* and b^* values were best fitted to the first-order kinetic model with high R^2 value while the values of a^* and total color difference (ΔE) followed a zero-order kinetic model. The results are in agreement with the several studies which have reported that the first-order kinetic model was better for L^* and b^* values of double-concentrated tomato paste (Barreiro et al. 1997), kiwifruits (Maskan, 2001), pineapple (Chutintrasri and Noomhorn, 2007) and peach puree (Avila et al., 1999) and zero-order kinetic model was better for a^* and total color change (ΔE) values of kiwifruits (Maskan, 2001), pineapple (Chutintrasri and Noomhorn, 2007). The estimated kinetic parameters of these models and

the statistical values of coefficients of determination R^2 are represented in Table 4.2 for all the sections of drying chamber.

Table 4.2: The estimated kinetic parameters and the statistical values of zero-order and first-order kinetics models for L^*, a^*, b^* and total-color difference (ΔE) at five sections along the length of drying chamber.

Drying Temperature (°C)	**Parameters**	**Section**	**Zero Order Model**			**First Order Model**		
			k_o (1/hr)	**C_o**	**R^2**	**k_1(1/hr)**	**C_o**	**R^2**
60	*L** (Lightness-darkness)	0-2	-3.5380	83.2110	0.9727	-0.0447	83.3000	0.9752
		2-4	-2.2202	82.2291	0.9659	-0.0277	82.2512	0.9665
		4-6	-2.9526	84.2960	0.9595	-0.0362	84.3323	0.9604
		6-8	-4.4193	84.5551	0.9808	-0.0555	84.6701	0.9908
		8-10	-3.5469	85.4751	0.9808	-0.0435	85.5536	0.9907
	*a** (Redness-greenness)	0-2	1.6585	12.9230	0.9826	0.1117	13.0358	0.9748
		2-4	1.6769	12.9780	0.9838	0.1132	13.0802	0.9669
		4-6	2.4099	10.886	0.9829	0.1761	11.1172	0.9758
		6-8	2.2107	10.5910	0.9824	0.1703	10.7984	0.9806
		8-10	2.0231	11.2850	0.9903	0.1575	11.3702	0.9886
	*b** (Yellowness/ blueness)	0-2	-0.3974	37.4660	0.9577	-0.0106	37.4684	0.9669
		2-4	-0.1290	36.2860	0.8317	-0.0035	36.2812	0.8506
		4-6	-0.6742	36.8040	0.9376	-0.0186	36.8074	0.9384
		6-8	-0.1254	35.7480	0.8849	-0.0034	35.7339	0.8961
		8-10	-0.1491	35.3480	0.7885	-0.0042	35.3465	0.8897
	ΔE (Total color difference)	0-2	3.4386	-0.5556	0.9820	1.3174	-0.5880	0.9281
		2-4	2.6373	1.2545	0.9781	0.7205	0.5537	0.9191
		4-6	3.7900	1.0606	0.9834	0.9197	0.4864	0.8563
		6-8	4.8137	0.7298	0.9907	0.9598	0.5901	0.9023
		8-10	3.9316	0.8095	0.9923	0.9518	0.4451	0.8831

The values of kinetic rate constants of both models (zero and first order) for all color parameters are found to be almost similar for all the sections of the drying chamber. This implies that the color formation or degradation was found to be uniform throughout the drying chamber due to uniform temperature distribution because kinetic rate constant depends mainly on drying temperature (Lozano et al; 2000). The color degradation rate increases with high drying temperature due to high energy transferred to the inside of drying material and vice versa. So, uniform distribution of drying temperature is of much importance to get uniform quality dried products throughout the drying chamber.

The values of color parameters presented in Figure 4.4, Table 4.1 and Table 4.2 represent values for different sections of drying chamber. As discussed earlier that each section (2m distance) had five food buckets, so the values of color parameters for a section were the average of those values measured for these five buckets.

4.4 Conclusion

A diagonal-airflow batch dryer developed for spatial drying homogeneity has been evaluated for uniform quality drying. For this, color changes of food material (potato slices, 5mm thick) throughout the drying chamber were measured non-destructively. Results showed that the rate of change of studied quality parameters at all sections of the drying chamber were found similar. This shows that the food product along the entire length of drying chamber dried with almost same rate which ultimately gave dried product of uniform final quality. Non-linear regression analysis showed high value of coefficient of determination for the measured and calculated data of color parameters for each section of the drying chamber.

The spatial uniform distribution of drying temperature enabled this dryer to give dried product of uniform quality at all of its sections. These results ascertain the fact that drying temperature is critical to quality of dried food product during a drying process. Therefore, the spatial uniform distribution of drying temperature is of much importance to reduce the factor of over and under drying and consequently to get product of uniform quality throughout the drying chamber. For this, design of airflow in the drying chamber is the main factor to be considered. Diagonal airflow design gave good temperature distribution which is important in reducing the heterogeneity of quality parameters in the drying chamber.

5 Thermodynamic analysis of the drying process in diagonal-batch dryer

Optimized air distribution is important for the energy consumption in a batch drying process. Energy and exergy analyses for an innovative diagonal-batch dryer were performed using potato slices of 5mm and 8mm thicknesses at 55°C and 65°C. The exergetic efficiency, improvement potential rate (1P) and exergetic factor (*f*) were taken as performance parameters. The main component for improving the system efficiency was found to be the fan-heater combination, possessing low exergy efficiency, high IP and high *f* values. The energy utilization, energy utilization ratio, exergy losses and exergy efficiency varied between 1.82-12.52 kJ/s, 0.04-0.59, 1.3-4.89 kJ/kg and 0.41-0.94, respectively for potato slices. The specific evaporation energy and specific product energy were found to be in the range of 4.78-6.13 MJ/kg and 16.24-20.63 MJ/kg respectively. The outcomes of the analysis will provide insights into the optimization of a batch dryer for the maximum retention of quality parameters and energy saving.

5.1 Introduction

Dehydration is an energy intensive unit operation due to high latent heat of water evaporation and the inherent inefficiency of using hot air as drying medium. Mostly, through-flow or cross-flow type's convective dryers (more than 85% of industrial dryers are convective) are used for the drying of many fruits and vegetables but a common problem of these food dryers is their high use of energy which is an important parameter in the selection of a drying process (Sagar and Suresh Kumar, 2010). Thus, for the industrial batch drying, it is important to reduce the energy consumption along with the quality drying and optimized air distribution plays a vital role for it. In this regard, it is essential to perform an effective thermal analysis of the drying process or system which has designed to provide energy saving and optimum processing conditions (Syahrul et al., 2002). For this purpose, energy analysis, particularly the exergy analysis provide a better understanding of the influence of thermodynamic phenomena on the process, comparison of the importance of different thermodynamic factors, and the determination of the most efficient ways of improving the process under consideration (Sogut et al., 2010).

The above mentioned aspects provide the prima motivation behind performing the thermodynamic analysis of diagonal-batch dryer developed for spatial drying homogeneity.

Energy and exergy analyses are rarely made for food processes. In case of potatoes, only Akpinar et al. (2005) worked on the single layer drying process of potatoes via a convective hot-air cyclone type dryer reported by Aghbashlo et al. (2008). So, this part of the study present energy and exergy analyses of drying process for the developed dryer using potato. This would also provide another way to overcome the problems related to energy and exergy throughout the drying process of potato slices using different drying unit. The objectives of the current study are (1) conducting energy and exergy analyses of single-layer convective drying of potato slices at different drying parameters (drying temperature and sample size) (2) splitting the dryer into components and evaluating the efficiency of the dryer and its components in term of exergetic efficiency, improvement potential rate and exergetic factor (3) comparing the results (energy and exergy analyses) obtained for the system under consideration with that of reported in the literature for hot-air batch drying.

5.2 Materials and methods

5.2.1 Dryer description

The developed diagonal batch dryer was used to conduct drying experiments in order to evaluate its thermal analysis. The description and operational principle of the dryer has been explained in chapter 3.

5.2.2 Experimental procedure

The experiments were carried out using locally available potatoes (variety: Anuschka). Potatoes were washed and sliced of thickness 5mm and 8mm using a slicer machine Alexander Solia-M30 SK (1.9 kW). The drying material (150 kg potato slices/experiment) was loaded in 25 buckets; each of them had five trays at successive interval of 0.058 m. The area of each tray was 0.206 m^2 and trays were loaded with a single layer of potato slices at a loading density of 5.82 kg/m^2. It was the maximum value of loading density for this dryer to avoid the possibility of slice overlapping. Experiments were conducted at drying temperatures of 55^oC and 65^oC. The rate of air flow in the drying chamber (within all the food buckets) was uniform and constant (avg. 1.5m/s). The variance in slice thickness and drying air temperature were based on the fact that these parameters significantly affect the drying process. Normally, the drying temperature is set in the range of 50^oC-80^oC for

convective drying of potatoes. So, two different temperatures with difference of 10°C were used to assess their effects on energy and exergy profiles. Temperatures of drying air at different points (inlet air, outlet air, ambient air, mixed air) were measured using thermocouples (K-type ± 1.5 k), connected to a data logger (Agilent 34970A, Malaysia). Mini data logger (MSR-145 ± 2%, Swiss) was used both at inlet and outlet positions of the drying chamber to measure the change in relative humidity. Potato slices were dried from an initial moisture content of 80% to the final moisture content of 12% and an electronic balance (BIZERBA-Sartorius, ±0.1g) was used for weighing of dried material in each bucket at the end of the drying process. The electric energy consumption (E) was quantified by a kWh-meter (ABB cewe) installed on the electric supply and its values were used to calculate specific evaporation energy (SEE) and specific production energy (SPE) using the following equations.

$$\text{SEE} = \frac{E_t}{M_{ew}} \tag{1}$$

Where E_t is the total energy supplied to the dryer in the form of electric energy and M_{ew} is the mass of water evaporated from the product.

$$\text{SPE} = \frac{E_t}{M_p} \tag{2}$$

Where M_p is the final mass of dried product.

5.2.3 Experimental uncertainty

Errors and uncertainties are inherent in both the instruments used and the measurements made during an experiment. Such errors can arise from the instrument selection, instrument calibration, observation and reading (Akpinar et al., 2005). Therefore, a detailed uncertainty analysis was performed for the experimental measurements of the parameters and total uncertainties of the calculated values are listed in Table 5.1. Considering the dimensionless relative error in the individual factors denoted by *xn*, the process of error estimation was done using the following equation (Holman, 2001).

$$U = [(x_1)^2 + (x_2)^2 + \ldots\ldots + (x_n)^2]^{1/2} \tag{3}$$

Table 5.1: Uncertainties of the experimental measurements and total uncertainties for the calculated values

Parameter	Unit	Comment
Experimental measurements		
Heater inlet temperature	°C	±0.270
Heater outlet temperature	°C	±0.230
Drying chamber inlet temperature	°C	±0.254
Drying chamber outlet temperature	°C	±0.301
Relative humidity of air	%	±0.2
Ambient temperature	°C	±0.472
Predicted/calculated values		
Total uncertainty for energy inflow	kJ/s	±0.435%
Total uncertainty for energy utilization	kJ/s	±0.798%
Total uncertainty for exergy inflow	kJ/s	±1.186%
Total uncertainty for exergy outflow	kJ/s	±2.831%
Total uncertainty for exergy loss	kJ/s	±1.247%

5.3 Analysis

For the energy and mass balance analysis, a schematic diagram of the drying chamber is shown in Figure 5.1. Heating and humidification of the drying air occurred throughout the drying process. These processes can be modelled and analysed by applying the principles of conservation of mass and energy (Midilli and Kucuk, 2003).

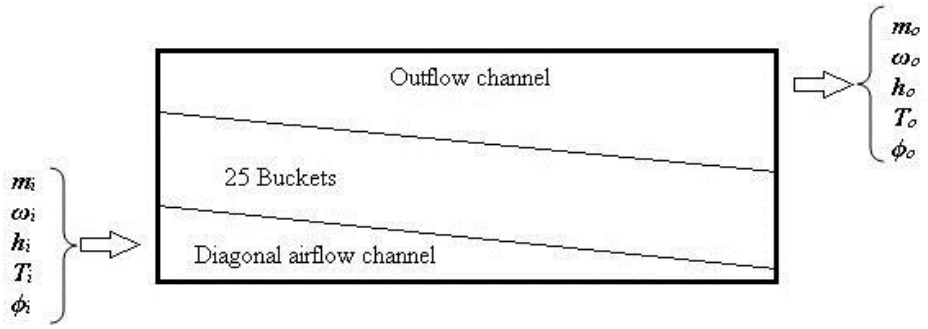

Figure 5.1: Schematic illustration of the drying chamber for energy balance

Conservation of mass for dry air

$$\sum m_i = \sum m_o \tag{4}$$

Where the subscripts *i* and *o* stand for positions at inlet and outlet respectively.

Conservation of mass for water vapors

$$\sum(m_{iw} + m_{ew}) = \sum m_{ow} \quad (5)$$

Where the subscripts *iw* , *ew* and *ow* stand for the amounts of the moisture coming with the inlet air, the evaporated moisture added to the air and the moisture leaving the outflow air respectively.

The general equation for conservation of energy can be written as (Prommas et al., 2010).

$$\mathrm{Q_{net}} - \mathrm{W} = \sum m_o \left(h_o + \frac{V_o^2}{2}\right) - \sum m_i \left(h_i + \frac{V_i^2}{2}\right)$$

It can be expressed as,

$$\mathrm{Q_{net}} - \mathrm{W} = \sum m_o \left(h_o - h_i + \frac{V_o^2 + V_i^2}{2}\right) \quad (6)$$

5.3.1 Description of the air conditions in the dryer

Figure 5.2 shows a schematic diagram of the dryer for the thermal analysis of the drying process. The analysis was divided into two phases, heating and humidification of the drying air.

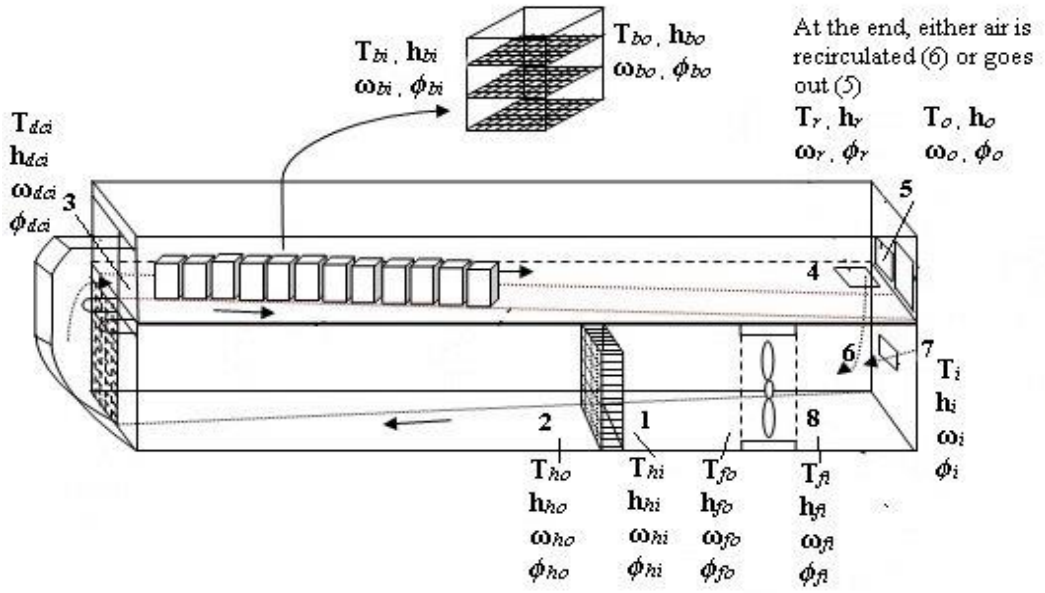

Figure 5.2: Schematic diagram of the dryer showing air conditions at its various positions. (1) Total inlet air (air added by fan + mixed air) (2) Heated air from heat exchanger (3) Inlet air

entering into the drying chamber i.e. Heated air, (4) Outflow air, (5) Outlet air i.e. exhaust air, (6) Recycled air (7) Inlet ambient air, (8) Mixed air (recycled and ambient air).

Inlet and outlet conditions of heater:

Starting from point 1, it is assumed that there is no loss between the fan and the heater so the inlet air conditions for the heater are equal to the outlet air conditions of the fan.

$$\omega_{hi} = \omega_{fo}\ ,\ T_{hi} = T_{fo}\ ,\ h_{hi} = h_{fo},\ \phi_{hi} = \phi_{fo} \quad (7)$$

Where the subscripts *hi* and *fo* define the heater inlet and fan outlet respectively.

The amount of heat transferred to the drying air by the heater can be calculated using the air temperature measured at the inlet and the outlet of the heater as,

$$Q_{1-2} = mc_p(T_2 - T_1) \quad (8)$$

Inlet conditions of the drying chamber:

The air conditions at the inlet (point 3) of the drying chamber are the same as at the outlet of the heater.

$$\omega_{dci} = \omega_{ho}\ ,\ T_{dci} = T_{ho}\ ,\ h_{dci} = h_{ho},\ \phi_{dci} = \phi_{ho} \quad (9)$$

Where the subscripts *dci* and *ho* define the drying chamber inlet and the heater outlet respectively.

Experimental measurements showed identical values for temperatures at the heater outlet and at the drying chamber inlet, indicating that there was no loss of energy from the heater to the inlet point (due to insulation of the dyer walls with polyurethane foam). So the temperatures at points 2 and 3 were equal. The heat available at the drying chamber inlet can be calculated as,

$$Q_{heat\ available} = mc_p(T_3 - T_1) \quad (10)$$

Outlet conditions of the drying chamber:

Air conditions at the outlet of the dryer depend on the amount of heat used in the drying chamber. Energy is used to increase the food temperature and to evaporate the moisture but the former has less effect in the calculations of energy utilization. The inlet air condition for

each food bucket was same as at the inlet of the drying chamber (point 3) due to the diagonal airflow channel as shown in Figure 5.3, illustrating the air conditions across the food buckets.

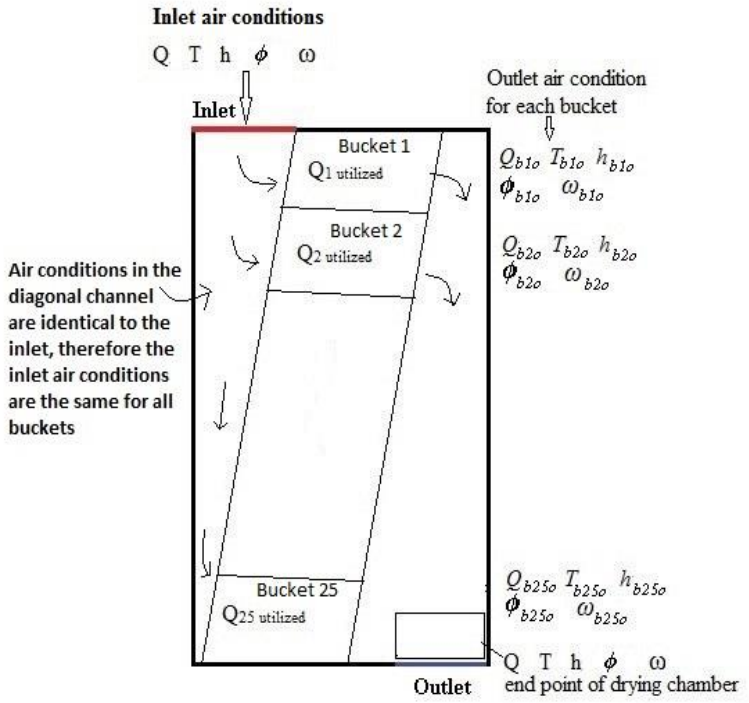

Figure 5.3: Symbolized air conditions in the drying chamber across the food buckets

It is assumed that the air velocity (avg.1.5m/s) is uniform through all the food buckets leading to the possibility of uniform moisture removal. This consideration can be justified through the numerical and experimental results of airflow through the drying chamber (Amjad et al., 2015b). Therefore, the inlet conditions of the buckets were assumed as equal to that of the drying chamber and can be written as,

$$T_{dci}, h_{dci}, \phi_{dci}, \omega_{dci} = T_{b1_{in}}, h_{b1_{in}}, \phi_{b1_{in}}, \omega_{b1_{in}} = T_{b2_{in}}, h_{b2_{in}}, \phi_{b2_{in}}, \omega_{b2_{in}} = \cdots$$
$$T_{b25_{in}}, h_{b25_{in}}, \phi_{b25_{in}}, \omega_{b25_{in}} \quad (11)$$

Where the subscript "*b*" stands for bucket and the numeric values "*1,2*....25" indicate the bucket's number while "*in*" indicates the inlet side of a bucket.

5.3.2 Conservation of the mass

5.3.2.1 During heating

The energy of the air increased as it passed through the heat exchanger. Increase of dry bulb temperature decreased the relative humidity of the air. Assuming steady state conditions and taking a control volume of the heat exchanger, the mass balance for the air can be written as,

$$m_1 = m_2 \tag{12}$$

According to equation 9, the humidity of the heated air at point 3 is the same as at point 2.

$$\omega_2 = \omega_3 \tag{13}$$

5.3.2.2 During humidification

The amount of the moisture at the outlet of the drying chamber (at point 4 in Figure 5.2) is the sum of moisture that was already present in the inlet air (negligible amount) and the moisture taken from the moist food in all the food buckets. This can be expressed as,

$$m_4\omega_4 = m_3\omega_3 + m_b\omega_b \tag{14}$$

The subscript "*b*" stands for bucket (25 in total).

Equation 14 can be applied to each bucket separately. The amount of moisture at the outlet of a bucket is equal to the amount of the moisture coming with inlet air for that bucket and the evaporated moisture added to the air as it passed through that bucket. So the moisture balance equation for each food bucket can be written as,

$$\begin{aligned} &m_{b1_{in}}.\omega_{b1_{in}} + m_{b1_{inside}}.\omega_{b1_{ev}} = m_{b1_o}.\omega_{b1_o} \\ &m_{b2_{in}}.\omega_{b2_{in}} + m_{b2_{inside}}.\omega_{b2_{ev}} = m_{b2_o}.\omega_{b2_o} \\ &\vdots \\ &m_{b25_{in}}.\omega_{b25_{in}} + m_{b25_{inside}}.\omega_{b25_{ev}} = m_{b25_o}.\omega_{b25_o} \end{aligned} \tag{15}$$

Where the subscripts *b*, *in, ev, o* and numeric values *(1, 2…n)* stand for bucket, the inlet of the bucket, evaporation, the outlet of the bucket and the bucket's number respectively.

From the equations 14 and 15, the total amount of moisture at the outlet of the drying chamber (point 4 in Figure 5.2) can be written as.

$$m_4\omega_4 = m_3\omega_3 + m_b\omega_{ev} = \sum_{i=1}^{25} m_{b_o}\omega_{b_o} \tag{16}$$

5.3.3 Conservation of energy

5.3.3.1 During heating:

An energy balance equation for the control volume of the heating unit can be written as,

$$Q_{1-2}\ or\ Q_{net\ availble} = m_2 h_2 - m_1 h_1 \quad (17)$$

The subscripts *1, 2* indicate the positions of the dryer illustrated in Figure 5.2.

The change in enthalpy both for air and water is associated with the temperature difference and each can be given by $c_p \Delta T$. This heat transfer is referred as sensible heat. So the energy balance during the heating process can also be represented as,

$$Q_{1-2} = mc_p(T_2 - T_1) \quad (18)$$

This is the available energy in the heated air as discussed earlier in equation 10.

5.3.3.2 During humidification

Saturated air conditions at the outlet of a dryer depend on several factors i.e. dryer insulation, convective heat transfer of the product, initial moisture contents, temperature of the drying air and density of the product. Practically, it is not possible to grab the potential of the heated air at full extent due to the sorption of the product. It means that a part of heat energy which remained unused is wasted along with the exhaust air or it is recirculated and can be written as,

$$Q_{wasted/recirculated}(m_4 h_4) = \mathrm{Q_{net\ available}} - \mathrm{Q_{Energy\ utilized}} \quad (19)$$

The amount of unused energy at the outlet of a bucket is the difference between the available inlet energy and the energy used for that bucket. So the energy balance equation for each food bucket can be written as,

$$\begin{aligned} &m_{b1_{in}}.h_{b1_{in}} - m_{b1_{inside}}.h_{b1_{ev}} = m_{b1_o}.h_{b1_o} \\ &m_{b2_{in}}.h_{b2_{in}} - m_{b2_{inside}}.h_{b2_{ev}} = m_{b2_o}.h_{b2_o} \\ &\vdots \\ &m_{b25_{in}}.h_{b25_{in}} - m_{b25_{inside}}.h_{b25_{ev}} = m_{b25_o}.h_{b25_o} \end{aligned} \quad (20)$$

Where the subscripts *b*, *in, ev, o and* numeric values *(1, 2…n)* stand for bucket, the inlet of the bucket, evaporation, the outlet of the bucket and the bucket's number respectively.

From equations 19 and 20, the total amount of air energy at the outlet of the dryer (point 4 in Figure 5.2) can be written as.

$$m_4 h_4 = \sum_{i=1}^{25} m_{b_o} h_{b_o} \quad (21)$$

Following the same principle as for equation 18, the heat utilized can be written as,

$$Q_{3-4} = mc_p(T_3 - T_4) \quad (22)$$

So the energy utilization ratio (EUR) of the drying chamber can be calculated using the following equation (Mujumdar, 1995).

$$EUR = \frac{heat\ utilized}{heat\ supplied} = \frac{(C_{pi}T_i - C_{po}T_o)}{(C_{pi}T_i - C_{pa}T_a)} \quad (23)$$

Where c_p, *T,* and subscripts *in, a,* and *o* stand for specific heat of air, temperature, inlet, ambient and outlet respectively.

5.3.4 Exergy analysis

The exergy based performance evaluation and subsequent optimization of food dryers have been growing interest (among the researchers) in recent years (Aghbashlo et al., 2013). Exergy analysis uses the conservation of mass and energy principles together with the second law of thermodynamics for the goals of design, assessment, optimization and improvement of energy systems. It can be applied on both system and component level. The total exergy of inflow, outflow and losses were determined by using the general form of the applicable exergy equation (Akpinar et al., 2005-2006; Aghbashlo et al., 2008).

$$\text{Exergy} = c_{pda}\left[(T - T_a) - T_a \ln \frac{T}{T_a}\right] \quad (24)$$

The subscript '*a'* denotes the reference conditions i.e. ambient condition.

Depending on the inlet and outlet temperatures of the drying chamber, the specific exergy inflow and outflow can be determined using the above expression for the exergy analysis of the product used as drying material.

5.3.4.1 During heating

The exergy inflow at the drying chamber inlet can be written as,

$$Ex_{dci} = c_{pda}\left[(T_{dci} - T_a) - T_a \ln \frac{T_{dci}}{T_a}\right] \quad (25)$$

Inlet air condition for all the food buckets were same as that of the drying chamber (eq.11), so the value of exergy inflow for each food bucket was considered equal.

5.3.4.2 During humidification

Exergy losses or exergy destruction occur during humidification. Exergy outflow at the outlet of the drying chamber was the summation of exergy outflow from each bucket as were in case of moisture mass flow (eq. 16) and energy flow at the dryer's outlet (eq. 21). The exergy outflow at the drying chamber outlet can be written as

$$Ex_{dco} = c_{pda}\left[(T_{dco} - T_a) - T_a \ln \frac{T_{dco}}{T_a}\right] \quad (26)$$

Hence, from eq. 25 and 26, the exergy loss is determined as,

$$\text{Exergy loss} = \text{Exergy inflow} - \text{Exergy outflow} \quad (27)$$

The exergetic efficiency can be defined as the ratio of exergy outflow to exergy inflow for the chamber as outlined below (Midilli and Kucuk, 2003).

$$\text{Exergetic efficiency } (\eta_{Ex}) = \frac{\text{Exergy inflow} - \text{Exergy loss}}{\text{Exergy inflow}} = 1 - \frac{Ex_L}{Ex_i} \quad (28)$$

For the exergy analysis of the dryer, the system was divided into two main components named as, fan-heater combination (A) and the drying chamber (B) as shown in Figure 5.4.

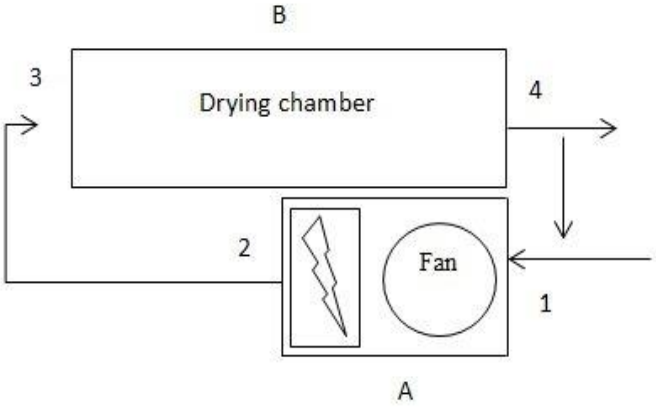

Figure 5.4: A schematic illustration of the dryer components for the exergy analysis

The exergy inflow and outflow for the each component were determined using equation 24. Beside the exergy efficiency, two different parameters were applied to investigate the performance of the dryer (Table 5.2). Van Gool (1997) reported that by decreasing the difference between the total exergy output and total exergy input, the irreversibility for a process can be decreased. Based on this, improvement potential rate was used to deduct the possible improvements in each component along with the whole system (Hammond and Stapleton 2001). Exergetic factor is another performance parameter used in the thermodynamic analysis of a system (Xiang et al., 2004) which shows the relative significance for the inflow exergy of a component on total exergetic inflow to the system. High exergetic factor for a system component means that high amount of exergy is being handled by that component in the system.

Table 5.2: Equations used for the exergy analysis of the system components.

Parameters	Equation	Remark	Equation Nr.
Exergy balance	$\sum E_{Xi} = \sum E_{Xo} + \sum E_{XL}$		(29)
Exergy rate	$E_{Xr} = E_X + m$		(30)
Performance parameters			
Efficiency	$\eta_{Ex} = \frac{E_{Xr2} - E_{Xr1}}{P_{Fan-heater}} \times 100$	For component A shown in Figure 5.4 (Fan-heater)	(31)
	$\eta_{Ex} = \frac{E_{Xr4}}{E_{Xr3}} \times 100$	For component B shown in Figure 5.4 (drying chamber)	(32)
Improvement potential	$\mathrm{IP} = (1 - \eta)(E_{Xi} - E_{Xo})$		(33)
Exergetic factor	$f = \frac{E_{Xi,k}}{E_{Xi,t}} \times 100$		(34)

5.4 Results and discussion

5.4.1 Energy analysis

Figure 5.5 shows the energy utilization as a function of drying time for different drying air temperatures and product thicknesses. The moisture of product is the base for energy utilization and therefore is an important parameter for thermal analysis of a drying process.

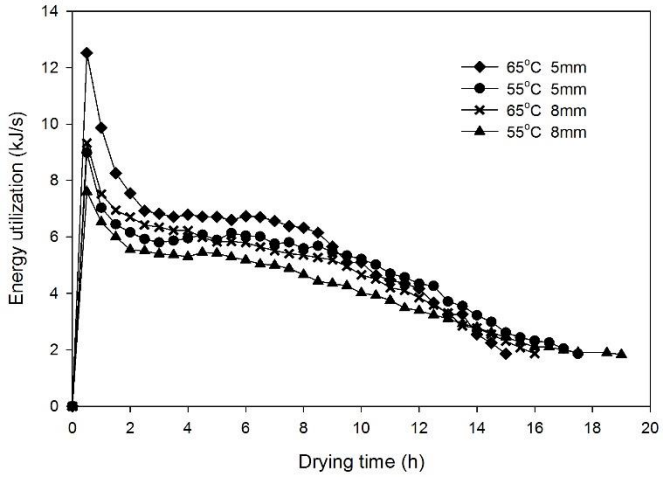

Figure 5.5: Effect of drying air temperatures and slice thicknesses on energy utilization

Due to the same inlet air conditions for all the food buckets (Figure 5.3, eq.11), the entire food product was exposed to the air uniformly, so the remarkable usual fact of under and over drying was reduced (Amjad et al., 2015b), important for the rate of energy utilization.

At constant sample thickness of 5 mm, the rate of energy utilization was higher at 65ºC than at 55ºC during the early stages of the drying process. This was due to the high removal of loosely bounded surface moisture of the food product. This moisture rapidly reduced due to less resistance to heat transfer inside the material. As drying proceeded, the hardened layer imposed a barrier against the dissipation of moisture across the product's surface and caused less removal of moisture, which ultimately decreased the rate of energy utilization (Bakal et al., 2011; Doymaz and Ismail, 2011).

The initial high rate of drying was due to the variation of the product surface temperature, which resulted in a change of convection rate of potato slices (Mohan and Talukdar, 2014). The decrease of drying temperature from 65ºC to 55ºC had increased the drying time by 10% and 18.75% for sample thicknesses of 5mm and 8mm respectively. By increasing the drying temperature at constant sample thickness, the increased rate of energy

utilization varied in the range of 0-39% (Table 5.3). The results are in agreement with several studies stating that increasing the drying air temperature results in an increase rate of drying and energy use for potato, banana and guava (Chua et al., 2000), pumpkin (Kongdej, 2011), tomato (Abano et al., 2011) and quinces (Tzempelikosa et al., 2012).

Table 5.3: Effect of drying parameters on energy analysis of potato

		Energy utilization (kJ/s)			EUR (%)		
		55°C	65°C	Δ (%)	55°C	65°C	Δ (%)
Effect of temperature	5mm	0-8.98	0-12.52	0-39	0-52	0-59	0-13
	8mm	0-7.60	0-9.33	0-22	0-49	0-54	0-10
		Energy utilization (kJ/s)			EUR (%)		
		8mm	5mm	Δ (%)	8mm	5mm	Δ (%)
Effect of thickness	65°C	0-9.33	0-12.52	0-34	0-54	0-59	0-9.25
	55°C	0-7.60	0-8.98	0-18	0-49	0-52	0-6.12

Figure 5.6 shows the calculated results for energy utilization ratio (EUR) and it can be observed that EUR increased as drying temperature increased and sample thickness decreased. This trend was more prevalent at the early stages of the drying process and it gradually reduced. The EUR of the drying chamber decreased with the drying time because of the reduced rate of moisture removal from the product for the same energy input.

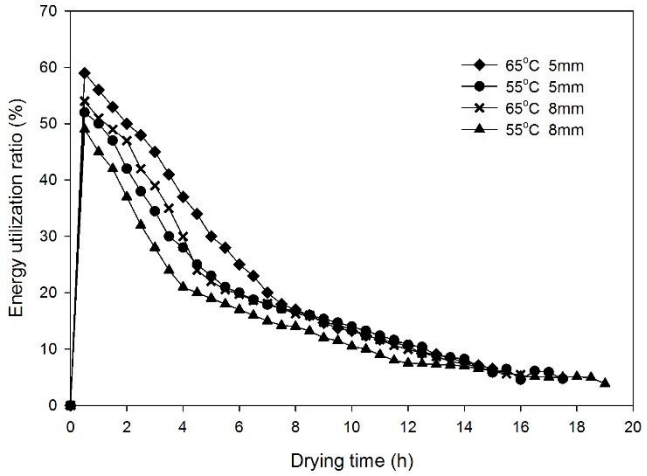

Figure 5.6: Variation of energy utilization ratio as a function of drying time

Potato slice thickness also played a role in energy consumption. Higher thickness caused less energy utilization due to less surface area and thick core of product which caused hindrance in moisture removal. The increase of sample thickness from 5mm to 8mm had prolonged the drying time by 6.67% and 8.57% for drying temperatures of 65°C and 55°C

respectively as shown in Figure 5.5. During the drying process, the increased rate of energy utilization varied in the range of 0-34% and 0-18% when sample thickness was decreased from 8mm to 5mm at 65ºC and 55ºC respectively (Table 5.3). EUR varied between 0-59.83%, 0-54.23%, 0-52.14% and 0-49.41% in the drying chamber for sample thicknesses of 5mm and 8mm at 65ºC, and for sample thicknesses of 5-8 mm at 55ºC respectively (Table 5.3).

Samples of low thickness dried more rapidly due to greater overall moisture transfer from the food product which in turn depended on internal and external resistances to mass transfer (Kumar and Singh, 2011). Primarily, the diffusion process controlled the internal resistance to mass transfer within a sample which was relatively low for 5mm thick samples due to minimum moisture travel path. Similarly, external resistance (depends on surface convective mass transfer) also reduced due to larger exposed surface area per unit mass in case of less sample thickness. Similar effects of product thicknesses on the drying rate were reported in the literature (Rahman and Kumar, 2007 for apple, Kongdej 2011 for pumpkin, Nguyen and Price, 2007 for banana and Fernando et al., 2008 for Papaya and Garlic).

The rate of energy consumption of a product varies due to variation the product geometrical configurations and different operating drying conditions which needs to be optimized with product quality. The energy utilization was high during the initial phase of the drying (Figure 5.5) which resulted due to higher moisture removal. Following moisture reduction, the energy absorbed by the product decreased. The average amount of energy used in the form of electricity to produce one kilogram of dried potato samples (SPE) and to evaporate one kilogram of water (SEE) were calculated to be lower; 16.24MJ/kg and 4.78MJ/kg respectively at high temperature of 65ºC and sample thickness of 5mm as shown in table 5.4.

Table 5.4: Dryer performance characteristics at bulk moisture content of 12% w.b

	5 mm		**8 mm**	
	65ºC	**55ºC**	**65ºC**	**55ºC**
Fresh weight (kg)	150	150	150	150
Dry weight Mp (kg)	34.12	34.25	34.25	34.37
Water removed, Mew (kg)	115.87	115.70	115.75	115.62
Electrical energy (MJ)	554.4	658.8	612	709.2
Energy used for moisture removal (MJ)	278.1	277.8	277.8	277.5
Energy efficiency (%)	50.16	45.39	42.16	39.12
Specific evaporation energy, SEE (MJ/kg)	4.78	5.69	5.28	6.13
Specific production energy, SPE (MJ/kg)	16.24	19.23	17.86	20.63

5.4.2 Exergy analysis

5.4.2.1 Exergy analysis for the product (drying chamber)

Figure 5.7 shows the exergy loss curves for potato slices as influenced by air temperature and slice thickness. The exergy losses decreased with the increase of drying time and it can be explained with the same fact that has been explained earlier for energy utilization. The moisture contents of the slices decreased with drying time and their capacity to absorb and use exergy for evaporation decreased.

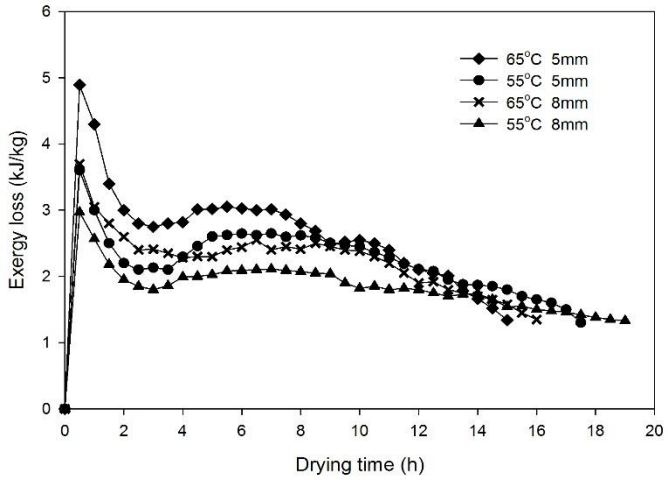

Figure 5.7: Variation of exergy losses as a function of drying time

The maximum and minimum values of exergy losses were found to be 4.89 kJ/kg (at 65°C and 5mm slice thickness) and 1.3 kJ/kg (at 55°C and 8mm slice thickness) respectively. So, exergy losses increased with the increase of drying temperature especially at the beginning of the drying process due to high removal of water. The exergy losses went up with the increase of the energy utilization. Energy utilization and exergy losses were influenced more by drying temperature than sample thickness as can be noticed from the values tabulated in Table 5.3 and Table 5.5 respectively. Similar findings regarding the effect of drying temperature on exergy losses have been reported by Akpinar et al. (2005-2006). Taking into account the effect of slice thickness, it was noticed that exergy losses increased in case of using small sample thickness because of higher contact area between the drying air and samples which increased the heat and mass transfer rate.

Table 5.5: Effect of drying parameters on exergy analysis of potato

		Exergy loss (kJ/kg)			Exergetic efficiency (%)	
		55°C	65°C	Δ (%)	55°C	65°C
Effect of temperature	5mm	0-3.60	0-4.89	0-36	0-90	0-92
	8mm	0-2.97	0-3.70	0-24	0-92	0-95
		Exergy loss (kJ/kg)			Exergetic efficiency (%)	
		8mm	5mm	Δ (%)	8mm	5mm
Effect of thickness	65°C	0-3.70	0-4.89	0-32	0-95	0-92
	55°C	0-2.97	0-3.60	0-20	0-92	0-90

Figure 5.8 presents the variation of the exergetic efficiency as a function of drying time for the drying chamber. The values of exergetic efficiency were based on the inflow, outflow and loss of exergy calculated using equations 25-28. It can be observed that exergetic

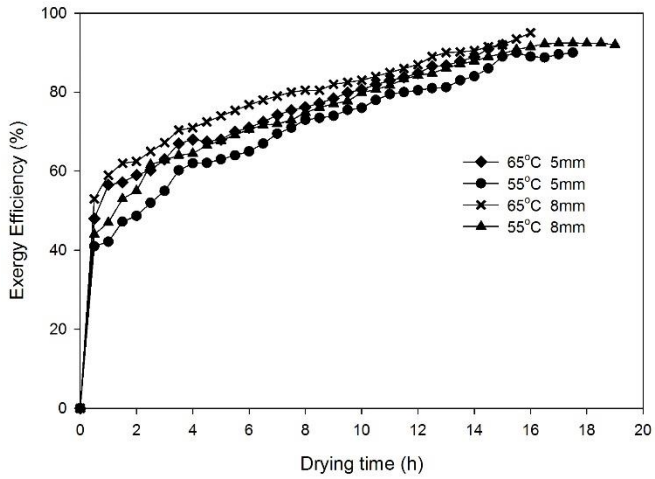

Figure 5.8: Variation of exergy efficiency with drying time under different drying variables

efficiency of the drying chamber increased with the increase of drying time. It was because of the fact that the available energy in the drying chamber increased with the drying time, since the amount of moisture decreased with time. Exergetic efficiency increased as drying temperature increased, although, increase in drying temperature resulted in an increase of exergy loss but this loss was lower than the increased amount of exergy entered in the drying chamber (exergy inflow) due to that increased temperature. Therefore, exergy efficiency increased with increasing drying air temperature (Table 5.5), according to equation 28. Higher thickness of potato slices increased the exergy efficiency due to decreased exergy losses, as explained earlier.

5.4.2.2 Exergy analysis of the overall system

The results of the exergy analysis, performed for the diagonal-batch dryer are summarized in Table 5.6. These results were calculated by using eq. 29-34 (Table 5.2). It can be observed that fan-heater combination handled major amount of the exergy in the system (exergetic factor), than the drying chamber. It had low exergetic efficiency and high improvement potential rate, which shows that this component significantly affected the system efficiency. Therefore, improvements should focus on this component.

Table 5.6: Results obtained from the exergy analysis of the dryer

	Component	Exergy inflow rate (kJ/s)		Exergy outflow rate (kJ/s)		Exergy loss rate (kJ/s)		Exergetic efficiency (%)		Improvement potential rate (kJ/s)		Exergetic factor (%)	
		65°C	55°C	65°C	55°C	65°C	55°C	65°C	55°C	65°C	55°C	65°C	55°C
05 mm	Fan-heater (A)	22.10	18.39	16.78	13.65	5.32	4.74	52.11	46.43	2.548	2.539	54.28	54.26
	Drying chamber (B)	18.61	15.50	17.22	14.01	1.39	1.49	92.51	90.39	0.104	0.143	45.72	45.74
	Overall system (A-B)	40.71	33.89	34.00	27.66	6.71	6.23	83.51	81.62	1.107	1.145	100.0	100.0
08 mm	Fan-heater (A)	19.87	17.24	14.67	12.34	5.20	4.90	50.93	47.99	2.552	2.548	54.25	54.40
	Drying chamber (B)	16.76	14.45	15.87	13.27	0.89	1.18	94.69	91.83	0.047	0.096	45.75	45.60
	Overall system (A-B)	36.63	31.69	30.54	25.61	6.09	6.08	83.37	80.81	1.013	1.167	100.0	100.0

There was no significant change in the improvement potential rate for both the system components with the change of temperature, showing that the insulation made in the dryer was good (Erbay and Icier, 2011). This can also be observed from the thermal images (Figure 5.9) of the dryer which showed heat distribution on the dryer's walls during the drying process. Band representing low temperature values (blue) were found dominant at the walls expect at the points of joints (two wall components). The product thickness had no significant effects on the exergy analysis of the system. On the other hand, the efficiency values for the fan-heater combination and the overall system increased with the increase of the drying temperature.

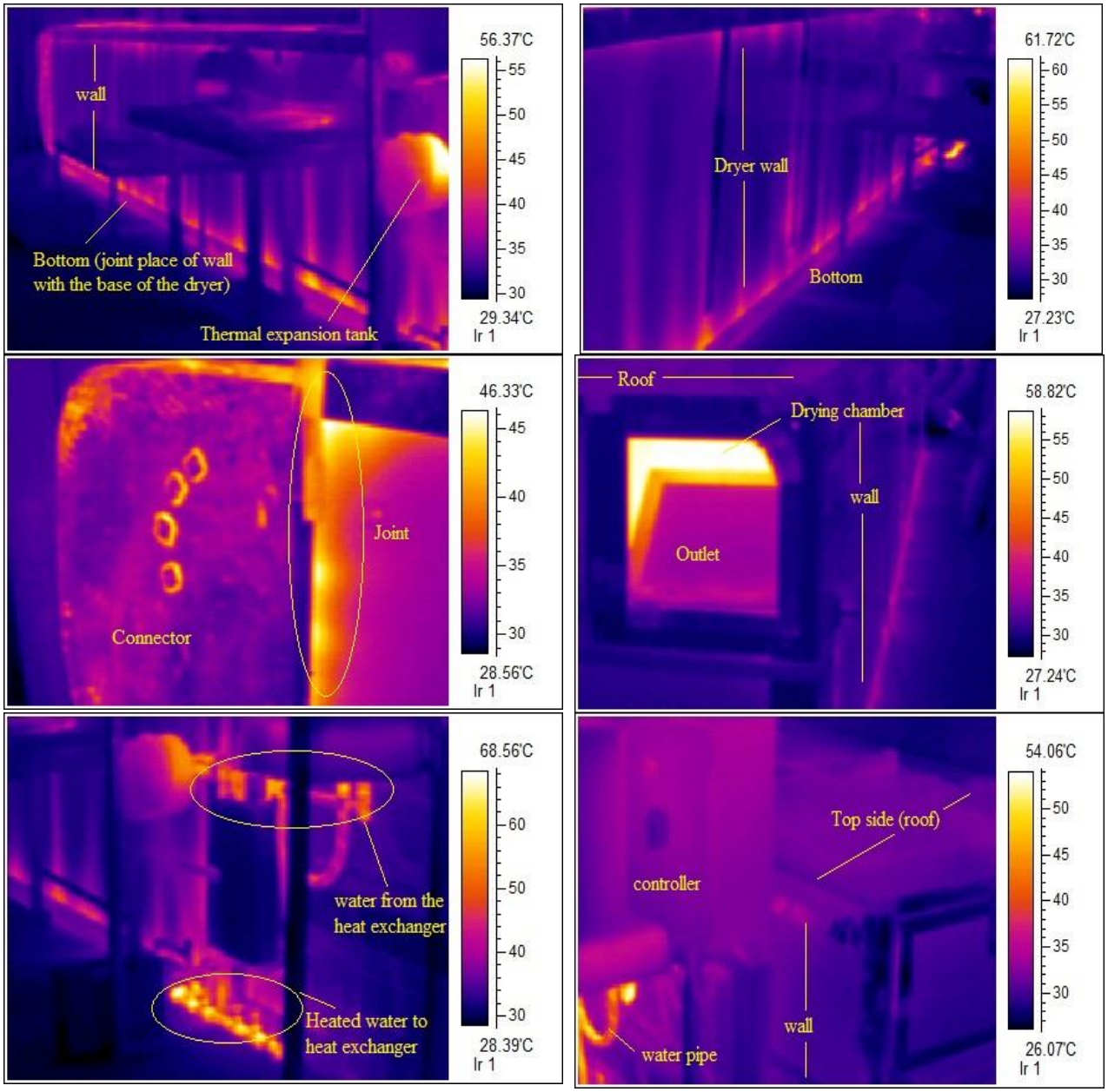

Figure 5.9: Thermal images of different positions of the dryer when operating at 60ºC

5.5 Experimental and predicted results

The parameters used for the analyses were calculated from the experimental data. In order to relate the experimental data with model data, all the studied parameters as functions of drying time were found best fitted in polynomial cubic using Sigmaplot-12. The coefficient of determination (R^2) was used to determine the suitability of fitness. Equation 35 gives the basic polynomial cubic equation used for fitting and the results for all the parameters investigated are reported in table 5.7.

$$y = y_o + ax + bx^2 + cx^3 \quad (35)$$

Table 5.7: The results for the fitting of all parameters investigated

Parameter	Drying condition	yo	a	b	c	R^2
Energy utilization (kJ/s)	T=65°C, thick=5mm	11.3449	-1.7915	0.2073	-0.0089	0.9196
	T=55°C, thick=5mm	7.5147	-0.4505	0.0384	-0.0019	0.9292
	T=65°C, thick=8mm	8.5110	-0.8348	0.0785	-0.0034	0.9659
	T=55°C, thick=8mm	6.6449	-0.2609	-0.0016	6.449E-5	0.9653
Energy utilization ratio (EUR)	T=65°C, thick=5mm	65.4030	-8.7742	0.3972	-0.0043	0.9952
	T=55°C, thick=5mm	58.1259	-9.9399	0.7402	-0.0201	0.9942
	T=65°C, thick=8mm	62.5116	-11.0848	0.8414	-0.0234	0.9874
	T=55°C, thick=8mm	52.3853	-9.4207	0.6831	-0.0171	0.9867
Exergy loss (kJ/kg)	T=65°C, thick=5mm	4.5437	-0.6761	0.0845	-0.0036	0.8625
	T=55°C, thick=5mm	2.8946	-0.1704	0.0217	-0.0010	0.7107
	T=65°C, thick=8mm	3.3902	-0.4017	0.0501	-0.002	0.8713
	T=55°C, thick=8mm	2.4948	-0.1522	0.0140	-0.0005	0.7544
Exergy efficiency (%)	T=65°C, thick=5mm	48.5637	5.8446	-0.4061	0.0141	0.9910
	T=55°C, thick=5mm	37.5675	6.8062	-0.3875	0.0100	0.9924
	T=65°C, thick=8mm	51.9202	6.4334	-0.4771	0.0153	0.9976
	T=55°C, thick=8mm	44.6165	5.7298	-0.2687	0.0055	0.9866

The plotted responses in Figure 5.10 show that the data points followed similar trend both for experimental and model predicted values for energy utilization (Figure 5.10a), energy utilization ratio (Figure 5.10b), exergy loss (Figure 5.10c) and exergy efficiency (Figure 5.10d). The results showed that for the energetic and exergetic parameters and drying conditions, model could estimate the experimental data with high R^2. For batch drying of potato slices, the model predicted results reasonably agreed with the experimental results of parameters studied. It can be used to provide the design data and for the optimal design of the dryer.

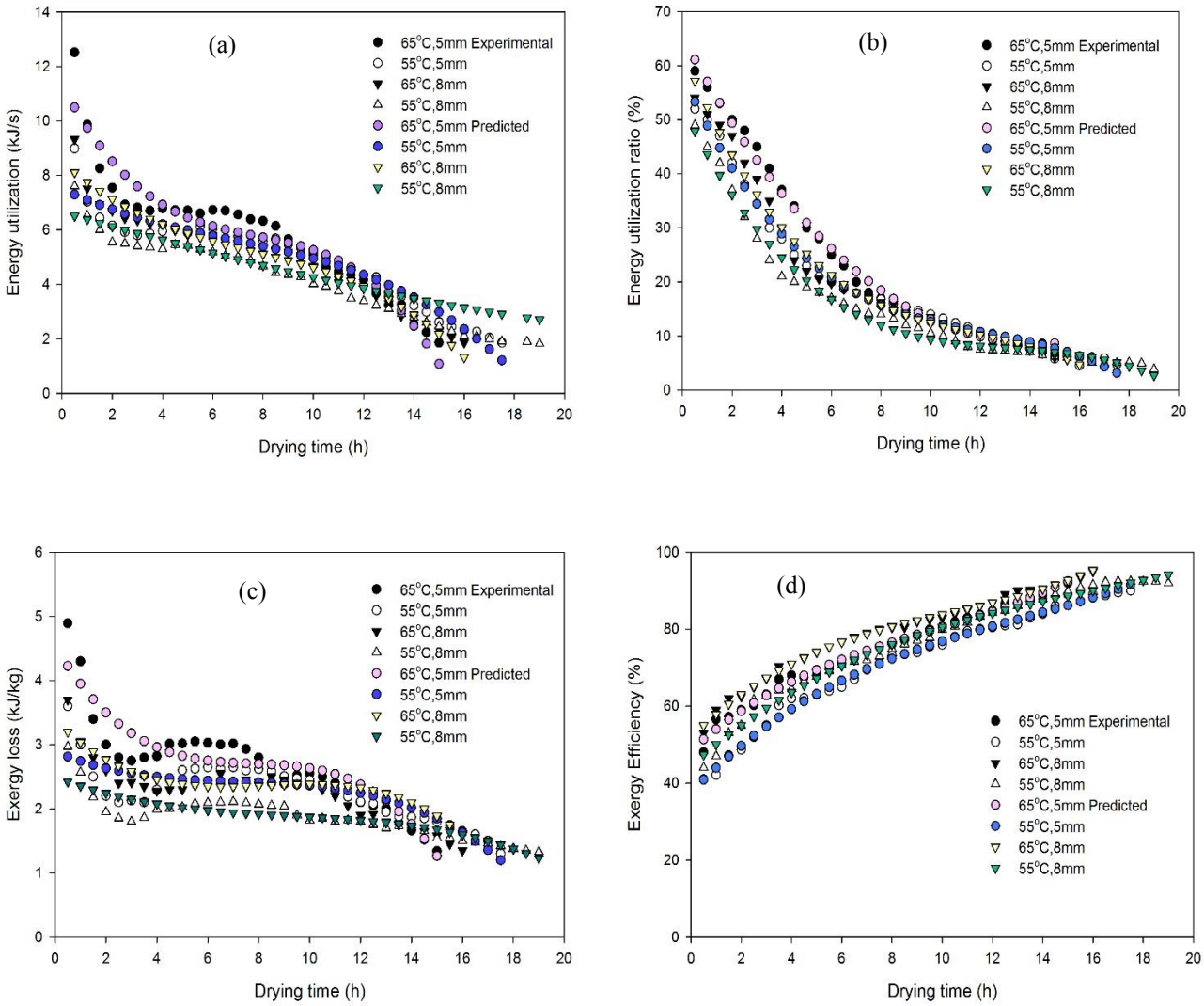

Figure 5.10: Comparison between experimental and predicted variations of energy utilization (a), energy utilization ratio (b), exergy losses (c) and exergy efficiency (d) as functions of drying time under different drying conditions.

5.6 Comparative view

Table 5.8 summarizes some of the recent studies about energy and exergy analyses to evaluate the hot air, tray or batch dryer's performance using different products. The range of drying temperature, mass flow rate of drying air, capacity of dryer and type of heater (electrical, fuel-powered, etc.) are the important parameters for the rate of energy utilization of batch dryer. It can be observed from the tabulated values in Tables 5.3, 5.5 and 5.8 that the diagonal batch dryer gave good results of energy and exergy analyses. It was because of

drying uniformity obtained with uniform airflow distribution through the drying chamber (Amjad et al., 2015b), required for successful operation (increased energy utilization).

Table 5.8: Some of the recent studies of thermal analysis to evaluate hot-air batch dryer's performance

Dryer type	Product	Drying variables	Energy utilization	EUR	Exergy losses	Exergetic efficiency	Reference
Laboratory tray dryer	Red pepper slices	T=55-70^{o}C V=1.5m/s	0.2-3.73 kJ/s	0-18.16%	0.9-1.488 kJ/kg	67.27-97.92%	Akpinar et al. (2004)
Experimental tray dryer	Strawberry slices	T=60-85^{o}C V=0.5-1.5m/s	0- 4.75 kJ/s	0-51.16%	0-0.715 kJ/s	24.81-100%	Akpinar (2006)
Two-tray hot air Cyclone type dryer	Potato slices	T=60-80^{o}C V=1-1.5m/s	0-7.1 kJ/s	0-61.62%	0-1.796 kJ/s	18-100%	Akpinar et al. (2005)
Two-tray hot air Cyclone type dryer	Apple slices	T=60-80^{o}C V=1.5m/s	0-4.51 kJ/s	0-34%	0-1.243 kJ/s	32-100%	Akpinar et al. 2004
Two-tray hot air Cyclone type dryer	Pumpkin slices	T=60-80^{o}C V=1-1.5m/s	0-4.10 kJ/s	0-56.85%	0-1.165kJ/s	19.40-100%	Akpinar et al. (2006)
Experimental tray dryer	Broccoli Florets	T=50-70^{o}C V=0.5-1.5m/s	-	-	0.037–0.074 kJ/s	59.70 - 81.92%	Icier et al. (2010)
Forced convection solar dryer	Pistachio	T=40-60^{o}C V=1.23m/s	0.9-2.66 kJ/s	0-59.7%	0.15–3.08 kJ/kg	15.65-100%	Midilli and Kucuk (2003)
Rotary column cylindrical solar dryer	Apricots	T=38-57^{o}C V=2.3m/s 2.25rpm	-	-	0.137-0.561kJ/kg	0.77-22.65%	Akpinar and Sarsilmaz (2004)

Energy consumption mainly varies with the type of the product used. In the current study, potato slices were used for the thermal analysis of the drying system. Akpinar et al. (2005) reported maximum energy utilization and exergy loss of 7.1kJ/s and 1.79 kJ/s respectively at 80^{o}C when energy utilization ratio was 61.62% in a cyclone type hot air dryer. The respective values found 12.52 kJ/s and 5.38 kJ/s in diagonal-batch dryer at 65^{o}C (15^{o}C less drying air temperature than used by Akpinar) with maximum EUR of 59% for the same product. Similarly energy utilization for other products (Table 5.8) would also expect to increase when process in the diagonal-batch dryer due to its feature of spatial drying uniformity.

Potato drying is a highly energy consuming process, significantly affected by the drying methods. Aghbashli et al. (2008) reported energy and exergy analyses of potato slices using semi-industrial continuous band dryer. Continuous dryers provide higher efficiency than tray dryer with low energy consumption. A comparison was made to show the difference

between the results of thermal analysis of the reported batch dryers and continuous dryer using potato as drying product (Table 5.9). The maximum values of energy utilization and exergy loss reported for cyclone type hot-air dryer were more than three times less and more than six times less respectively than that of values reported for continuous band dryer.

Table 5.9: Comparison of thermal analysis of potato slices in hot-air batch dryers and continuous dryer

Dryer type	Drying variables	Energy utilization (kJ/s)	EUR (%)	Exergy losses (kJ/s)	Exergetic efficiency (%)
Two-tray hot air Cyclone type dryer By Akpinar et al (2005)	T=60-80^{o}C V=1-1.5m/s	0-7.1	0-61.62	0-1.796	18-100
Diagonal-batch dryer (Current study)	T=55-65^{o}C Vavg=1.5m/s	0-12.52	0-59	* 0-5.38	41.12- 94
Semi-industrial continuous band dryer By Aghbashli et al. (2008)	T=50-70^{o}C m=0.61-1.83kg/s	3.75-24.05	15-37	0.6–13.71	57.13- 94.05

*By multiplying the mass airflow rates (at inlet and outlet) with calculated values of exergy inflow and outflow of the system respectively.

On the other hand, in case of diagonal-batch dryer, these values were found almost two times lower than the values reported for continuous band dryer. For diagonal batch dryer, the less difference in these values from that of the continuous dryer comparative to cyclone hot air dryer was due to uniform air distribution in the drying chamber. Spatial uniform air distribution facilitated the removal of moisture equally throughout the drying chamber which increased the rate of energy utilization.

5.7 Conclusion

In this study, the concept of energy and exergy analyses was applied to a newly developed diagonal-batch dryer using potato slices. The components of the drying system were also separately analyzed. The main conclusion of the current study can be listed as follows:

i. Energy utilization, energy utilization ratio and exergy losses increased with the increase of drying air temperature while decreased with the increase of potato slice thickness. The maximum exergy efficiency for potato slices was observed when

higher drying air temperature and larger sample thickness were used for the drying experiment.

ii. From the exergy analysis, it was found that system component A (fan-heater combination) affect the overall system efficiency more than component B (drying chamber). Increasing the efficiency of this component would enhance the overall system efficiency. Almost similar improvement potential rates were found for both the system components at different drying temperatures, showing that the insulation of the system was good.

iii. Consumption of electrical energy to evaporate one unit mass of moisture and to produce one unit mass of dried potato slices was found lower at 65^{o}C and 5mm slice thickness. Single layer with thin sample size is helpful to increase the energy utilization and decrease of the drying time.

iv. Uniform air distribution is important to increase the rate of energy utilization of a product during a drying process in hot air tray dryers. Due to drying uniformity, system gave good results of energy and exergy analysis when compared with other hot air drying systems.

v. Taking these results into consideration, the energy utilization during the drying process of this system could be increased to its maximum value by optimization and controlling of drying parameters to get optimum quality of dried material with shorter drying time. Moreover, the optimization of the drying process in the diagonal-dryer using other biological materials should also be done in future studies.

6 Mathematical Modelling of the Diagonal batch dryer for the convective drying of Potato

The mathematical drying model of the diagonal-batch dryer, designed for spatial drying homogeneity, has been developed using potato slices as drying material. For this process, heat and mass transfer equations were solved simultaneously to get a dryer model comprising a material model and an equipment model. The material model describes the drying kinetics of the product (instantaneous temperature and moisture distribution) while the equipment model deals with the dynamics of the dryer (transfer process in the dryer and predicts the instantaneous temperature and humidity of the air). The most of the parameters and physical properties required to solve the model were determined experimentally and some were taken from the literature. The outcomes showed an initial decline in air temperature at the time of entrance into the dyer due to high rate of moisture removal but later on stabilized. The product temperature also increased with drying time while its moisture contents decreased. The model results agreed closely to experimental data on batch drying of potato slices under used drying conditions.

6.1 Introduction

Most of the convective drying operations for fruits and vegetables are of batch drying (Mujumdar, 2006). Therefore, the design of batch dryers is important to size the drying equipment and drying chamber accordingly to meet the desired operating conditions. But for the biological materials, it is a complex process because of the dependence of food physicochemical properties and drying kinetics on water content and operating variables which need to consider for solving the model equations (Ratti et al., 2009). One of the main problems with batch type dryers is the lack of the airflow uniformity in the drying chamber, causing hindrance to get uniform moisture distribution (Karim et al., 2005).

Kerkhof (1994) pointed out the following difficulties for the quantitative understanding of the drying processes: (a) highly nonlinear physical processes (b) complicated exchanges and interaction processes; (c) the dominating process depend on drying conditions and can change even during the drying process (d) the material properties are highly dependent on the moisture content and temperature. In order to reduce the

complexity of the solution, an appropriate drying model should be developed predicting closely the experimental data.

Ratti and Crapiste (1992) proposed generalized drying curve to develop a material model for the drying process of apple, carrot and potato. It has been shown that the drying parameter is only dependent on the product moisture rather the drying conditions, food geometry and type of product. Hawlader et al. (1997) developed a drying simulation model for tunnel dryer by taking into account the product shrinkage. Experimental and simulated results of moisture contents showed good agreement. Dagde and Nmegbu (2014) developed a mathematical model for a hot air batch tray dryer by applying the conservation principle to mass and energy both for product and air.

In this study a mathematical model has been developed to find the drying potential of the air to dry the product up to desired moisture content under the used drying condition in diagonal-batch dryer. In order to get the required moisture content, several drying parameters are expected to be involved leading to complex modelling process. A simplified and accurate methodology has proposed by Chua et al. (1997) for batch dryers. The methodology incorporates a material model, describes the drying behavior of the product and an equipment model which expresses the effect of heat and mass transfer in the product on the drying air. The process was simulated under real operating conditions based on experimental drying kinetics. Experimental results of potato drying were used to calibrate the model.

6.2 Model development

The mathematical model of a dryer consists in the energy and mass balances for the air and the food material. For this, four heat and mass transfer equations are required to represent the design of a batch dryer (Ratii et al., 2009). After solving, these equations will give information about moisture content and temperature of the product (material model), humidity, and temperature of the air during hot air drying (equipment model).

6.2.1 Material model

The change in product temperature and moisture during drying process is described by this model. The air was uniformly distributed through the drying chamber (Amjad et al., 2015b), so in this study a case of single food bucket was taken. To simplify the model, the following assumptions were made.

1. The moisture movement and heat transfer are one dimensional.
2. The system is adiabatic, no energy losses through the walls of dryer.
3. The material to material contact is negligible.
4. The moisture content in the potato sample is uniform.
5. Thermochemical properties of material, air and moisture are constant i.e. no chemical reaction during the drying process.

The material model equations were derived from the process of heat and mass transfer between product and the drying air (Appendix 2).

The moisture content of the product,

$$X_{t+1} = X_t - \Delta t * DR \left(\frac{A_p}{M_p}\right) \quad 1$$

The temperature of the product,

$$T_p^{t+1} = T_p^t + \frac{\Delta t * A_p\left[h\left(\bar{T}_a - \bar{T}_p\right) + DR\{(Cp_w - Cp_v) * \bar{T}_p - L\}\right]}{M_p\left(Cp_p + Cp_w \bar{X}\right)} \quad 2$$

These equations were used for each time interval during the drying process to calculate the change in product moisture and temperature. The detail of abbreviations for each respective used term can be found in the list of nomenclature.

6.2.2 Equipment model

The equipment model was developed to characterize the heat and mass balance of the drying air as it came to contact with product in the drying chamber. Taking a single food bucket as a control volume, schematic illustration of air heat and mass balance is shown in Figure 6.1.

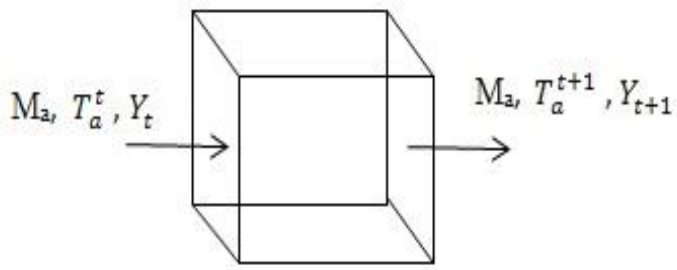

Figure 6.1: Scheme of a control volume showing air undergoing a drying process

In order to describe the changes in the drying air due to the heat and mass transfer in the product, the following assumptions were made:

1. Thermal properties of moisture and air are constant.
2. Product size and product distribution is uniform in the drying chamber.
3. The process of heat and mass transfer is one dimensional.

Equations 3 and 4 are derived to describe the change in air moisture and temperature. Derivation details are in appendix 2.

Humidity (moisture) of the drying air,

$$Y_{t+1} = Y_t + DR\left(\frac{A_p}{M_a}\right) \quad 3$$

Temperature of the air,

$$T_a^{t+1} = T_a^t - \frac{\Delta t * A_p[(\bar{T}_a - \bar{T}_p)(h - DRCp_v)] - Q}{M_a(Cp_a + Cp_v\bar{Y})} \quad 4$$

The change in moisture and temperature both for air and product, thermal communication area of product, mass flow rate of air and drying rate were determined from the experimental data. The convective heat transfer coefficient (h_c) of potato was calculated for each time interval using following equation (Tripathy et al., 2014).

$$h_c = \frac{(V_p/A_p)\left[\rho Cp_p(1+X)\left(\frac{dT_p}{dt}\right) + \rho L\left(\frac{dX}{dt}\right)\right]}{(T_a - T_p)} \quad 5$$

The thermo-physical properties of potato (heat of sorption, density and specific heat) were calculated as:

Latent heat of vaporization was calculated by using the equation modelled by Youcef-Ali et al. (2001) for potato.

$$L = 4.1868\left\{597 - 0.56\left(T_p + 273\right)\right\} \quad 6$$

Density of the potato was calculated by using the expression given by Wang et al. (1994) for potato under different operating temperatures.

$$\rho = \{A + B\exp(CX^2)\} \times 1000 \qquad 7$$

Where A, B, and C are correlation coefficients and values used at 65°C were 1.081, 0.1955, and -0.442 respectively. It was calculated for each time interval using respective value of product moisture for that time interval. The volume of the product was calculated from the value of density and respective mass of the product.

The values for specific heat of water (c_{pw}) and vapour (c_{pv}) were 4.2 kJ/kg k and 1.871 kJ/kg k respectively for the used drying temperature (Robert et al. 1997). The value for specific heat of potato was 3.515 kJ/kg k (Marcus and Lund, 2003). It can also be calculated using the expression developed by Wang and Brennan (1993) for potato.

6.3 Experiments

The drying experiments were same as described in chapter 5 (section 5.2.2). The required experimental values were used to solve the model equations. The first drying condition (65°C and 5mm thickness) was used in this study. The previous studies (chapters 3-5) showed the drying uniformity among the food buckets. So, the periodic weight of one representative food bucket was measured during the drying process for model development due to the difficulties of unloading and reloading of all the buckets after each time interval. Therefore, all the respective values such as airflow rate, product temperature, and moisture change were used for a single bucket. The inlet air conditions (air temperature, air humidity) were same for all the food buckets (chapter 5, section 5.3.1, and eq. 11).

6.4 Results and discussion

6.4.1 Validation of material model

The experimental measured changes in the product moisture content and temperature during the drying process were compared with model predicted values. The weight of the potato slices was continuously measured after every thirty minutes interval. For each time interval, the model equations were solved by using respective experimental measured values for that

time interval. It was repeated until the desired final moisture content was obtained. The modelled results from material model showed good agreement with experimental data as shown in Figure 6.2a. The mean difference between experimental and predicted values for moisture content and product temperature were 3.125% and 3.50% for each interval of time respectively. It can be observed from Figure 6.2b that changes in product temperature at early time intervals were more visible due to the rapid change in the product moisture. This trend became lower as drying proceeded to end.

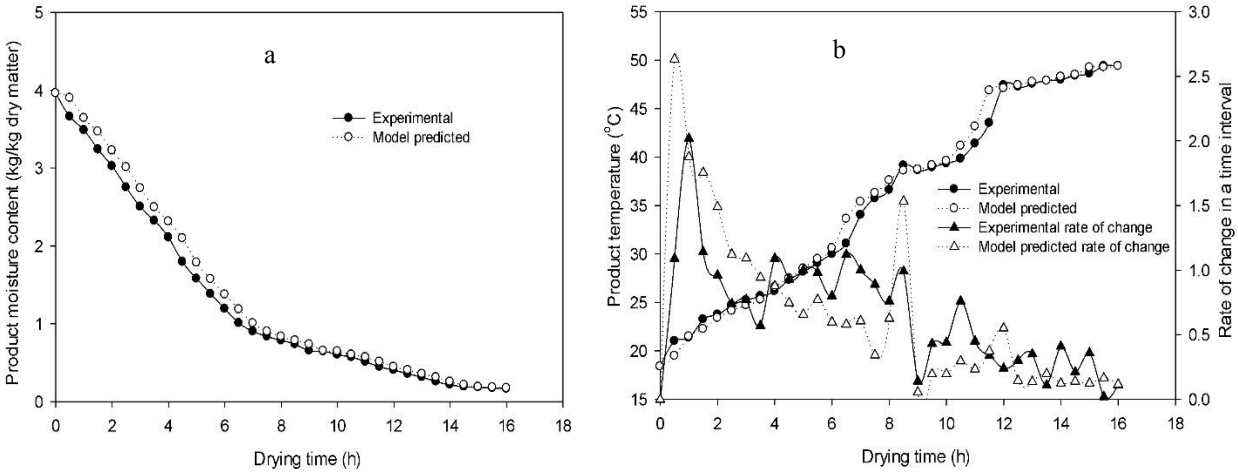

Figure 6.2: Comparison between experimental and predicted drying kinetics for product moisture (a) and temperature (b)

6.4.2 Validation of equipment model

During the drying process, the changes in product moisture content and temperature bring change in the drying air condition due to the process of heat transfer from air to product and mass transfer from product to air. For the same time interval as stated above the experimental measured and model predicted changes in air humidity and temperature showed good agreement (Figure 6.3). The air got more humid at the early time intervals due to high moisture removal rate from the product resulted the decline of air temperature. The mean difference between experimental and model predicted values in air moisture and temperature was calculated almost of same value 3.03%.

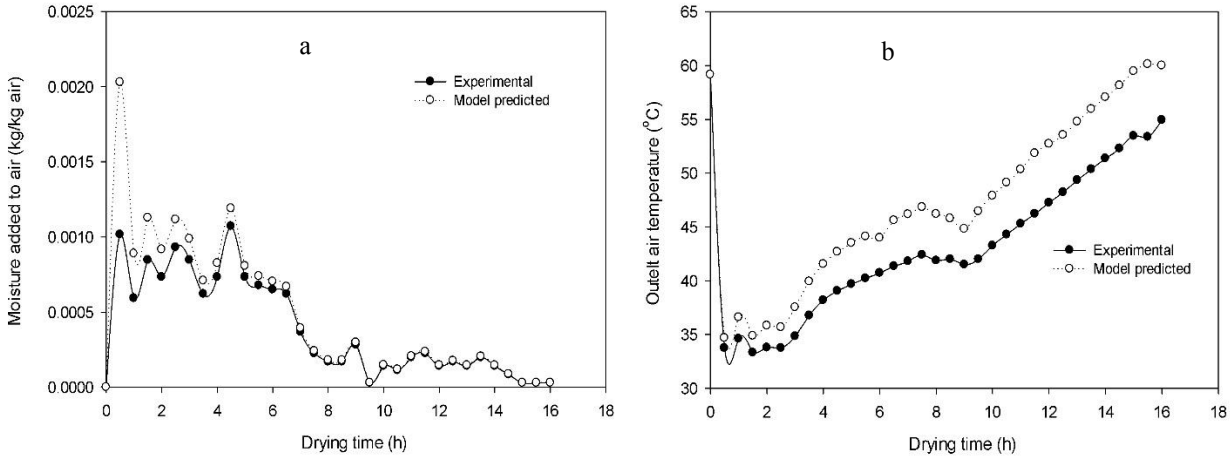

Figure 6.3: Comparison between experimental and predicted change in air moisture (a) and temperature (b)

6.4.3 Overall dryer model

The overall dryer model described by equations 1 to 4 is one dimensional. Figure 6.4 shows the relationships among the parameters calculated from the material model and the equipment model. More moisture added to the drying air at early stages of the drying process due to high moisture removal rate as product had more moisture at initial time intervals (Figure 6.4a). This decline of product moisture content caused an increase of product temperature (Figure 6.4b).

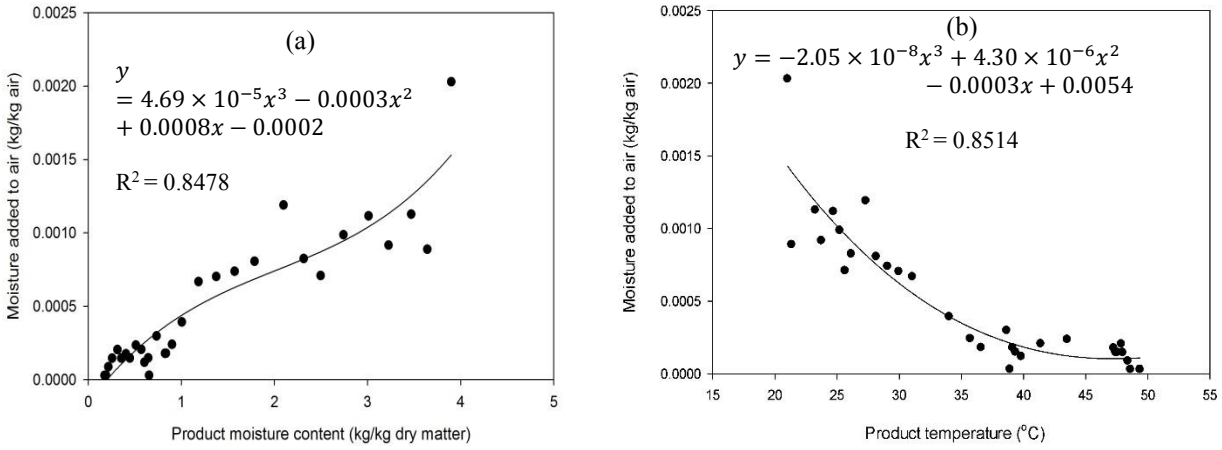

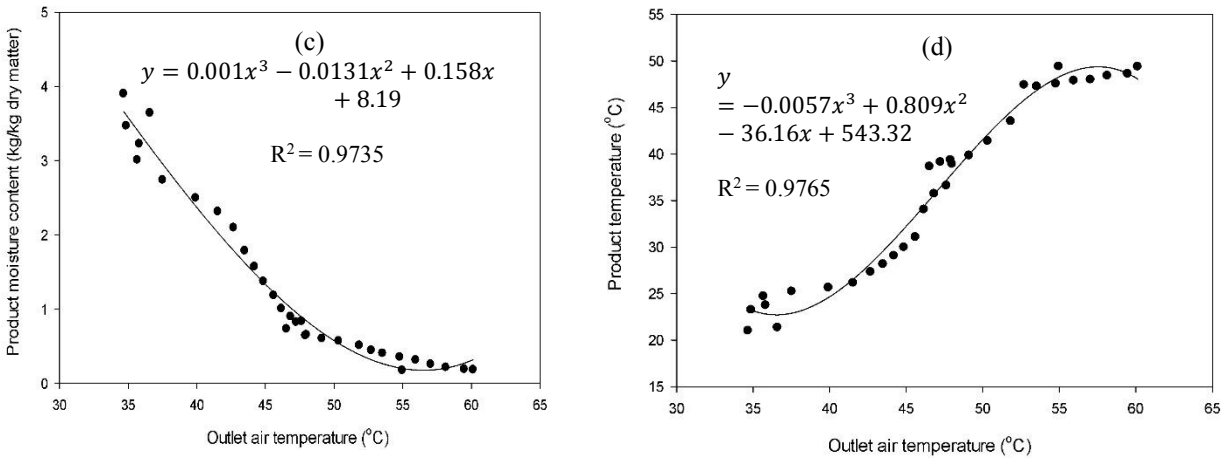

Figure 6.4: Relationship between models predicted change in air humidity with product moisture (a) change in air humidity with product temperature (b) change in product moisture with air temperature (c) change of product temperature with air temperature (d)

As the drying time increased, product moisture decreased and adding less water to the air. Therefore, the temperate of outlet air started to rise with the decrease of product moisture content and increase of product temperature due to low air humidity (Figure 6.4c &d). These relationships show the interdependency of the calculated parameters and can be interlinked in various ways. In case of one parameter obtained from experiment or calculated using respective model equation, the other parameter can be predicted without knowing its experimental value or calculation via model equation for that parameter. The equations of best fitted curves for these relationships were polynomial cubic with good values of coefficient of determinant (R^2) 0.8478, 0.8514, 0.9735 and 0.9765 for Figure 6.4a, 6.4b, 6.4c, and 6.4d respectively using Sigma-plot 12.3.

6.5 Conclusion

A mathematical model to predict the drying of potato slices in a diagonal batch dryer was developed. The dynamic behavior of the dryer was described by the equations. These equations were obtained by applying the conservation principle to the mass of product moisture, mass of air moisture (air humidity), product energy and air energy. Results show that more the moisture in the product, more water will be added to the air to increase air humidity. Both the potato temperature and air temperature increased with the increase of drying time. The experimental and model data were found in close agreement. The

mathematical model can be used to analyze the influence of various drying conditions on the drying time and be helpful to overcome the practical difficulties in getting optimum dryer design and drying conditions.

7 General discussion

Convective air drying is a widely used method for food preservation and storage. Drying homogeneity is key factor for the reduction of drying time, energy consumption and production of uniform quality dried product. Generally fruits and vegetables possess high initial moisture content and properties which are sensitive to drying temperature (color, texture, and nutritional aspect). Several factors affect the required amount of energy for specific product such as initial moisture content, drying temperature, air humidity and air flow rate. But uniform exposure of all the food material to same air conditions is important to get dried product of uniform quality. The design for air distribution is one of the important factors in designing batch type food dryers. It is difficult to resolve the problem of flow heterogeneity in industrial convective air dryers. The factors which need to be considered while designing airflow distribution are the drying medium and geometry of the drying chamber. The use of air deflectors in batch drying systems is common practice to overcome the drying heterogeneity. Their use make the dryer's geometry complicate which not only increase the dryer construction cost but also result in velocity pressure drop. In industrial air dryers, the effect of flow heterogeneity is particularly difficult to resolve. The present study deals with the design, construction and evaluation of a new batch type food dryer named as Diagonal-dryer due to diagonal airflow channel along with the entire length of the dryer.

7.1 Development of diagonal-airflow batch dryer with numerical and experimental evaluation for spatial drying homogeneity

Most of the research in batch drying processes dealt with the effect of drying temperature and air velocity as primary influencing parameters on the quality of dried products while the lack of airflow uniformity is a crucial factor. Normally, in convective dryers, the air moves from one side (inlet) of the drying chamber to the other side (outlet) of the drying chamber causing over and under drying of material respectively. The present study was conducted to design a new batch type food dryer named as diagonal-batch dryer due to its diagonal airflow design for uniform exposure of entire product to air.

Experimental and CFD based simulation results showed good agreement for air distribution in the drying chamber. In case of simulation conducted using ANSYS-Fluent, the design of the drying chamber with diagonal-airflow channel gave uniform air distribution

profiles comparative to non-diagonal airflow channel (straight airflow channel). In straight airflow channel, air flow was direct towards the end of the drying chamber as was expected which created zones of high and low airflow distribution. On the other hand, simulated outcomes for velocity profiles showed uniform air distribution in the drying chamber. Due to the diagonal angle of the channel, the air converged as it moved towards the end of the drying chamber.

A series of drying experiments were conducted using potato as drying material, showed almost uniform spatial drying homogeneity. The slight span of moisture content was observed among buckets lying at first two meter distance of the drying chamber and last ten buckets (at 8m and 10m distance) comparative to the buckets lying in the middle of the drying chamber (at 4m and 6m distance). As the air entered into the drying chamber, it moved towards the end of the dryer and built a velocity pressure within the diagonal airflow channel due to its convergence. It was also observed from the results of airflow simulation that air flow was not much smooth just at the entrance of the diagonal airflow channel due to some pushing effect exerted by the incoming air. So, the velocity pressure settled smoother at the middle of airflow channel. These variations in the moisture content were observed during constant rate of drying because of surface moisture which is loosely bounded and its evaporation rate significantly varies with the slight variation in the air flow. Secondly, each experiment was conducted separately for every two meter distance of the drying chamber and initial moisture content of the product was taken uniform for all the experiments although it was measure separately with slightly differ values. So slight variation in the results could be due to the actual variations in the moisture. But all the drying material in each set of experiments gave an almost equal final moisture contents during the phase of second falling rate. The drying material in all the food buckets was being exposed to incoming warm air uniformly which facilitated the uniform drying. Comparison between the results of air velocity extracted from simulation (average predicted) and measured through experiments (average measured) revealed good agreement (correlation coefficient of 87.09%). The numerical and experimental results of air distribution ascertain the diagonal airflow design for uniform drying.

After the successful results of drying homogeneity, effect of uniform air distribution on the quality of dried product was on-line investigated along with the entire length of the drying chamber. Change in color was selected as quality parameter to be investigated. Results showed that the rate of color change of product (potato slices) at all sections of the drying chamber was found similar. Drying temperature mainly influence the quality parameter so the

change in the studied quality parameter is directly linked with uniformity of drying temperature. The lightness (L^*) of the slices decreased with the decrease of moisture content which could be attributed to the non-enzymatic browning. It might also be related to an increase in samples opacity resulting from structural shrinkage due to the moisture evaporation. Temperature of the product under drying also effect the value of lightness, increase of product temperature results decline in lightness. Therefore, uniform decline in lightness of the product samples at all sections ascertain the fact of uniform temperature availability in the drying chamber. It could be related to uniform air distribution within the drying chamber as temperature distribution is associated with airflow in the drying chamber. Similarly the change in redness (a^*) and yellowness (b^*) was also similar at all the sections of the dryer.

These results showed that the rate of change of these quality parameters at all sections of the drying chamber were found similar. Drying temperature mainly influence the quality parameter so the change in these quality parameters is directly linked with uniformity of drying temperature. Therefore, the spatial uniform distribution of drying temperature is of much importance to reduce the factor of over and under drying and consequently to get product of uniform quality throughout the drying chamber. For this, design of airflow in the drying chamber is the main factor to be considered. Diagonal airflow design gave good temperature distribution which helped in reducing the heterogeneity of quality parameters in the drying chamber. The distribution of drying temperature is linked with air flow, therefore uniform air distribution over the food trays is required for successful operation both from drying rate and energy consumption points of view.

7.2 Energy and exergy analysis of the drying process and mathematical modelling of the diagonal-airflow batch dryer

Food drying is an energy consuming process especially when deal with fruits and vegetables. Therefore, well understanding of the drying process is very important not only for optimizing the product quality but also for the system efficiency. For any newly developed drying system, thermodynamic analysis helps to optimize the process effectively. For this purpose, energy analysis, particularly the exergy analysis provides a better understanding of the thermodynamic phenomena and useful information in the design of the drying system. Energy and exergy analyses for the diagonal-batch dryer were performed using potato slices of 5 mm and 8 mm thicknesses at 55^{o}C and 65^{o}C drying temperature. The rates of drying and

energy use increase with the increase of drying temperature. Therefore, at same sample thickness, the rate of energy utilization was found higher when temperature changed from 55^{o}C to 65^{o}C. This was due to the high removal of loosely bounded surface moisture of the food product. As drying proceeded, the rate of moisture dissipation decreased ultimately decreased the rate of energy utilization. The effect of sample thickness on energy utilization is inversely proportional i.e. higher the sample thickness less the energy utilization due to less surface area and thick core of product which caused hindrance in moisture removal. The maximum energy efficiency of the dryer was found 50.16% at 65^{o}C with 5mm sample thickness. In case of exergy analysis, the exergy losses went up with the increase of the energy utilization. Energy utilization and exergy losses were influenced more by drying temperature than sample thickness. The maximum and minimum values of exergy losses were found to be 4.89 kJ/kg (at 65^{o}C and 5mm slice thickness) and 1.3 kJ/kg (at 55^{o}C and 8mm slice thickness) respectively. Exergetic efficiency increased as drying temperature increased, although, increase in drying temperature resulted in an increase of exergy loss but this loss was lower than the increased amount of exergy entered in the drying chamber (exergy inflow) due to that increased temperature. Therefore, exergy efficiency increased with increasing drying air temperature.

The main purpose of exergy analysis was to diagnose the system parts affecting the system efficiency so that one can easily make assessment, optimization and improvement of energy systems. The main component for improving the system efficiency was found to be the fan-heater combination, possessing low exergy efficiency of 46.43-52.11%, high improvement potential rate (IP) of 2.53-2.55 and high exergetic factor (*f*) of values 54.26-54.40% under the used drying conditions. Exergetic factor (*f*) shows the relative significance for the inflow exergy of a component on total exergetic inflow to the system. High exergetic factor for a system component means that high amount of exergy is being handled by that component in the system. These results show that fan-heater combination handled major amount of the exergy in the system (exergetic factor), than the drying chamber. It had low exergetic efficiency and high improvement potential rate, which shows that this component significantly affected the system efficiency. Therefore, improvements should focus on this component. There was no significant change in the improvement potential rate for both the system components with the change of temperature, showing that the insulation made in the dryer was good (Erbay and Icier, 2011). The product thickness had no significant effects on the exergy analysis of the system. On the other hand, the efficiency values for the fan-heater combination and the overall system increased with the increase of the drying temperature.

The outcomes of these analyses mainly vary depending upon the dryer configuration and the product being used. Therefore, dryers with different designs can give different values of energy and exergy analyses for the same product. Thus, the ultimate objective of a modified or new design is to improve the results in the form of less energy consumption and better product quality. Energy and exergy analyses are rarely made for food processes. Detailed literature review has shown that little work has been done on the energetic and exergetic analyses for the hot air batch drying of fruits and vegetables. In case of potatoes, only Akpinar et al. (2005) worked on the single layer drying process of potatoes via a convective hot-air cyclone type dryer reported by Aghbashlo et al. (2008). In order to compare the system, almost same drying conditions (reported for other two dryers) were used for the thermal analysis of diagonal-dryer. Comparative results (Table 5.9) showed lower values for the rates of energy utilization and exergy loss reported for cyclone type hot-air dryer comparative to continuous band dryer. On the other hand, these differences were calculated less in case of diagonal-batch dryer. For diagonal batch dryer, the less difference in these values from that of the continuous dryer comparative to cyclone hot air dryer was due to uniform air distribution in the drying chamber. Spatial uniform air distribution facilitated the removal of moisture equally throughout the drying chamber which increased the rate of energy utilization.

Mathematical modelling of the drying process is an important aspect in the field of food processing. It enable the researchers and designers to select appropriate drying conditions for desired results and then resize the dying system to meet these drying operating conditions. The solved mathematically equations for a drying process are helpful in predicting the parameters at any time during the drying process based on initial conditions (Hawlader et al. 1997). But for the biological materials, it is a complex process because of the dependence of food physicochemical properties and drying kinetics on water content and operating variables which need to consider for solving the model equations (Ratti et al., 2009). One of the main problems with batch type dryers is the lack of the airflow uniformity in the drying chamber, causing hindrance to get uniform moisture distribution (Karim et al., 2005). Diagonal batch dryer specifically developed for spatial drying homogeneity. So, a set of mathematical equations were solved that could adequately characterize the system. These equations were obtained by applying the conservation principle to the mass of product moisture, mass of air moisture (air humidity), product energy and air energy. Results showed that more the moisture in the product, more water will be added to the air to increase air

humidity. Both the potato temperature and air temperature increased with the increase of drying time. The experimental and model data were found in close agreement.

Both numerical and experimental based research methodology was applied for the design of dryer. The design objectives cannot be expressed in the form of simple algebra. In this context a computer-based approach is best for design optimization to search for the best design according to specified criteria. The repetitive process of modelling and iteration for solution using different solver models and boundary conditions to get appropriate and logical results not only save the research time but economical as well. Computer simulation systematically adjusts the influencing variables to find the solution that has the best performance but produce results that are implied by the premises and cannot provide new empirical data. Only experiments can help to know the things that are not logically implied in our prior knowledge. Prior knowledge to run simulation is not the same as that required to conduct a good experiment. Therefore, experimental evaluation of an empirical system in its real geometrical form is important for proper functionality.

7.3 Further research

After getting a design for spatial drying homogeneity, the next challenge is to get dried food products with acceptable shape, size, color and texture. For this, further research should be in the direction to monitor and control the drying conditions dynamically (in real time manner). Food processes are complex due to interaction of numerous factors and traditional off-line evaluations are unable to get optimum operating conditions and processing quality. Therefore, for dynamic control of the drying conditions application of computer vision would be a viable technique for better understanding of ill-defined drying process and this will really help to further increase the energy efficiency.

Secondly, the development of a diagonal batch dryer needs to be investigated with aspect of drying capacity. For this, a computer simulation based thematic view of development has been presented in appendix 3.

8 Summary

The process of food drying is extensively applied to make the product more stable for the longer period of time. Fruits and vegetables are highly perishable because of high moisture content and deteriorate quickly due to biochemical activities in the product, inappropriate storage conditions, and inadequate transport facilities. Therefore, to get rid of such losses, direct method of drying is the oldest method in human history which is outdated to face the current challenges. In order to meet the quality standard and drying capacity, lot of developments were made in food drying sector in the form of various food dryers available in the market presently. Most of them are indirect type to develop a temperature differential for effective drying process. Different drying methods are used for food drying like steam drying, microwave drying, vacuum drying but more than 85% of industrial dryers are of the convective type with hot air as the drying medium. Batch type convective dryers are common and easy to use even for food growers in the developing countries due to simple design configuration. The drying is achieved by air circulation over the product which is critical in defining the final quality of the dried product. But problem of uneven air distribution encounter in most batch type drying systems. The effect of drying temperature, relative humidity and air velocity have been considered by many researchers as primary influencing parameters on the quality of the dried products while the lack of uniformity in air flow is a crucial factor. Non-uniform air distribution causes non-uniformity in air velocity and drying temperature which translates into drying heterogeneity in the dryer. It is particularly difficult to resolve the effect of flow heterogeneity in large air dryers.

In this study a new batch type dryer named “diagonal-batch dryer” has been developed with diagonal airflow channel along with the length of the drying chamber without baffle plates/air guiders. Apart of the benefits to use air guiders, they cause not only increase in dryer construction cost but also results in velocity pressure drop. So, more energy is consumed in the drying process. In order to get spatial uniform drying without air guiders, the food buckets were arranged diagonally along with the length of dryer. The main purpose of diagonal channel was to expose the entire product uniformly to the incoming hot air. The detail of the dryer configuration can be found in chapter 3. The airflow simulation of the system was carried out using ANSYS-Fluent in the ANSYS Workbench platform. Two different geometries of the drying chamber, diagonal and non-diagonal were modelled and results for uniform air distribution were obtained from diagonal airflow design. Practically, a

series of experiments were conducted to assess the design. Potato slices were used as drying material as they were easily available from the University agricultural farm. The measured span of moisture content among the food buckets was found low at a given drying time (Table 3.2) in the form of standard deviation which showed the occurrence of spatial drying homogeneity. The results of calculated average velocity through the buckets were compared with those extracted from simulation. The result of statistical analysis showed good value of coefficient of determinant (87.09%) for airflow distribution between the average predicted and the average experimental measured velocity. The numerical and experimental air distribution with diagonal airflow design strengthen the design for uniform drying.

The quality of dried product is significantly affected by the drying temperature. As convective heat transfer (h_c) of a product varies with its position in the drying chamber and drying time, so variation in the drying rates effect the quality parameters of drying materials. Therefore, it becomes important to distribute that temperature uniformly to get products of similar change in quality. In order to assess the effect of uniform air distribution on the quality change, color of the product was on-line investigated along with the entire length of the drying chamber. An imaging box was developed for this purpose comprising a camera and lights (chapter 4). Spatial variations of this quality parameter were selected as criteria to assess the uniform quality drying throughout the dryer's chamber. The change in lightness, redness and yellowness retention ratio of potato slices at all sections of the drying chamber were found similar up to certain extent which ascertain the fact of uniform temperature availability throughout the drying chamber. It could be related to uniform air distribution within the drying chamber as temperature distribution is associated with airflow distribution. Therefore, it was concluded that uniform final quality could be retained to maximum with uniform air distribution.

The most important thing for a batch type food dryer is the energy consumption. Thermodynamic analysis of the dryer was performed (chapter 5). The energy efficiency of the system was calculated 50.16% within the used drying conditions and the average amount of energy used in the form of electricity to produce one kilogram of dried potato samples (SPE) and to evaporate one kilogram of water (SEE) were calculated to be lower 16.24MJ/kg and 4.78MJ/kg respectively at high temperature of 65^{o}C and sample thickness of 5mm (Table 5.4). This efficiency can be improved further by optimizing the fan and heater combination. Because the main component for improving the system efficiency was found to be the fan-heater combination based on exergy analysis, possessing low exergy efficiency of 46.43-52.11%, high improvement potential rate (IP) of 2.53-2.55 and high exergetic factor (*f*) of

values 54.26-54.40% under the used drying conditions. The energy and exerggy analyses for diagonal batch dryer were also compared with other reported batch tray dryers (Table 5.8). The range of drying temperature, mass flow rate of the drying air, capacity of dryer and type of heater (electrical, fuel-powered, etc.) are the important parameters for the rate of energy utilization of batch dryer. The comparison revealed that the diagonal batch dryer gave good results of energy and exergy analyses. It was because of drying uniformity obtained with uniform airflow distribution through the drying chamber, required for successful operation (increased energy utilization). Mathematical drying model was also developed to describe the drying kinetics of the product and the dynamics of the dryer.

The development of diagonal-batch dryer provides a useful and an effective way to get possibility for spatial drying homogeneity. This design is able to expose the entire product to air uniformly in the drying chamber rather to pass the air from one food tray to the next. Further work could be in the direction of optimizing drying condition non-destructively to increase the energy efficiency, more importantly is to increase the drying capacity using this diagonal airflow concept.

Zusammenfassung

Das Verfahren der Lebensmitteltrocknung wird häufig angewendet, um ein Produkt für längere Zeit haltbar zu machen. Obst und Gemüse sind aufgrund ihres hohen Wassergehalts leicht verderblich durch biochemische Vorgänge innerhalb des Produktes, nicht sachgemäße Lagerung und unzureichende Transportmöglichkeiten. Um solche Verluste zu vermeiden wird die direkte Trocknung eingesetzt, welche die älteste Methode zum langfristigen haltbarmachen ist. Diese Methode ist jedoch veraltet und kann den heutigen Herausforderungen nicht gerecht werden.

Um eine standardisierte Qualität und Trocknungskapazität zu erreichen, sind im Bereich der Lebensmitteltrocknung viele technische Lösungen entwickelt worden was in der Fülle der derzeitig auf dem Markt befindlichen Anlagen widergespiegelt ist. Die meisten basieren zur effektiven Trocknung indirekt auf der Erzeugung eines Temperaturdifferentials. Zur Trocknung von Lebensmitteln werden verschiedene Verfahren angewandt, z.B. Dampf-, Mikrowellen und Vakuumtrocknung, jedoch sind mehr als 85 % der Industrietrockner Konvektionstrockner mit erwärmter Luft als Trocknungsmedium. Chargentrockner sind die gängige Variante und einfach zu bedienen, auch für Erzeuger in Entwicklungsländern aufgrund der einfachen Ausführung. Eine Trocknung wird durch die über das Produkt zirkulierende Luft erreicht, und deren Zustand entscheidet über die Endqualität des Produktes. Jedoch treten in den meisten Chargentrocknern Probleme durch ungleiche Luftverteilung auf. Die Effekte von Trocknungstemperatur, relativer Luftfeuchte und Strömungsgeschwindigkeit werden von vielen Forschern als die bedeutendsten angesehen, bezüglich ihres Einflusses auf Qualitätsparameter getrockneter Produkte. Ein ungleichmäßiger Luftstrom jedoch ist der entscheidende Faktor. Eine ungleichförmige Luftverteilung führt zu ungleichmäßigen Luftgeschwindigkeiten, was zu Trocknungsheterogenitäten im Trockner führt.

In der vorliegenden Arbeit wurde ein neuer Chargentrockner, der “Diagonal-Chargentrockner, mit diagonalem Luftstömungskanal entlang der Länge des Trocknungsraumes und ohne Umlenkblech/Leitblech entwickelt. Neben dem unbestreitbaren Nutzen der Verwendung von Leitblechen, erhöhen diese jedoch die Konstruktionskosten und führen auch zu einer Erhöhung des Druckverlustes. Dadurch wird im Trocknungsprozess mehr Energie verbraucht. Um eine räumlich gleichmäßige Trocknung ohne Leitbleche zu erreichen, wurden die Lebensmittelbehälter diagonal entlang der Länge des Trockners

platziert. Das vorrangige Ziel des diagonalen Kanals war, die einströmende, warme Luft gleichmäßig auf das gesamte Produkt auszurichten. Details zu den Einstellungen können dem Kapitel 3 entnommen werden. Die Simulation des Luftstroms wurde mit ANSYS-Fluent in der ANSYS Workbench Plattform durchgeführt. Zwei verschiedene Geometrien der Trocknungskammer, diagonal und nicht diagonal, wurden modelliert und die Ergebnisse für eine gleichmäßige Luftverteilung aus dem diagonalen Luftströmungsdesign erhalten. Es wurde eine Reihe von Experimenten durchgeführt, um das Design zu bewerten. Kartoffelscheiben dienten als Trocknungsgut, da sie leicht vom universitätseigenen Versuchsbetrieb zu beziehen waren. Die räumliche Spreizung der gemessenen Feuchtegehalte in Lebensmittelbehälter war zu jeder gegebenen Trocknungszeit niedrig (Tabelle 3.2), auch bezüglich der Standardabweichung, was eine vorhandene räumliche Trocknungshomogenität nachweist. Die Ergebnisse der kalkulierten durchschnittlichen Strömungsgeschwindigkeiten durch die Behälter wurden mit denen der Simulation verglichen. Die statistischen Ergebnisse zeigen einen guten Korrelationskoeffizienten für die Luftstromverteilung (87,09 %) zwischen dem durchschnittlich vorhergesagten und der durchschnittlichen gemessenen Strömungsgeschwindigkeit. Die modellierte und experimentelle Luftverteilung mit diagonalem Luftstrom-Design verbesserten die Dimensionierung für gleichmäßige Trocknung.

Die Qualität getrockneter Produkte wird maßgeblich von der Trocknungstemperatur beeinflusst. Da die konvektive Wärmeübertragung (hc) eines Produktes mit seiner Position in der Trocknungskammer und der Trocknungszeit variiert, beeinflussen Variationen der Trocknungsrate die Qualitätsparameter des Trocknungsgutes. Daher ist es wichtig, eine gute Temperaturverteilung zu erreichen, um eine gleichmäßige Veränderung in der Qualität der Produkte im ganzen Trockner zu erreichen. Um den Effekt der gleichmäßigen Luftverteilung auf die Veränderung der Qualität zu bewerten, wurde die Farbe des Produktes, entlang der gesamten Länge der Trocknungskammer kontaktfrei im on-line-Verfahren bestimmt. Zu diesem Zweck wurde eine Imaging-Box, bestehend aus Kamera und Beleuchtung (s. Kapitel 4), entwickelt. Räumliche Unterschiede dieses Qualitätsparameters wurden als Kriterium gewählt, um die gleichmäßige Trocknungsqualität in der Trocknungskammer zu bewerten. Die Veränderung der Erhaltungsquote Helligkeit (L^*), Rotfärbung (a^*) und Gelbfärbung (b^*) der Kartoffelscheiben in allen Bereichen der Trocknungskammer waren bis zu einem gewissen Maße ähnlich, was eine konstante Temperaturbereitstellung über die gesamte Trocknungskammer bekräftigt. Dies könnte an der einheitlichen Luftverteilung innerhalb der Trocknungskammer liegen, da die Temperaturverteilung mit der Luftverteilung

zusammenhängt. Daraus kann geschlossen werden, dass eine einheitliche Endproduktqualität durch eine gleichmäßige Luftverteilung maximiert werden kann.

Entscheidend beim Lebensmittel-Chargentrockner ist sein Energieverbrauch. Dafür wurden thermodynamische Analysen des Trockners durchgeführt (Kapitel 5). Die Energieeffizienz des Systems wurde bei den genutzten Trocknungsbedingungen mit 50,16 % kalkuliert. Die durchschnittlich genutzten Energie in Form von Elektrizität zur Herstellung von 1 kg getrockneter Kartoffeln (SPE) wurde mit weniger als 16,24 MJ/kg und weniger als 4,78 MJ/kg Wasser zum verdampfen (SEE, bei einer sehr hohen Temperatur von jeweils 65 °C und Scheibendicken von 5 mm kalkuliert (Tabelle 5.4). Die Effizienz kann durch Optimierung der Ventilator-Heizungs-Kombination noch verbessert werden. Die Ventilator-Heizungs-Kombination wurde als Hauptkomponente zur Verbesserung der Systemeffizienz ermittelt. Dies basiert auf einer Exergie-Analyse, mit einer geringen Exergieeffizienz von 46,43-52,11 %, einem hohen Verbesserungspotential (IP) von 2,53-2,55 und einem hohen exergetischen Faktor (f) von 54,26-54,40 % bei den verwendeten Trocknungsbedingungen. Die Energie- und Exergieanalysen für diagonale Chargentrockner wurden zudem mit denen anderer Chargentrockner verglichen (Tabelle 5.8). Die Auswahl von Trocknungstemperatur, Massenflussrate der Trocknungsluft, Trocknerkapazität und Heiztyp (elektrisch, Treibstoff, etc.) sind die wichtigen Parameter zur Bewertung der genutzten Energie von Chargentrocknern. Der Vergleich zeigt, dass der diagonale Chargentrockner gute Ergebnisse für die Energie- und Exergieanalyse liefert. Dies beruht auf einer gleichmäßigen Trocknung durch eine gleichmäßige Luftstromverteilung durch die Trocknungskammer, die für einen erfolgreichen Ablauf benötigt wird (verbesserte Energienutzung). Um die Trocknungskinetik des Produktes und die Dynamik des Trockners zu beschreiben wurde ein mathematisches Trocknungsmodell entwickelt.

Die Entwicklung des diagonalen Chargentrockners bietet eine nützliche und effektive Lösung zur Ermöglichung einer räumlichen Trocknungshomogenität. Das Design erlaubt es, das gesamte Produkt in der Trocknungskammer gleichmäßigen Luftverhältnissen auszusetzen, statt die Luft von einer Horde zur nächsten zu leiten. Weiterer Forschungsbedarf besteht im Bereich der Optimierung der Trocknungsbedingungen unter Einsatz nicht-invasiver Methoden um die Energieeffizienz zu verbessern. Wichtiger jedoch scheint die Erhöhung der Trocknungsleistung durch den Einsatz Prinzips der diagonalen Luftführung.

Appendix

Appendix 1: Dryer's technical data

Mode of operation	Batch
Heat input type	Convection
State of material in dryer	Stationary
Operating pressure	Atmospheric
Drying medium	Air
Number of stages	Single
Configuration	10m × 1.20m × 1.25m
Inlet cross sectional area	0.07 m^2
Air flow rate at inlet	1.155-1.70 m3/sec
Outlet cross sectional area	0.045 m^2
Total Area (cross sectional)	12 m^2
Total volume	15 m^3
Drying chamber volume	4.68 m^3
Temperature range	Max. 75 °C
Fan size	Dia: 0.7 m
No. of food buckets	25
Area of a bucket	0.24m^2
No. of trays per bucket	4-5
Tray perforation	69.45%
Loading density	Max 5.28 kg/m^3
Batch capacity	100-150 kg
Drying material	Perishable (fruits, vegetables)

Appendix 2: Derivation of model equations

Moisture mass balance in the potato

$$\frac{dX}{dt} = -DR\left(\frac{A_p}{M_p}\right) \quad \text{A1}$$

Negative (-) sign indicate the decline in product moisture content with the drying time

Re-writing the equation (A1) in expanded form, we get

$$\frac{X_t - X_{t+1}}{\Delta t} = DR\left(\frac{A_p}{M_p}\right)$$

$$X_{t+1} = X_t - \Delta t * DR\left(\frac{A_p}{M_p}\right)$$

$$\begin{bmatrix} Moisture\ content \\ after\ time\ interval \\ (t+1) \end{bmatrix} = \begin{bmatrix} moisture\ content\ at \\ the\ start\ of \\ time\ interval \end{bmatrix} - \begin{bmatrix} Length\ of\ the \\ time\ interval \end{bmatrix} * \begin{bmatrix} Rate\ of\ moisture\ removed \\ per\ unit\ area \end{bmatrix} * \begin{bmatrix} area\ of\ the\ product \\ per\ unit\ mass \end{bmatrix}$$

Moisture mass balance in the air (air humidity)

$$\begin{bmatrix} Initial\ humidity \\ of\ the\ drying\ air \end{bmatrix} + \begin{bmatrix} moisture\ content \\ added\ to\ the\ air\ in \\ time\ interval \\ (rate\ of\ moisture\ removal \\ per\ unit\ area * thermal \\ communication\ area) \end{bmatrix} - \begin{bmatrix} Final\ moisture\ content\ of \\ air\ after\ time\ interval \\ (t+1) \end{bmatrix} = 0$$

$$M_a Y_t + DR * A - M_a Y_{t+1} = 0 \qquad \text{A2}$$

Re-writing the equation (A2), we obtain,

$$M_a Y_{t+1} = M_a Y_t + DR * A \qquad \text{A3}$$

Dividing both sides of equation (A3) by Ma, we get,

$$Y_{t+1} = Y_t + DR \left(\frac{A_p}{M_a}\right)$$

Energy balance in the potato

The heat that is transferred from the drying air to the product brings the change in the product temperature by moisture evaporation. The heat and mass balance equation describes an expression for the change in the product temperature as.

$$\begin{bmatrix} \text{Change in sensible heat of product} \\ \text{due to change in its temperature} \end{bmatrix} = \begin{bmatrix} \text{Heat of vaporization of the moisture} \\ \text{leaving the product} \end{bmatrix}$$

$$\mathrm{hA_p}\left(\overline{\mathrm{T}}_\mathrm{a} - \overline{\mathrm{T}}_\mathrm{p}\right)\Delta\mathrm{t} = \mathrm{M_p}\left[\left\{\left(\mathrm{Cp_p} + \mathrm{XCp_w}\right)\Delta\mathrm{T_p}\right\} + \left\{\Delta\mathrm{X}(\mathrm{Cp_w} - \mathrm{Cp_v})\overline{\mathrm{T}}_\mathrm{p} + \mathrm{L}\right\}\right] \qquad \text{A4}$$

Dividing both sides of equation A4 with mp and rearranging,

$$\frac{\Delta T_p}{\Delta t} + \left(\mathrm{Cp_p} + \overline{\mathrm{X}}\mathrm{Cp_w}\right) = \frac{hA_p\left(\overline{\mathrm{T}}_\mathrm{a} - \overline{\mathrm{T}}_\mathrm{p}\right)}{M_p} - \left[\Delta X(\mathrm{Cp_w} - \mathrm{Cp_v})\overline{\mathrm{T}}_\mathrm{p} + \mathrm{L}\right] \qquad \text{A5}$$

Put the value of ΔX in equation A5 from the equation A1

$$\frac{\Delta T_p}{\Delta t}\left(\mathrm{Cp_p} + \overline{\mathrm{X}}\mathrm{Cp_w}\right) = \frac{hA_p(\overline{\mathrm{T}}_\mathrm{a} - \overline{\mathrm{T}}_\mathrm{p})}{M_p} - \left[-DR\left(\frac{A_P}{m_p}\right)(\mathrm{Cp_w} - \mathrm{Cp_v})\overline{\mathrm{T}}_\mathrm{p} + \mathrm{L}\right] \quad \text{A6}$$

Taking $\frac{A_P}{m_p}$ common from right side term of equation A6 and rearranging it, we get

$$\frac{\Delta T_p}{\Delta t} = \frac{A_p\left[h(\overline{\mathrm{T}}_\mathrm{a} - \overline{\mathrm{T}}_\mathrm{p}) + DR(\mathrm{Cp_w} - \mathrm{Cp_v})\overline{\mathrm{T}}_\mathrm{p} - \mathrm{L}\right]}{M_p(\mathrm{Cp_p} + \overline{\mathrm{X}}\mathrm{Cp_w})}$$

Energy balance in the air

The drying air entering the drying chamber undergoes the heat and mass transfer process. Thus, the enthalpy balance between the product and the air after a time interval, described by the equation as,

$$\begin{bmatrix}\text{Change in specific enthalpy of air}\\ \text{passing through dryer}\end{bmatrix} + \begin{bmatrix}\text{Change in specific enthalpy of air}\\ \text{due to heat supplied per unit time}\end{bmatrix} = \begin{bmatrix}\text{Change in specific enthalpy of product}\\ \text{due to an increase insensible heat}\\ \text{transfered from the air to the product}\end{bmatrix}$$

$$M_a[(\mathrm{Cp_a} + \mathrm{Cp_v}Y_t)T_a^t - (\mathrm{Cp_a} + \mathrm{Cp_v}Y_{t+1})T_a^{t+1} - \mathrm{Cp_v}T_a^{t+1}(Y_{t+1} - Y_t)] + Q =$$
$$A_P\left[h\left(\overline{\mathrm{T}}_\mathrm{a} - \overline{\mathrm{T}}_\mathrm{p}\right) - DR\mathrm{Cp_v}\left(\overline{\mathrm{T}}_\mathrm{a} - \overline{\mathrm{T}}_\mathrm{p}\right)\right]\Delta t \quad \text{A7}$$

Taking T_a^{t+1} common from the left term of equation A7 and rewrite it,

$$M_a[(\mathrm{Cp_a} + \mathrm{Cp_v}\bar{Y})T_a^t - T_a^{t+1}\{(\mathrm{Cp_a} + \mathrm{Cp_v}Y_{t+1}) - \mathrm{Cp_v}(Y_{t+1} - Y_t)\}] =$$
$$A_P\left[h\left(\overline{\mathrm{T}}_\mathrm{a} - \overline{\mathrm{T}}_\mathrm{p}\right) - DR\mathrm{Cp_v}\left(\overline{\mathrm{T}}_\mathrm{a} - \overline{\mathrm{T}}_\mathrm{p}\right)\right]\Delta t - Q$$

$$M_a[(\mathrm{Cp_a} + \mathrm{Cp_v}\bar{Y})(T_a^t - T_a^{t+1})] = A_P\left[h\left(\overline{\mathrm{T}}_\mathrm{a} - \overline{\mathrm{T}}_\mathrm{p}\right) - DR\mathrm{Cp_v}\left(\overline{\mathrm{T}}_\mathrm{a} - \overline{\mathrm{T}}_\mathrm{p}\right)\right]\Delta t - Q \quad \text{A8}$$

Rearranging equation A8,

$$\frac{\Delta T_a}{\Delta t} = \frac{A_p[(\overline{\mathrm{T}}_\mathrm{a} - \overline{\mathrm{T}}_\mathrm{p})(\mathrm{h} - \mathrm{DRCp_v})] - Q}{M_a(\mathrm{Cp_a} + \bar{Y}\mathrm{Cp_v})}$$

Appendix 3: Diagonal airflow channel optimization

The following figures show the configuration of the diagonal airflow channel. In order to modifiy its dimentions by keeping same diagonal angle (1.42°), it has been divided into five sections. The measured and calculated values of average air velocity, average area and flow rate for each section is tabulated in the table.

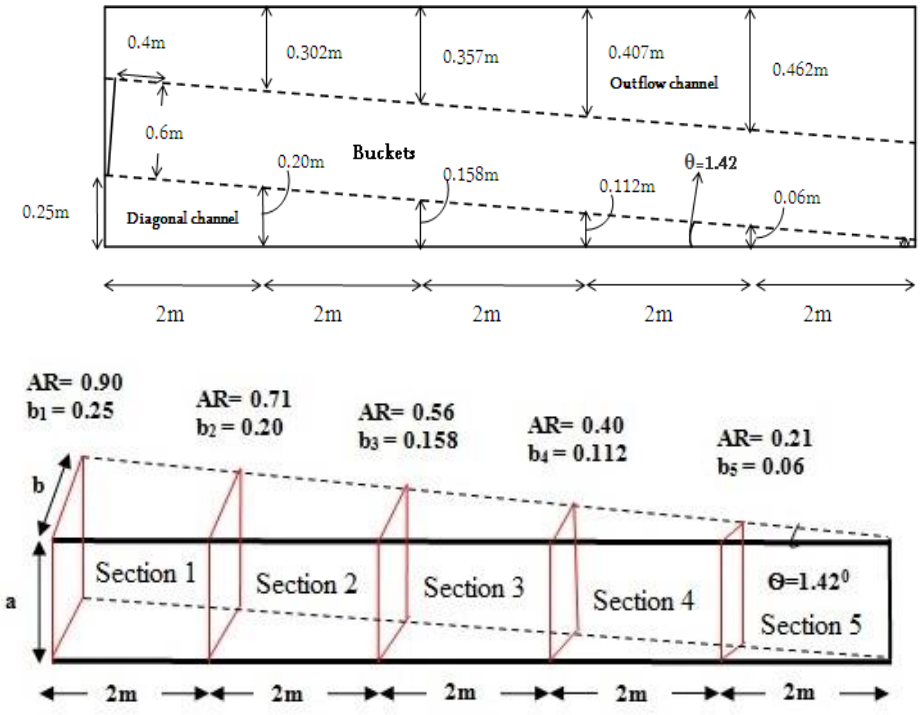

a = channel height = 0.28m (constant)
b = channel width = m (decreases along the channel length)

Section	avg.Velocity (m/s)	avg.A (m^2)	avg.Q (m^3/s)
1	16	0.063	1.008
2	14	0.050	0.70
3	11	0.037	0.40
4	06	0.024	0.14
5	04	0.019	0.078

After getting an appropriate diagonal angle, any change in the dimensions (width or length) of the channel can be adjusted by taking these values as scale to get the same diagonal angle.The height of the channel (a) is constat (0.28m) while width of the channel (b) contimously decreased with an average value of 0.048m for evey 2m distance along the dryer length. So by using the first value of width at zero distance, the next values after every 2m distance can be automatically calculated. This has been descibed as below,

Area of channel

Position (m)	Height, a (m)	Width, b (m)	Aspect ratio (AR)	cross sectional Area (m^2)
0	0.28	0.250	0.89	0.07
2	0.28	0.202	0.72	0.05656
4	0.28	0.158	0.55	0.04312
6	0.28	0.106	0.38	0.02968
8	0.28	0.058	0.21	0.01624
10	0.28	0.010	0.04	0.0028

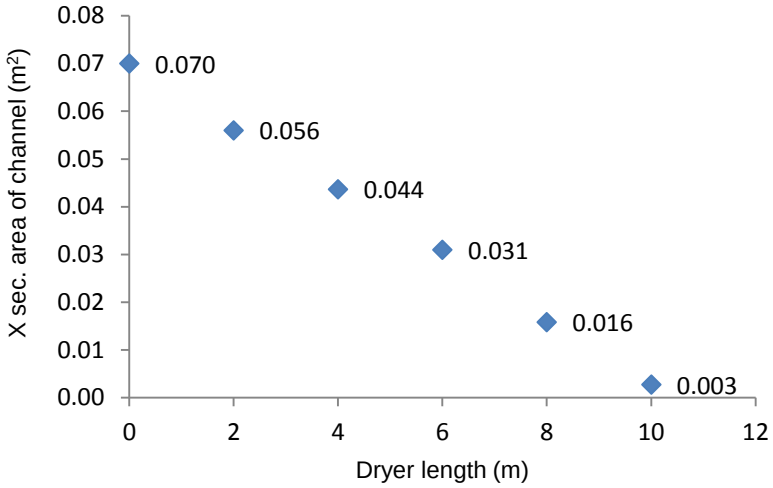

Length of the dryer

a. Changing the width of the channel- Height constant

By increasing or decreasing the cross sectional width (b) of the diagonal channel, the overall length of the drying chamber will increase or decrease by 2m respectively to give same diagonal angle.

Channel Width at start, b1 (m)	Channel length (m)	Diagonal angle (degree)
0.25	10	1.43
0.3	12	1.43
0.35	14	1.43

Once the width of the channel has been changed, the flow rate at inlet will increase due to the change in cross section area if we get same velocity. As channel length would increase with the increase of channel width, so this higher flow rate will enable the air to flow with same airflow rate to the end of the channel.

In case of increasing or decreasing area by changing the width of channel (b), the flow rate towards the buckets will remain same due to same cross sectional area of the buckets. It is not wise able to increase the width of the channel due to the following reasons,

- It only increases the capacity of dyer by the addition of just five buckets (2m length increment)
- The increase in length of the dryer will require more space

So it's better to increase the height of the channel.

b. Changing the height of the channel- Width constant

Once we increase the channel height (a) to increase the dryer capacity (increased sizes of food buckets), then flow towards the buckets or trolley/wagons will also increase due to their increased area.

In case of increment in the height of the channel, addition of perforation plate may be needed to maintain the air column and to straighten the airflow in the channel with increased height. For this different options had been simulated using ANSYS-Fluent.

This is the 3D view of the proposed diagonal dryer for higher batch capacity. The height of the food shelves has increased to increase the batch size.

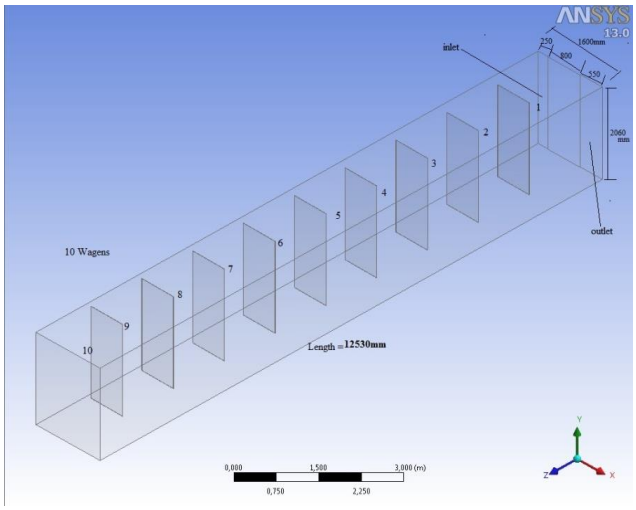

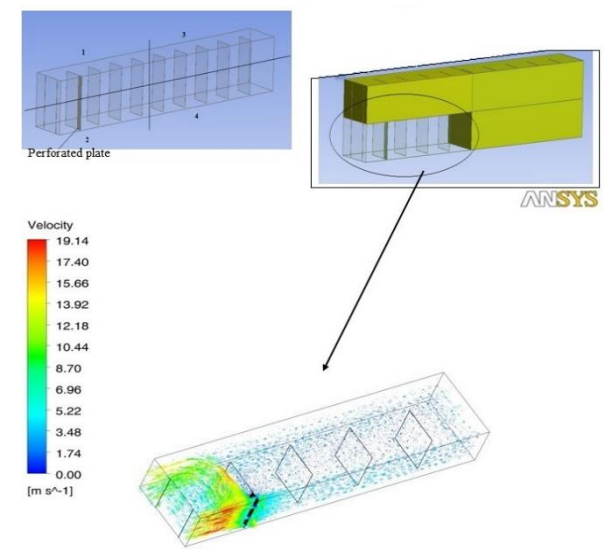

1

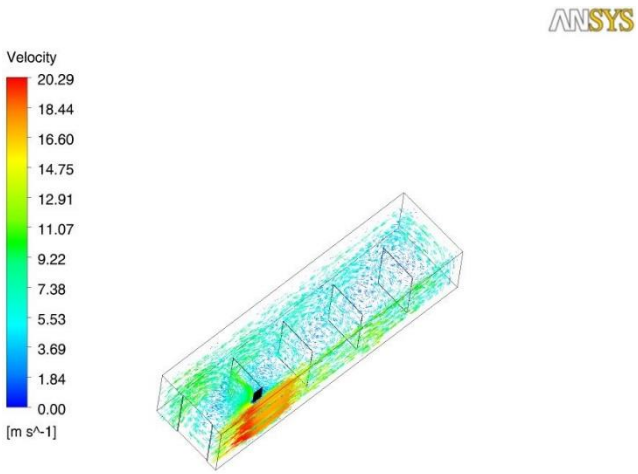

2

In order to get simulated analysis of the airflow, the geometry was modelled and analyzed in ANSYS workbench. The symmetric command was used to get quick analysis and to simplify the geometry. In the first case, a perforated plate was used in the diagonal-channel just along the side of first food shelf. It created a strong back pressure even by varying the perforation.
In second case the same perforated plate was shifted to the inner side of shelf wall, parallel to the direction of airflow. The back pressure and swirling effect which was found in case 1, was reduced at some extent.

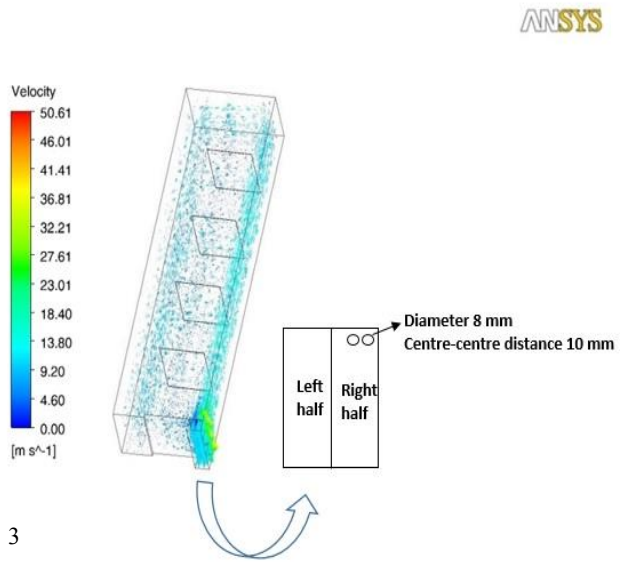

3

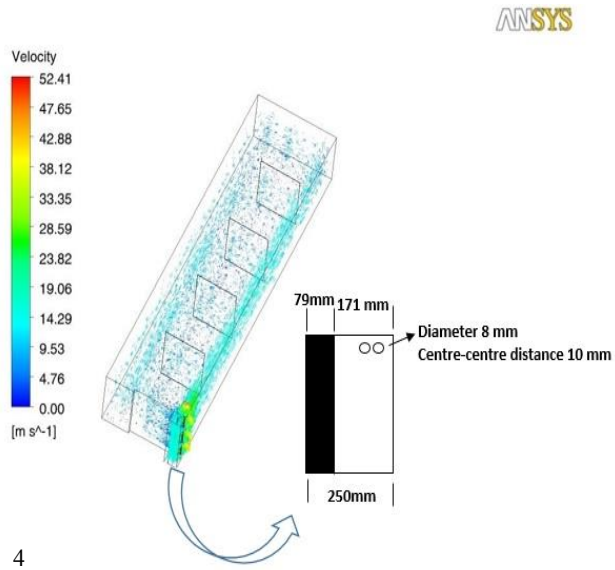

4

In the third case, perforated plate was shifted near to the inlet of the channel. The plate was divided into two halved and only one half (right side) was perforated. It eliminated the factor of comparative high airflow toward the first food shelf as was observed in second case. But it would cause back pressure to fan due to less perforation. Therefore, in fourth analysis of this case, almost fourth part of perforated plate was kept unperforated. It gave good airflow distribution in the diagonal airflow channel but still need to avoid the airflow to be struck more with the sides of the food shelves.

In fifth case, the same perforated plate used in the fourth analysis was shifted at the inlet of the channel. It gave quite good flow distribution in the channel.

So depending upon the batch requirement, the size of the diagonal-channel can be calculated and its proposed configuration can be pre-evaluated using simulation technique.

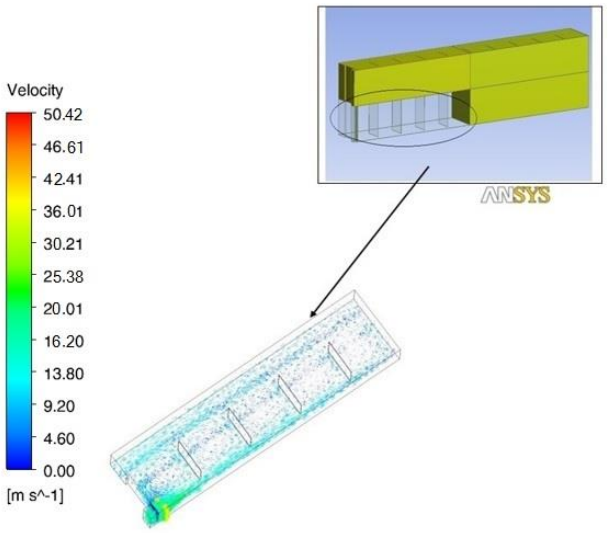

List of References

Amanlou, Y., Zomorodian, A. (2010). Applying CFD for designing a new fruit cabinet dryer. Journal of Food Engineering, 101: 8–15

Abano, E.E., Ma, H., Qu, W. (2011). Influence of air temperature on the drying kinetics and quality of tomato slices. Journal of Food Processing & Technology, 2 (5):1-9.

Abdullah, M.Z., Guan, L.C., Lim, K.C., Karim, A.A. (2004). The applications of computer vision systems and tomographic radar imaging for assessing physical properties of food. Journal of Food Engineering, 61(1): 125–135.

Adams, R.L., Thompson, J.F. (1985). Improving drying uniformity in concurrent flow tunnel dehydrators. Trans ASAE, 28(3): 890–892.

Aghbashlo, M., Kianmehr, M.H., Arabhosseini, A. (2008). Energy and exergy analyses of thin layer drying of potato slices in a semi-industrial continuous band dryer. Drying Technology, 26(12): 1501-1508.

Aghbashlo, M., Mobli, H., Rafiee, S., Madadlou, A. (2013). A review on exergy analysis of drying processes and systems. Renewable and Sustainable Energy Reviews, 22: 1–22.

Akpinar, E.K. (2004). Energy and exergy analyses of drying of red pepper slices in convective type dryer. International Communications in Heat and Mass Transfer, 31(8): 1165-1176.

Akpinar, E.K. (2007). Thermodynamic analysis of strawberry drying process in a cyclone type dryer. Journal of Scientific and Industrial Research, 66(2): 152–161.

Akpinar, E.K., Midilli, A., Bicer, Y. (2005). Energy and exergy of potato drying process via cyclone type dryer. Energy Conversion and Management, 46 (15-16): 2530-2552.

Akpinar, E.K., Midilli, A., Bicer, Y. (2006). The first and second law analyses of thermodynamic of pumpkin drying process. Journal of Food Engineering, 72 (4): 320–331.

Akpinar, E.K., Sarsilmaz, C. (2004). Energy and exergy analyses of drying of apricots in a rotary solar dryer. International Journal of Exergy, 1(4): 457–474.

Alireza, Y., Acefeh, L., and M. Reza. (2009). New method for determination of potato slice shrinkage during drying. Computer and Electronics in Agriculture, 65: 268-274.

Amjad, W., Hensel, O., Munir, A. Esper, A. (2015a). Batch drying of potato slices: Kinetic changes of color & shrinkage in response of uniformly distributed drying temperature. Agricultural Engineering International: CIGR Journal, 17(3): 296-308.

Amjad, W., Munir, A., Esper A., Hensel, O. (2015b). Spatial homogeneity of drying in a batch type food dryer with diagonal air flow design. Journal of Food Engineering, 144: 148-155.

Araya-Farias, M., Ratti, C. (2008). Dehydration of foods. In: Ratti C (ed) Advances in food dehydration. Contemporary food engineering. CRC Press, Boca Raton, pp 1–36

Avila, I.M.L.B, and C.L.M. Silva. (1999). Modelling kinetics of thermal degradation of color of peach puree. Journal of Food Engineering, 39(2): 161-166.

Axtell, B. (2002). Drying food for profit: A guide for small business. (Ed.). London: Intermediate Technology Development Group Publishing Ltd. 85-103 p.

Ayensu, A., Asiedu-Bondzie, (1986). Solar drying with convective self-flow and energy storage. Solar and Wind Technology, 3(4): 273-279.

Babalis, S.J., Belessiotis, V.G. (2004). Influence of the drying conditions on the drying constants and moisture diffusivity during the thin-layer drying of figs. Journal of Food Engineering, 65(3): 449–58.

Babalis, S.J., Papariсolaou, E., & Belessiotis, V.G. (2005). Impact of alternating drying-air flow direction on the drying kinetics of agricultural products. 3rd IASME/WSEAS Int. Conf. on Heat Transfer, Thermal Engineering And Environment, Corfu, Greece, August 20-22, 2005 (pp300-305).

Barreiro, J.A., Milano, M., Sandoval, J.A. (1997). Kinetics of color change of double concentrated tomato paste during thermal treatment. Journal of Food Engineering, 33(3): 359-371

Bakal, S.B., Sharma, G.P., Sonawan, S.P., Verma, R.C. (2011). Kinetics of potato drying using fluidized bed dryer. Journal of Food Science & Technology, 49(5): 608- 613.

Bartzanas, T., Boulard, T., Kittas, C. (2004). Effect of vent arrangement on windward ventilation of a tunnel greenhouse. Biosystem Engineering, 88: 479–90.

Chandra Mohan, V. P., Talukdar, P. (2014). Experimental studies for convective drying of Potato. Heat Transfer Engineering, 35(14–15): 1288–1297.

Chauhan, P.S., Kumar, A., Tekasakul, P. (2015). Application of software in solar drying systems: A review. Renewable and sustainable energy reviews 51: 1326-1337.

Chen, H.H., Huang, T.C., Tsai, C.H., Mujumdar A.S. (2008). Development and performance analysis of a new solar energy-assisted photocatalytic dryer. Drying Technology, 26: 503–7

Chen, Y., Martynenko, A. (2013). Computer Vision for Real-Time Measurements of Shrinkage and Color Changes in Blueberry Convective Drying. Drying Technology, 31: 1114–1123.

Chua, K. J., Mujumdar, A. S., Chou, S. K., Hawlader, M. N. A., Ho, J. C. (2000). Convective drying of banana, guava and potato pieces: Effect of cyclical variations of air temperature on drying kinetics and color change. Drying Technology, 18(4-5): 907–936.

Chua, K.J., Hawlader, M.N.A., Chou, S.K., Ho, J.C. (2002). On the study of time-varying temperature drying effect on drying kinetics and product quality. Drying Technology, 20 (8): 1559–1577.

Chutintrasri, B., and Noomhorm, A. (2007). Colour degradation kinetics of pineapple puree during thermal processing. LWT, 40: 300-306.

Colak, N., Hepbasli, A. (2007). Performance analysis of drying of green olive in a tray dryer. Journal of Food Engineering, 80 (4): 1188–1193.

Contreras, C., Martin-Esparza, M.E. Chiralt, A., Martinez-Navarrete, N. (2008). Influence of microwave application on convective drying: effects on drying kinetics and optical and mechanical properties of apple and strawberry. Journal of Food Engineering 88 (1): 55– 64.

Corzo, O., Bracho, N., Vasquez, A., Pereira, A. (2008). Energy and exergy analyses of thin layer drying of coroba slices. Journal of Food Engineering, 86(2): 151-61.

Cristina Ratti & Guillermo H. Crapiste (2009). Modeling of Batch Dryers for Shrinkable Biological Materials. Food and Bioprocess Technology, 2: 248–256

Chou, S. K., Hawlader, M. N. A., Chua, K. J., Teo, C. C. (1997). A methodology for tunnel dryer chamber design. International journal of energy research, 21: 395-410.

Darabi, H., Zomorodin, A., Akbari, M.H., Lorestani, A.N. (2013). Design of cabinet dryer with two geometric configurations using CFD. Journal of Food Science & Technology, 52(1): 359–366.

Diamante, L., Durand, M., Savage, G., Vanhanen, L. (2010). Effect of temperature on the drying characteristics, colour and ascorbic acid content of green and gold kiwifruits. International Food Research Journal, 17: 441-451.

Doymaz, I., Ismail, O. (2011). Drying characteristics of sweet cherry. Food and Bio-products Processing, 89(1): 31-38.

Ehiem, J.C., Irtwange, S.V., Obetta, S.E. (2009). Design and development of an industrial fruit and vegetable dryer. Research Journal of Applied Sciences, Engineering and Technology, 1(2): 44-53.

Elamin, O.M., and Akoy. (2014). Effect of Drying Temperature on Some Quality attributes of mango slices. International Journal of Innovation and Scientific Research, 4(2): 91-99

Erbay, Z., Icier, F. (2011). Energy and exergy analyses on drying of olive leaves (olea europaea) in tray drier. Journal of Food Process Engineering, 34(6): 2105–2123.

Farias, A.M. and C. Ratti. (2008). Dehydration of foods. In: Ratti C (ed) Advances in food dehydration. Contemporary food engineering. CRC Press, Boca Raton, pp 1–36

Fernandez, L., Castillero, C., Aguilera. J.M. (2005). An application of image analysis to dehydration of apple discs. Journal of Food Engineering, 67: 185–193.

Fernando R. L., and L. Cisneros-Zevallos. (2007). Degradation kinetics and colour of anthocyanins in aqueous extracts of purple- red-flesh potatoes (Solanum tuberosum L.) Journal of Food Chemistry, 100: 885-894.

Fernando, W. J. N., Ahmad, A. L., Shukor, S. R. A., Lok, Y. H., (2008). A model for constant temperature drying rates of case hardened slices of papaya and garlic. Journal of Food Engineering, 88(2): 229–238.

Fluent 6.3 user's Guide (2005). Fluent documentation. Fluent Inc, Lebanon.

Ghiaus, A.G., Gavriliuc, R. (2007). Simulation of air flow and dehydration process in tray drying systems. U.P.B. Sci. Bull., Series D, 69(4): 41-50.

Gül ah Çakmak, Cengiz Y ld z, (2009). Design of a new solar dryer system with swirling flow for drying seeded grape. International Communications in Heat and Mass Transfer, 36(9): 984-990.

Hammond, G. P., Stapleton, A. J. (2001). Exergy analysis of the United Kingdom energy system. Proc. IMechE, Part A: Journal of Power and Energy, 215(A2): 141–162.

Hancioglu, E., Hepbasli, A., Icier, F., Erbay, Z., Colak, N. (2010). Performance investigation of the drying of parsley in a tray dryer system. International Journal of Exergy, 7(2): 193-210.

Hassan, O. A. B., and Z. Yue. (2002). Pressure drop in and noise radiation from rectangular and round ducts-literature survey. The third European conference on energy performance & indoor Climate in Buildings, France, pp. 387-392.

Hatcher, D. W., Symons, S. J., Manivannan, U. (2004). Developments in the use of image analysis for the assessment of oriental noodle appearance and colour. Journal of Food Engineering, 61(1): 109–117.

Holman, J.P. (1994). Experimental methods for engineers. (6th ed., International Ed.) McGraw-Hill, Singapore.

Hawlader, M.N.A., Chou, S.K., Chua, K.J. (1997). Development of design charts for tunnel dryers. International journal of energy research, 21: 1023–1037

Ichsani, D., Dyah, W. A. (2002). Design and experimental testing of a solar dryer combined with kerosene stoves to dry fish. American Society of Agricultural and Biological Engineers, 1-3.

Icier, F., Colak, N., Erbay, Z., Kuzgunkaya, E.H., Hepbasli, A. (2010). A comparative study on exergetic performance assessment for drying of broccoli florets in three different drying systems. Drying Technology, 28(2): 193–204.

Jacek, S., Andrzej, J.N., & Dawid, R. (2010). Improved 3-D temperature uniformity in a laboratory drying oven based on experimentally validated CFD computations, Journal of Food Engineering, 97: 373-383.

Janjai, S., Intawee, P., Chaichoet, C., Mahayothee, B., Haewsungcharern, M., Muller, J. (2006). Improvement of the air flow and temperature distribution in a conventional longan dryer. International symposium towards sustainable livelihoods & ecosystem in mountaneous regions, Chiang Mai, Thailand.

Jasim Ahmed and Mohammad Shafiur Rahman. Handbook of food process design. Volume 1 2012, Blackwell Publishing Ltd. chapter 19, page 552

Jayas, D.S., Paliwal, J., Visen, N.S. (2000). Multi-layer neural networks for image analysis of agricultural product. Journal of Agricultural Engineering Research, 72(2): 119–128.

Kerkhof, J. A. M. (1994). The role of theoretical and mathematical modelling in scale-up, Drying Technol., 12(1&2): 1-46.

Kiranoudis, C.T., Karathanos, V.T., & Markatos, N.C. (1999) Computational fluid dynamics of industrial batch dryers of fruits, Drying Technology. 17(1&2): 1-25

Kongdej, L. (2011). Effects of Temperature and Slice Thickness on Drying Kinetics of Pumpkin Slices. Walailak Journal of Science and Technology, 8(2): 159-166.

Krawczyk, P., Badyda, K. (2011). Two-dimensional CFD modeling of the heat and mass transfer process during sewage sludge drying in a solar dryer. Archives of Thermodynamics, 32: 3–16.

Kro¨ll, K. (1978). Trockner und Trocknungsverfahren (2nd ed.).In Trocknungstechnik, Vol. 2 springer, Berlin.

Krokida M.K., Karathanos V.T., Maroulis Z.B. and D.K. Marinos. (2003). Drying kinetics of some vegetables. Journal of Food Engineering, 59: 391–403.

Krokida, M.K., Karathanos, V.T., Maroulis, Z.B., Marinos Kouris, D. (2003). Drying kinetics of some vegetables. Journal of Food Engineering, 59(4): 391–403.

Krokida, M.K., Tsami, E., and Z.B. Maroulis. (1998). Kinetics on color changes during drying of some fruits and vegetables. Drying Technology, 16 (3–5): 667–685.

Kudra, T. (2004). Energy Aspects in Drying. Drying Technology: An International Journal, 22(5): 917-932.

Kumar, S., Singh, S. (2011). Performance evaluation of forced convection mixed-mode solar dryer: Experimental Investigation. 978-0-9564263-4/5/25.00©2011 IEEE.

Lee, H.S., ând G.A. Coates. (1999). Thermal pasteurization effects on color of red grapefruit juices. Journal of Food Science, 64: 663-666.

Leo´ n, K.; Mery, D.; Pedreschi, F.; Leo´ n, J. (2006). Color measurement in L*a* b* units from RGB digital images. Food Research International, 39(10): 1084–1091.

Lozano, J.E., and A. Ibarz. (1997). Color changes in concentrated fruit pulp during heating at high temperatures. Journal of Food Engineering, 31: 365-373.

Lozano, J.E., Cristina Anon, and G.V. Barbosa-Canovas. (2000). Trends in food engineering. Technomic Publisher 2007 USA ISBN: 1-56676-991-4.

Marcel, E., Alexis, K., François, G. (2014). Effect of Thermal Process and Drying Principle on Color Loss of Pineapple Slices. American Journal of Food Science and Technology, 2(1): 17-20.

Marcus Karel, Daryl B. Lund (2003). Physical Principles of Food Preservation: Revised and Expanded. Volume 129 of Food science and technology, Edition 2 revised, CRC Press, 2003.

Margaris, D.P., Ghiaus, A.G. (2006). Dried product quality improvement by air flow manipulation in tray dryers. Journal of Food Engineering, 75: 542–550.

Martynenko, A. (2006). Computer vision system for control of drying process. Drying Technology, 24: 879–888.

Mathioulakis, E., Karathanos, V.T., Belessiotis, V.G. (1998). Simulation of air movement in a dryer by computational fluid dynamics: application for the drying of fruits. Journal of Food Engineering, 36 (2): 183–200.

Mayor, L., and A.M. Sereno. (2004). Modeling shrinkage during convective drying of food materials: a review, Journal of Food Engineering, 61 (3): 373-386.

Midilli, A., Kucuk, H. (2003). Energy and exergy analyses of solar drying process of pistachio. Energy, 28: 539–56.

Mirade, P.S. (2003). Prediction of the air velocity field in modern meat dryers using unsteady computational fluid dynamics (CFD) models. Journal of Food Engineering, 60: 41–48.

Misha, S., Mat, S., Ruslan, M.H., Sopian, K., Salleh, E. (2013). Review on the application of a tray dryer system for agricultural products. World Applied Science Journal, 22 (3): 424-433.

Mujumdar, A. S. (1995). Handbook of industrial drying, 2nd edn. Marcel Dekker, New York.

Mujumdar, A. S. (2006a). Handbook of industrial drying, 3rd ed. New York, USA: CRC.

Mujumdar, A.S. (2000). Drying technology in agricultural and food science. Science publishers, Inc. Plymoth, UK, pp: 61-98 and pp: 253-286.

Mujumdar, A.S. (2006b). Some recent developments in drying technologies appropriate for postharvest processing. International Journal of Postharvest Technology and Innovation, 1: 76–92.

Mujumdar, A.S. (2007). Principles, classifications, and selection of dryers. Handbook of industrial drying (3rd ed., pp. 1-32). Boca Raton, FL: Taylor & Francis.

Müller, J and Mühlbauer, W. (2012). Modern Drying Technology: Energy Savings, Volume 4 Doi: 10.1002/9783527631681.ch6 Published Online: 26 JAN 2012

Müller, J., Heindl, A. (2006). Drying of medicinal plants. In R. J. Bogers, L. E. Craker, & D. Lange (Eds.), Medicinal and aromatic plants: Agricultural, commercial, ecological, legal, pharmacological and social aspects (pp. 237-252). Dordrecht: Springer.

Muskan, M. (2001). Kinetics of colour change of kiwifruits during hot air and microwave drying. Journal of Food Engineering, 48 (2): 169–175

Nagle, M., Carlos, J., Azcárraga, G., Mahayothee, B., Haewsungcharern, M., Janjai, S., Müller, J. (2010). Improved quality and energy performance of a fixed-bed longan dryer by thermodynamic modifications. Journal of Food Engineering, 99: 392–399

Nguyen, M.N., Price, W.E. (2007). Air-drying of banana: Influence of experimental parameters, slab thickness, banana maturity and harvesting season. Journal of Food Engineering, 79(1): 200-207.

Niamnuy, C., Devahastin, S., Soponronnarit, S., Vijaya Raghavan, G.S. (2008). Kinetics of astaxanthin degradation and colour changes of dried shrimp during storage. Journal of Food Engineering, 87(4): 591–600.

Norton, T., Sun, D.W. (2006). Computational fluid dynamics (CFD) e an effective and efficient design and analysis tool for the food industry: A review. Trends in Food Science & Technology, 17: 600-620.

Orikasa, T., Wu, L., Shiina, T., Tagawa, A. (2008). Drying characteristics of kiwifruit during hot air drying. Journal of Food Engineering, 85: 303-308.

Pedreschi, F., Leo´n, J., Mery, D., Moyano, P. (2006). Development of a computer vision system to measure the colour of potato chips. Food Research International 39: 1092–1098.

Pedreschi, F., Leo´n, J., Mery, D., Moyano, P., Pedreschi, R., Kaack, K., Granby. K. (2007). Colour development and acrylamide content of pre-dried potato chips. Journal of Food Engineering, 79: 786–793

Pereira, A. C., Reis, M. S., Saraiva, P. M. (2009). Quality control of food products using image analysis and multivariate statistical tools. Industrial and Engineering Chemistry Research, 48(2): 988–998.

Precoppe, M., Janjai, S., Mahayothee, B., Müller, J. (2014). Batch uniformity and energy efficiency improvements on a cabinet dryer suitable for smallholder farmers. Journal of Food Science & Technology, 52(8): 4819-4829.

Prommas, R., Rattanadecho, P., Cholaseuk, D. (2010). Energy and exergy analyses in drying process of porous media using hot air. International Communications in Heat and Mass Transfer, 37: 372–378.

Rafiq, A., Makroo, H., Sachdeva, P., Sharma, S. (2013). Application of Computer Vision System in Food Processing- A Review. Journal of Engineering Research and Applications, 3(6): 1197-1205

Rahman, N., Kumar, S. (2007). Influence of sample size and shape on transport parameters during drying of shrinking bodies. Journal of Food Process Engineering, 30(2): 186-203.

Ramallo, L.A., Mascheroni, R.H. (2012). Quality evaluation of pineapple fruit during drying process. Food and Bioproducts processing, 90: 275–283.

Ramos, I.N., Silva, C.L.M., Sereno, A.M., Aguilera, B.J.M. (2004). Quantification of microstructural changes during first stage air drying of grape tissue. Journal of Food Engineering, 62: 159–164.

Robert H. Perry, Don W. Green and James O. Maloney. Perry's Chemical Engineers' Handbook Seventh Edition. McGrawHill Companies, Inc NY, 1997. ISBN: 0-07-115448-5.

Roman, F., Strahl-schäfer, V., Hensel, O. (2012). Improvement of air distribution in a fixed-bed dryer using computational fluid dynamics. Biosystems Engineering, 112: 359-369.

Sagar, V. R., Suresh Kumar P. (2010). Recent advances in drying and dehydration of fruits and vegetables: A review. Journal of Food Science & Technology, 47(1): 15–26.

Sahin, S., Sumnu, S.G. (2006). Physical Properties of Foods, Food Science Text Series; Springer Science þBusiness Media, LLC: New York.

Segnini, S., Dejmek, P., & O¨ ste, R (1999). A low cost video technique for colour measurement of potato chips. Lebensmittel-Wissenschaft und-Technologie, 32: 216–222.

Shahab, M., Rafiee, S., Mohtasebi, S., Hosseinpour, S. (2013). Image analysis and green tea colour change kinetics during thin-layer drying. Food Science and Technology International, 0 (0): 1–12.

Shawik, D., Tapash, D., Srinivasa Rao, P., Jain, R.K. (2001). Development of an air recirculating tray dryer for high moisture biological materials. Journal of Food Engineering 50: 223–227.

Sogut, Z., Ilten, N., Oktay, Z. (2010). Energetic and exergetic performance evaluation of the quadruple-effect evaporator unit in tomato paste production. Energy, 35(9): 3821-3826.

Sturm, B., Anna-Maria N.V., Hofacker, W.C. (2014). Influence of process control strategies on drying kinetics, colour and shrinkage of air dried apples. Applied Thermal Engineering 62: 455-460.

Syahrul, S., Hamdullahpur, F., Dincer, I. (2002). Thermal analysis in fluidized bed drying of moist particles. Applied Thermal Engineering, 22(15): 1763-1775.

Tippayawong, N., Tantakitti, C., Thavornun, S., Peerawanitkul, V. (2009). Energy conservation in drying of peeled longan by forced convection and hot air recirculation. Biosystems Engineering, 104: 199–204

Tzempelikos, D.A., Vouros, A.P., Bardakas, A.V., Filio, A.E., Margaris, A.P. (2012). Analysis of air velocity distribution in a laboratory batch-type tray air dryer by computational

fluid dynamics. International Journal of Mathematics and Computers in Simulation, 6(5): 413-421.

Tripathy, P. P., Abhishek, S., Bhadoria, P. B. S. (2014). Determination of convective heat transfer coefficient and specific energy consumption of potato using an ingenious self-tracking solar dryer. Food Measure, 8: 36–45.

Van Gool,W. (1997). Energy policy: fairy tales and factualities. In Innovation and technology strategies and policies (Eds O.D.D. Soares, A.Martins da Cruz, G. Costa Pereira, I. M. R. T. Soares, and A. J. P. S. Reis), 1997, pp. 93–105 (Kluwer Academic Publishers, Dordrecht).

Wang, N., Brennan, J.G. (1995). Changes in structure, density and porosity of potato during dehydration. Journal of Food Engineering, 24(1): 61–76.

Wang, N., Brennan, J.G. (1993). The influence of moisture content and temperature on the specific heat of potato measured by differential scanning calorimetry. Journal of Food Engineering, 19(3): 303–310.

Xia, B., & Sun, D.W. (2002). Applications of computational fluid dynamics (CFD) in the food industry: a review. Computers and Electronics in Agriculture, 34: 5-24.

Xiang, J.Y., Cali, M., Santarelli, M. (2004). Calculation for physical and chemical exergy of flows in systems elaborating mixed-phase flows and a case study in an IRSOFC plant. International Journal of Energy Research, 28(2): 101–115.

Yam, K. L., & Papadakis, S. E. (2004). A simple digital imaging method for measuring and analyzing color of food surfaces. Journal of Food Engineering, 61(1): 137–142.

Yu, H., MacGregor, J. F., Haarsma, G., & Bourg, W. (2003). Digital imaging for online monitoring and control of industrial snack food processes. Industrial and Engineering Chemistry Research, 42(13): 3036–3044.

Youcef-Ali, S., Moummi, N., Desmons, J.Y., Abene, A.H., Messaoudi, M., Le, R. (2001). Numerical and experimental study of dryer in forced convection. International Journal of Energy Research, 25(6): 537–553.